

ISSN 1994-4136 (print)

ISSN 1997-3500 (online)

Myrmecological News

Volume 25

October 2017



Schriftleitung / editors

Florian M. STEINER, Herbert ZETTEL & Birgit C. SCHLICK-STEINER

Fachredakteure / subject editors

Jens DAUBER, Falko P. DRIJFHOUT, Evan ECONOMO, Heike FELDHAAR, Nicholas J. GOTELLI,
Heikki O. HELANTERÄ, Daniel J.C. KRONAUER, John S. LAPOLLA, Philip J. LESTER,
Timothy A. LINKSVAYER, Alexander S. MIKHEYEV, Ivette PERFECTO, Christian RABELING,
Bernhard RONACHER, Helge SCHLÜNS, Chris R. SMITH, Andrew V. SUAREZ

Wissenschaftliche Beratung / editorial advisory board

Barry BOLTON, Jacobus J. BOOMSMA, Alfred BUSCHINGER, Daniel CHERIX, Jacques H.C. DELABIE,
Katsuyuki EGUCHI, Xavier ESPADALER, Bert HÖLLDOBLER, Ajay NARENDRA, Zhanna REZNIKOVA,
Michael J. SAMWAYS, Bernhard SEIFERT, Philip S. WARD

Eigentümer, Herausgeber, Verleger / publisher

© 2017 **Österreichische Gesellschaft für Entomofaunistik**
c/o Naturhistorisches Museum Wien, Burgring 7, 1010 Wien, Österreich (*Austria*)



Light at the end of the tunnel: Integrative taxonomy delimits cryptic species in the *Tetramorium caespitum* complex (Hymenoptera: Formicidae)

Herbert C. WAGNER, Wolfgang ARTHOFER, Bernhard SEIFERT, Christoph MUSTER, Florian M. STEINER & Birgit C. SCHLICK-STEINER



Abstract

Species delimitation is fundamental for many biological studies; its importance extends from regional faunistics over behavioral research to the reconstruction of evolutionary history. However, species delimitation in the Palearctic *Tetramorium caespitum* species complex (formerly *Tetramorium caespitum* / *impurum* complex) has stayed ambiguous over a century. A 2006 study argued for the presence of eight Western Palearctic cryptic species but did not draw formal taxonomic conclusions due to multiple unresolved issues. Using 1428 nest samples in an in-depth integrative-taxonomy approach, we here revise the European species of the complex. Unsupervised analyses provide independent species hypotheses based on molecular and morphological disciplines. Following the unified species concept, we show the presence of ten clearly distinguishable European species differing in mitochondrial DNA, nuclear DNA, morphology of workers and males, and ecology. We explain the evolution of the observed mitochondrial-nuclear discordances by peripatric speciation, historical introgression, and recent hybridization, and that of morphological-nuclear discordances by interspecific similarity and intraspecific variability, that is, morphological crypsis. Based on the final species hypotheses, we confirm *T. caespitum* (LINNAEUS, 1758), *T. impurum* (FOERSTER, 1850), *T. indocile* SANTSCHI, 1927, *T. hungaricum* RÖSZLER, 1935, and *T. alpestre* STEINER, SCHLICK-STEINER & SEIFERT, 2010 as good species. We raise *T. fusciclava* CONSANI & ZANGHERI, 1952 stat.n., *T. staerckei* KRATOCHVÍL, 1944 sp.rev., and *T. immigrans* SANTSCHI, 1927 stat.n. (as an introduced species also in the Americas) to species rank and synonymize *T. semilaeve* var. *kutteri* SANTSCHI, 1927 under *T. indocile* and *T. staerckei* var. *gregori* KRATOCHVÍL, 1941 under *T. impurum*. Finally, we newly describe *T. breviscapus* sp.n. and *T. caucasicum* sp.n. We present dichotomous determination keys to workers and males and make freely available an online identification key to workers at <https://webapp.uibk.ac.at/ecology/tetramorium/>. Of relevance to resolving other highly complicated taxonomic problems, we highlight that no single data type was sufficient to disentangle the final species boundaries, which underlines the importance of integrating multiple data sources in taxonomy.

Key words: CO1 gene polyphyly, amplified fragment-length polymorphism, morphometrics, nest centroid clustering, interspecific hybridization, European pavement ants.

Myrmecol. News 25: 95-129

licensed under CC BY 3.0

ISSN 1994-4136 (print), ISSN 1997-3500 (online)

Received 13 March 2017; revision received 13 June 2017; accepted 14 July 2017

Subject Editor and ad-hoc Editor-in-Chief: Herbert Zettel

Herbert C. Wagner (contact author), Wolfgang Arthofer, Florian M. Steiner¹ & Birgit C. Schlick-Steiner¹, Molecular Ecology Group, Institute of Ecology, University of Innsbruck, Technikerstraße 25, 6020 Innsbruck, Austria. E-mail: heriwagner@yahoo.de; wolfgang.arthofer@uibk.ac.at; florian.m.steiner@uibk.ac.at; birgit.schlick-steiner@uibk.ac.at

Bernhard Seifert, Section Pterygota, Senckenberg Museum of Natural History, Am Museum 1, 02826 Görlitz, Germany. E-mail: bernhard.seifert@senckenberg.de

Christoph Muster, Neukamp 29, 18581 Putbus, Germany. E-mail: muster@rz.uni-leipzig.de

¹Equally contributing senior authors

Introduction

The species level is the basis of many biological studies – most research in, for example, conservation, phenology, morphology, behavior, and physiology, makes sense only if the study organism is correctly determined at the species level. Some species are, from a human point of view, cryptic, which means they are not morphologically distinguishable using conventional methods (BICKFORD & al. 2007, SMITH & al. 2008, SEIFERT 2009). Their delimitation challenges taxonomists and increasingly leads to inter-

disciplinary approaches (SCHLICK-STEINER & al. 2010). Species delimitation is also the basis of investigating the evolution of crypsis itself. Processes such as stasis, convergence, interspecific gene flow, and postglacial migration can only be understood using correctly delimited species units.

Ants have been considered as difficult to determine at the species level (SEIFERT 2007). Within ants, the genus *Tetramorium* seems to stand out in this quality, as its taxo-

nomical situation has remained unclear even in the relatively well studied Central European area (STEINER & al. 2002, CSŐSZ & MARKÓ 2004, SCHLICK-STEINER & al. 2005, 2006, SEIFERT 2007). Species of the *Tetramorium caespitum* complex (formerly *T. caespitum* / *impurum* complex sensu SCHLICK-STEINER & al. 2006) inhabit areas up to 2500 meters above sea level (m a.s.l.) and 63° N and include the most widespread and abundant *Tetramorium* ants of Central and Northern Europe. Representatives of the complex are found in open, xerothermous habitats such as dry grasslands, block fields, and urban areas. Dense forests are avoided, but light pine and oak woodlands in southern Europe are frequently inhabited.

Before the 20th century, two still valid species of the complex were described from Europe, *Tetramorium caespitum* (LINNAEUS, 1758) and *T. impurum* (FOERSTER, 1850). In the first half of the 20th century, multiple new *Tetramorium* species and subspecies names were assigned (e.g., EMERY 1925, SANTSCI 1927, RÖSZLER 1936, KRATOCHVÍL 1941, 1944), but strong delimitation arguments were missing in most cases. Hence, in the following decades, myrmecologists ignored those nomenclatural changes. CSŐSZ & MARKÓ (2004) found distinct differences between *T. caespitum* s.l. and *T. hungaricum* RÖSZLER, 1935 and redescribed the latter based on morphological arguments. After that, the detection of cryptic species by SCHLICK-STEINER & al. (2006) was based on sequences of the mitochondrial cytochrome C oxidase subunit I (CO1) gene, traditional morphometrics (TM), male genital morphology, and cuticular hydrocarbons. These authors proposed the presence of five further species additionally to *T. caespitum*, *T. impurum*, and *T. hungaricum* and handled them as operational taxonomic units labeled A - E. Additionally, they labeled six smaller CO1-haplotype (HT) clades (henceforth, CO1 clades) without data of other disciplines as U1 - U6. Since then, operational taxonomic unit A has been newly described as *T. alpestre* STEINER, SCHLICK-STEINER & SEIFERT, 2010 (STEINER & al. 2010) and C redescribed as *T. indocile* SANTSCI, 1927 (CSŐSZ & al. 2014b). Besides *T. tsushimae* (see STEINER & al. 2006b), species E has been shown to be the only species of the complex introduced to the Americas (STEINER & al. 2008).

In this study, we aimed to delimit the European species of the *Tetramorium caespitum* complex based on integrative taxonomy. Additionally, we showed the linkage between operational taxonomic units and type material, drew taxonomical consequences, and presented identification keys. Thereby, we provide the basis for reconstructing the evolutionary history of the cryptic species complex. Due to the obvious difficulties in delimiting species of the *T. caespitum* complex (SCHLICK-STEINER & al. 2006, STEINER & al. 2006a, SEIFERT 2007, STEINER & al. 2010), we used an in-depth integrative-taxonomy approach and applied genetic and morphological data on a high-density sample from most European regions. We chose mitochondrial DNA (CO1 gene), a whole-genome scan (amplified fragment-length polymorphism; AFLP), male genital morphology, TM of workers, geometric morphometrics (GM) of workers and gyne wings, and thermal niche as data sources for integrative species delimitation. We followed an established protocol to handle cryptic species by integrative taxonomy (SCHLICK-STEINER & al. 2010). To link operational taxonomic units with valid species names, we

investigated Palearctic type material from the west of the Johansen line in Siberia (see JOHANSEN 1955) as well as the type of a species introduced to the Americas (*T. immigrans* SANTSCI, 1927).

Material and methods

Diagnosis of the *Tetramorium caespitum* complex: At least 28 *Tetramorium* species are native to Europe (BOROWIEC 2014); most of these do not belong to the *Tetramorium caespitum* complex. The differentiation of complexes is not always simple since the traits of morphological characters often overlap. Therefore, the morphological criteria for inclusion into the *T. caespitum* complex are characterized in detail here (see Taxonomy, Diagnosis of the *T. caespitum* complex).

Integrative-taxonomy workflow: The study follows a coherent protocol for integrative taxonomy (SCHLICK-STEINER & al. 2010). As far as possible, data were generated by using the same individuals in all disciplines. In doing so, gasters of workers were cut off for DNA extraction, degastered workers mounted for morphometrics, and males from the same nests dissected for genital investigation. Data of CO1, AFLP, male genital morphology, TM, and GM were analyzed without prior hypotheses, that is, in an unsupervised fashion. The results of disciplines were compared and discordance rates between genetic and morphometric methods determined. The unified species concept (DE QUEIROZ 2007) was used; it defines species as independently evolving metapopulations and considers the ability of different disciplines to delimit species at different stages of speciation. Following ideas of WIENS & SERVEDIO (2000) and SEIFERT (2014), species delimitation criteria were decisions considering thresholds of evolutionary divergence. For the CO1 phylogeny, the multi-rate Poisson Tree Processes method (KAPLI & al. 2017) was used to delimit CO1 clades; after comparison with other results, these clades were treated either as intraspecific entities or species. For AFLP data, BAPS (CORANDER & al. 2008) clusters (MALLET 1995) with the highest marginal likelihood were considered either as intraspecific entities or as species, depending on morphological findings. Male genital morphology was qualitatively scanned for distinct trait differences; delimitable morphometric entities were considered to confirm or reject DNA-based species hypotheses. For morphometric species delimitation, Nest-Centroid clustering (SEIFERT & al. 2014b) was used; discordance rates between Nest-Centroid-clustering-based and DNA-based species hypotheses were calculated by pairwise comparisons of species; discordance rates < 5% of nests were accepted and considered to confirm DNA-based species hypotheses. Discordances between results of different data types required evolutionary explanations. Finally, operational taxonomic units were linked to type material and nomenclatural consequences drawn.

Sample: Material of the *Tetramorium caespitum* complex was collected from 31 nations in Europe and – to a lesser extent – from Asia and the Americas mainly between 1992 and 2015, resulting in more than 2400 nest samples. The material was stored at -20 °C in 96% ethanol at the Institute of Ecology, University of Innsbruck, Austria (Tab. S1, as digital supplementary material to this article, at the journal's web pages). Material outside the *T. caespitum* complex was used to delimit the species com-

plex within the *T. caespitum* group sensu BOLTON (1995) (see Taxonomy, Diagnosis of the *T. caespitum* complex). Only species of the *T. caespitum* complex occurring in Europe were considered for detailed analyses. First, a 1113-bp stretch of the CO1 gene of a worker of 1391 nests originating from all relevant biogeographical regions was sequenced (partly published in SCHLICK-STEINER & al. 2006, STEINER & al. 2010, CSŐSZ & al. 2014b, and KINZNER & al. 2015). Incomplete CO1 sequences were not used for phylogenetic reconstruction but for distribution maps whenever assignment to a CO1 clade was possible. The rationale for investigating samples under further, ideally all, disciplines was to representatively sample HT diversity and geographic distribution of CO1 clades. Material of 476, 96, 468, 245, and 81 nests was used for AFLP, male genital morphology, worker TM, worker GM, and gyne GM, respectively. Additionally to this material, for distribution maps and calculation of thermal niches, also data published by SCHLICK-STEINER & al. (2006), NEUMEYER (2008), WAGNER (2009, 2011a, b, 2012), STEINER & al. (2010), WAGNER & al. (2010, 2016), BRAČKO & al. (2014), and CSŐSZ & al. (2014b) were used, providing that the species determinations were plausible.

PCR amplification and sequencing of the CO1 gene:

Total genomic DNA of the gasters of one to two workers per nest was extracted with the GenElute Mammalian DNA Extraction Kit (Sigma, St. Louis, USA) following the instructions of the manufacturer. A 1280 bp fragment of the CO1 gene was amplified using the primers COI1f (5'-CCC CCC TCT ATT AGA TTA TTA TT-3'; STEINER & al. 2005) and UEA10 (5'-TCC AAT GCA CTA ATC TGC CAT ATT A-3'; LUNT & al. 1996). Standard PCR was performed using 1 × MyTaq buffer (Bioline, UK), 200 nM of each primer, 0.25 U MyTaq DNA polymerase (Bioline), 0.3% Bovine Serum Albumin (Roche, Switzerland), and ca. 50 ng template DNA in a total volume of 10 µl. When the standard PCR failed, reactions were repeated using 1 × RotorGene Probe PCR Master Mix (Qiagen, Germany), 100 nM of each primer, and ca. 50 ng template DNA in a total volume of 10 µl. Reactions were carried out on a UnoCycler (VWR, USA) with an initial denaturation at 95 °C for 3 min, followed by 35 cycles of 95 °C for 30 s, 48 °C for 45 s, and 72 °C for 2 min, and 10 min of final extension at 72 °C. PCR products were purified by incubation with 2 U Exonuclease I and 0.1 U FastAP (both Thermo Scientific, USA) at 37 °C for 15 min, followed by an inactivation step at 80 °C for 15 min. Purified PCR products were Sanger sequenced by a commercial sequencing facility (Eurofins MWG Operon, Germany) using both amplification primers. To eliminate PCR errors, sequences revealing singleton HTs were verified with an independent PCR.

CO1 alignment and nuclear mitochondrial sequences

(NUMT) detection: Sequences were aligned with the ClustalW algorithm implemented in MEGA5.05 (TAMURA & al. 2011) using default settings. A four-step workflow to detect nuclear copies of mtDNA (NUMTs; see SONG & al. 2008) was applied: (I) Electropherograms were checked for double peaks, translated, and controlled for correct amino acid sequence and premature stop codons. (II) A mitochondrial DNA enrichment protocol (TAMURA & AOTSUKA 1988) was used to check samples of 14 CO1 clades of which nests with > 15 workers were available.

(III) RNA of the nests 18538 (HT225) and 18535 (HT439), both stored in RNAlater (Qiagen) and belonging to CO1 clade U2 sensu SCHLICK-STEINER & al. (2006), was isolated using the Nucleospin RNA Kit (Macherey Nagel, Düren, Germany). Complementary DNA was synthesized with the RevertAid First Strand cDNA Synthesis Kit (Thermo Scientific) following the manufacturer's instructions and using the primer COI1f. The complementary DNA was amplified with the primers COI1f and neg0R, 5'-CCT CTT TCA TTT ATA ATA ATA TG-3'. (IV) Based on the CO1 polyphyly within *Tetramorium caespitum* (see results), we hypothesized that the Iberian nests of clade D sensu SCHLICK-STEINER & al. (2006), henceforth D_w, might have amplified NUMTs. As CO1 clade U2 (belonging to *T. caespitum* according to our final species hypotheses) occurs in the geographic area neighboring the samples of D_w and likewise belongs to *T. caespitum*, a forward-primer specific for the CO1 clade U2, u2_spec_f, 5'-TCA CTC GGA ATA ATT TAC GCC-3', was developed. Since some nests of CO1 clade D_w were morphometrically similar to and geographically overlapped with *T. impurum*, we developed also a CO1 forward-primer specific for *T. impurum*, imp2_spec_f, 5'-TAC AGC AAT TCT CCT TCT CC-3'. Extracts of all 23 D_w-nests were amplified using these forward primers and UEA10 using Rotor-Gene Probe PCR Master Mix as described in Section PCR amplification and sequencing of the CO1 gene. Only CO1 HTs without suspicious results in any of these four steps were used for the phylogenetic reconstruction; other sequences were considered as potential NUMTs and thus excluded. Sequences of new CO1 HTs and NUMTs were deposited in GenBank (Tab. S1).

Phylogenetic reconstruction and species delimitation

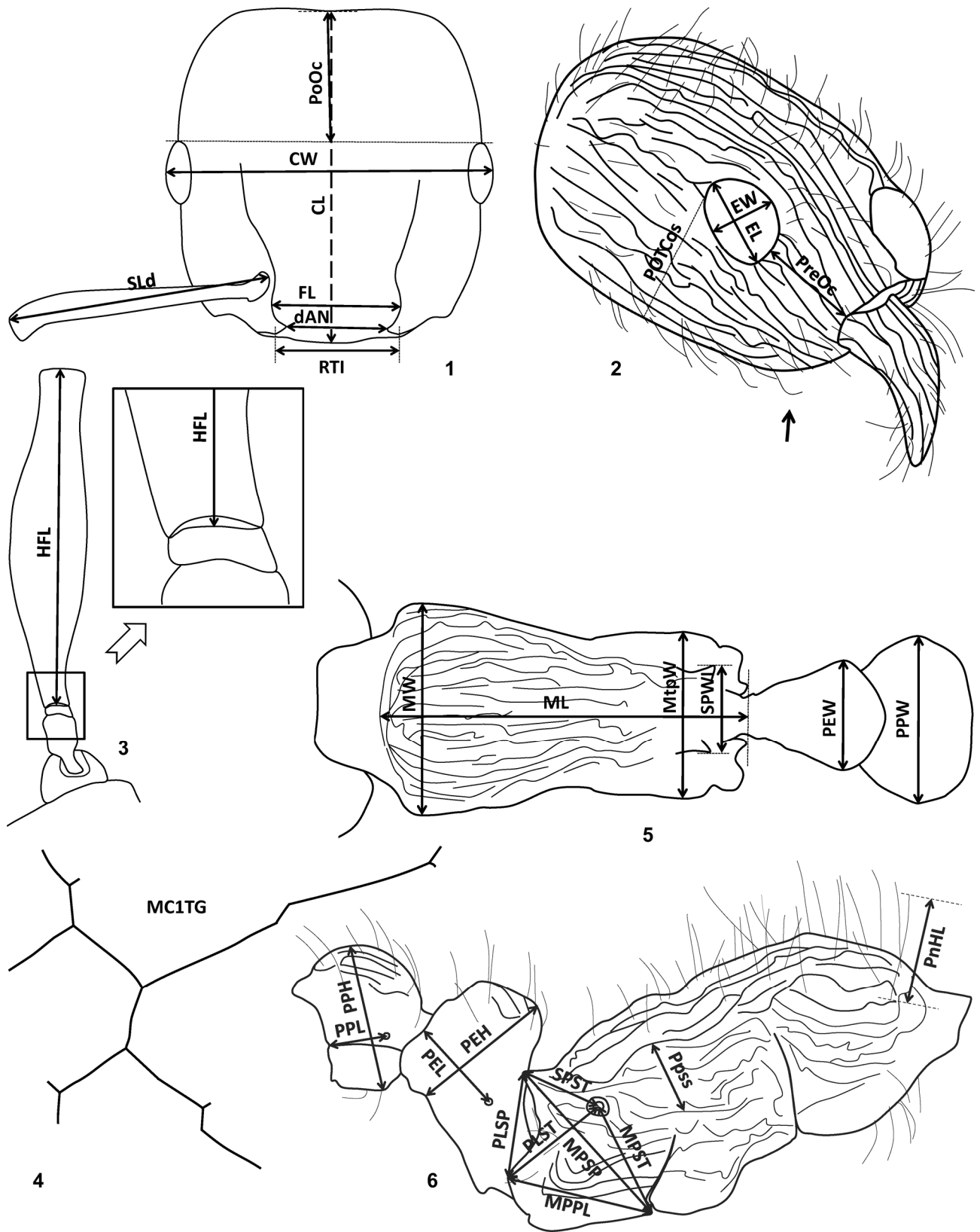
using CO1: For phylogenetic reconstruction, every HT was used only once. *Tetramorium capitale* (MCAREAVEY, 1949) (GenBank accession AY641664) was chosen as outgroup. For model selection, PartitionFinder v1.1.1 (LANFEAR & al. 2012) was used. TrN + G + I, F81, and GTR + G were suggested for codon positions 1, 2, and 3, respectively. These best-fit partitioning schemes were used for the Maximum-Likelihood (ML) tree reconstruction in Garli v2.0 (ZWICKL 2006). Phylogenetic trees were also reconstructed using a Bayesian approach (MrBayes v3.2.0; RONQUIST & al. 2012). Here, the alignment was partitioned into three codon positions as suggested by PartitionFinder. Two parallel runs, each consisting of four chains, were iterated for 8×10^6 generations using the algorithm "mixed". The first 25% were discarded as burn-in. The final average standard deviation of split frequencies was still above 0.01 (0.0144). Additional runs using 15×10^6 and 30×10^6 generations did not improve the standard deviation of split frequencies values (data not shown). Convergence of model parameters was checked using Tracer v1.6 (RAMBAUT & al. 2014). After resolving polytomies, the resulting tree was used for species delimitation based on the multi-rate Poisson Tree Processes method (KAPLI & al. 2017) excluding the outgroup.

Amplified fragment-length polymorphism (AFLP):

DNA of 508 *Tetramorium* workers (476 of the *T. caespitum* complex) was used for AFLP genotyping following a modified protocol of VOS & al. (1995), described in detail in WACHTER & al. (2012). Briefly, digestion was performed with the enzymes EcoRI and MseI; AFLP ad-

Tab. 1: Acronyms and definitions of the worker traditional morphometrics characters. For illustrations, see Figures 1 - 6.

Acronym	Definition
CL	Maximum cephalic length in median line (Fig. 1); head is carefully tilted to position with true maximum; excavations of occiput and / or clypeus reduce CL. Peaks due to sculpture are ignored and only valleys are considered.
CS	Arithmetic mean of CL and CW.
CW	Maximum cephalic width across eyes (Fig. 1).
dAN	Minimum distance between antennal fossae (Fig. 1); measured in dorsofrontal view.
EL	Maximum diameter of one eye. All structurally defined ommatidia, pigmented or not, are included (Fig. 2).
EW	Minimum diameter of one eye. All structurally defined ommatidia, pigmented or not, are included (Fig. 2).
EYE	Arithmetic mean of EL and EW.
FL	Maximum distance between external margins of frontal lobes (Fig. 1). If this distance is not defined because frontal carinae constantly converge frontad, FL is measured at FRS level (definition of FRS see SEIFERT 2003) as distance between the outer margins of frontal carinae.
HFL	Length of hind femur in dorsal view (Fig. 3). Second trochanter, which could appear to be portion of femur, must not be mistakenly included.
MC1TG	Quantification of stickman-like or reticulate microsculpture units on base of 1 st gastral tergite (use > 150 × magnification; Fig. 4): Number of connected lines building units and being separated by line intersections and by flections angled > 10° is counted. Also very short lines are full counts. Arithmetic means of at least three units per worker are taken.
ML	Mesosoma length measured in dorsal view from caudalmost portion of propodeum to dorsofrontal corner of pronotal slope (i.e., where coarsely structured dorsal shield meets finely structured pronotal neck; Fig. 5); equivalent measuring also possible in lateral view.
MPPL	Distance between most anteroventral point of metapleuron and most dorsocaudal point of propodeal lobe in lateral view (Fig. 6). If there are two points coming into question to be dorsocaudalmost point on propodeal lobe, the one which is provided with a carina is taken.
MPSP	Distance between most anteroventral point of lateral metapleuron and distalmost point of propodeal spine (it does not need to be uppermost point of spine; Fig. 6).
MPST	Distance between most anteroventral point of metapleuron and center of propodeal stigma (Fig. 6).
MtpW	Maximum metapleuron width measured in dorsal view (Fig. 5). (In most cases, maximum is at caudal and in few cases at central or frontal region of metapleuron.)
MW	Maximum mesosoma width (Fig. 5).
PEH	Petiole height. Measured from uppermost point of concave ventral margin to node top (Fig. 6).
PEL	Petiole length. Measured in lateral view from center of petiolar stigma to caudal margin of petiole (both measuring points on same focal level; Fig. 6).
PEW	Maximum petiole width (Fig. 5).
PLSP	Distance between most dorsocaudal point of propodeal lobe (if there are two points coming into question to be dorsocaudalmost point of propodeal lobe, the one which is provided with a carina is taken) and distalmost point of propodeal spine (it does not need to be uppermost point of spine; Fig. 6).
PLST	Distance between most dorsocaudal point of propodeal lobe and center of propodeal stigma (Fig. 6).
PnHL	Length of hair at frontolateral corner of pronotum (Fig. 6). Take longest hair of both sides.
PoOc	Postocular distance. Using cross-scaled ocular micrometer, head is adjusted to measuring position of CL; caudal measuring point: median posterior margin of head, microsculpture peaks are ignored and valleys are considered; frontal measuring point: median head crossing line between posterior eye margins (Fig. 1).
POTCos	Number of postoculo-temporal costae and costulae (Fig. 2). With head in lateral view and longitudinal axis of head adjusted horizontally, counted by focussing along perpendicular line from caudalmost point of eye down to underside of head. Costae / costulae just touching measuring line are counted as 0.5, those positioned just at ventral margin of head silhouette are not counted. Arithmetic mean of both sides.
PPH	Maximum postpetiole height (Fig. 6).
PPL	Postpetiole length; distance from center of postpetiolar stigma to caudalmost intersection point of tergite and sternite (both measuring points at same focal level; Fig. 6).
Ppss	Maximum height of smooth and shiny area on lateral side of propodeum (Fig. 6). This area is brought into visual plane; a line is positioned perpendicular to main costae on propodeum and maximum height of smooth and shiny area without any costulae and costae is measured. Take arithmetic means of both sides.
PPW	Maximum postpetiole width (Fig. 5).
PreOc	Preocular distance in lateral view. Measured as minimum distance between anterior eye margin and sharp frontal margin of gena (Fig. 2).
RTI	Distance between tops of ridges between antennal fossae and clypeus (Fig. 1). Tops are defined as dorsofrontalmost points of ridges, provided with a costa on clypeus. Measured in dorsoanterior view.
SLd	Maximum scape length, including scape lobe, excluding articular condyle (Fig. 1).
SPST	Distance between distalmost point of propodeal spine (it does not need to be uppermost point of spine) and center of propodeal stigma (Fig. 6).
SPWI	Maximum distance between outer margins of propodeal spines (Fig. 5). Measured in dorsoanterior view.



Figs. 1 - 6: Measurement lines for the morphometric characters: (1) CL, CW, dAN, FL, PoOc, RTI, and SLd; (2) EL, EW, and PreOc; including an artificial line for the meristic character POTCos, as well as a hind for the position of c-shaped, crinkly, or sinuous hairs (arrow); (3) HFL; (4) Meristic character MC1TG. In this example, MC1TG = 18; (5): ML, MtpW, MW, PEW, PPW, and SPWL; (6) MPPL, MPSP, MPST, PEH, PEL, PLSP, PLST, PnHL, PPH, PPL, Ppss, and SPST.

aptors were ligated simultaneously. Preselective amplification was carried out with the primers Eco-N and Mse-C. Selective amplification was performed using the five primer combinations tEco-AA / Mse-CAA, tEco-AA / Mse-CTA, tEco-AA / Mse-CTT, tEco-AC / Mse-CTA, and tEco-TG / Mse-CTA incorporating FAM / NED / PET labels by an M13-tail method. Plate position of samples was chosen randomly. As quality control, two kinds of replicas were used: (I) Preselective amplicon of four workers was included on each 96-well plate used in the selective PCR ("fixed replicas"). (II) DNA of eight randomly chosen workers per plate was replicated on another position of the same plate already in the digestion-ligation-step ("pairwise replicas"). Capillary electrophoresis was performed by a commercial sequencing facility (Comprehensive Cancer Center DNA Sequencing & Genotyping Facility, University of Chicago, USA) on an ABI 3730 sequencer (Applied Biosystems). Trace files were converted to comma separated tables using PeakScanner v1.0 (Applied Biosystems) and scored automatically using optiFLP v1.54 (ARTHOFER & al. 2011) with the same parameter space as in ARTHOFER & al. (2013: tab. 1). The quality of individual AFLP profiles was assessed in tinyFLP v1.40 (ARTHOFER 2010). Profiles falling into the 10th percentile of peak count in more than one primer set were considered of low quality and excluded from further analysis. For each primer set, a Neighbor Joining (NJ) tree was constructed with optiFLP, and tree topologies were compared as done by DEJACO & al. (2016); samples grouping into more than three NJ clades were excluded.

Bayesian clustering was performed using BAPS v5.3 (CORANDER & al. 2008). First, the "clustering of individuals" option was executed with $K = [1; 30]$ and all other parameters in default. The results were pipelined into the clustering-based admixture analysis using minimum population size = 3, 500 iterations, 50 reference individuals, and 50 iterations for reference individuals.

Male genital morphology: We qualitatively investigated male genital morphology of 96 males (Tab. S1). Mounted genitals were used for z-stack imaging with a Z6 APO macroscope (Leica, Wetzlar, Germany) providing a magnification of 72 ×, a Leica DFC 420 camera, and Leica Application Suite v3.6. Final images were composed with Helicon Focus v5.1 (Helicon Soft Ltd., Charkow, Ukraine). Representative images were used to draw anatomical figures (Fig. S1, as digital supplementary material to this article, at the journal's web pages). Terminology of the considered structure, the parameres, follows COLLINGWOOD (1979). Interspecific differences of male genital morphology allowed a qualitative assessment in most cases.

Traditional morphometrics (TM) of workers: Dissected gasters of workers were used for DNA extraction; the degastered bodies were mounted for morphometric analyses. Measurements were made using a Leica M165 C high-performance stereomicroscope with magnifications of 120 - 360 ×. Workers were positioned on a pin-holding stage permitting spatial adjustment in all directions. Measurements always referred to cuticular surface and not pubescence surface. A cross-scaled ocular micrometer with 120 graduation marks ranging over 52% of the visual field was used. Its measuring line was continuously kept in vertical position to avoid parallax error (SEIFERT 2002). A Schott KL 1500 LCD cold-light source equipped with two

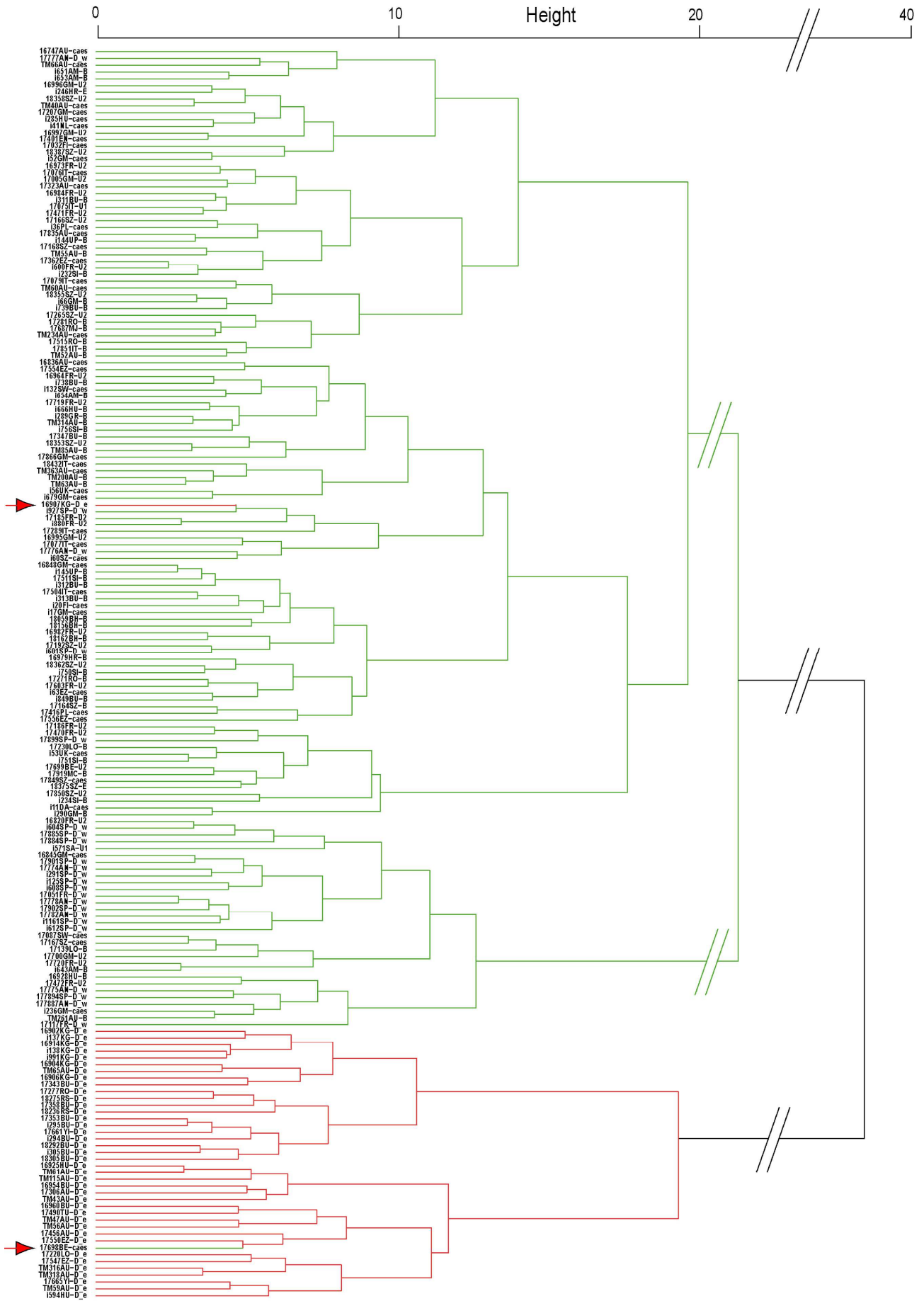
flexible light ducts combined with a Leica coaxial polarized-light illuminator was used.

Morphometric data of 968 workers from 468 nests were collected (on average, 2.1 workers per nest). For 459 and 237 of these individuals also CO1 and AFLP data, respectively, were available (min. one worker per nest). We defined 33 characters (Tab. 1; Figs. 1 - 6); 26 of them followed STEINER & al. (2006), SEIFERT (2007), and CSÖSZ & al. (2014b), and seven (dAN, HFL, MC1TG, MtpW, PPL, Ppss) were new. Twenty-nine characters were collected morphometrically, MC1TG and POTCos meristically; CS and EYE were arithmetic means of other characters.

Nest-Centroid clustering (SEIFERT & al. 2014b) was used as unsupervised approach to establish morphological species hypotheses independent from genetic data using R v3.0.1 and the packages MASS, ecodist, cluster, plyr, stringr, and scatterplot3d (R DEVELOPMENT CORE TEAM 2012). The hierarchical Nest-Centroid-Ward clustering was run first to build a species hypothesis. Afterwards, non-hierarchical Nest-Centroid-K-means clustering was performed with the number of classes suggested by Nest-Centroid-Ward. For a final evaluation, to minimize the number of mismatches, only pairwise species comparisons were used (Fig. 7). To assign samples to species pairs, the DNA-based species hypotheses were followed, that is in most cases, the AFLP results. Since AFLP data of ten small CO1 clades containing one or two HTs were missing, we usually assigned them to neighboring clades if no conflict with other disciplines was obvious. In doing so, we aimed to avoid oversplitting. In CO1 clade I (= *Tetramorium breviscapus*, see Results and discussion) only, the clade itself represented the DNA-based species hypotheses due to obvious morphologic differences of neighboring clades. Nests concordantly classified by Nest-Centroid-Ward and Nest-Centroid-K-means were fixed as either hypothesis "1" or "2", while discordantly classified nests were used as wild cards ("0"). The species hypotheses formed by this procedure were used in confirmative linear discriminant analyses (LDA) on the level of workers using the method "stepwise selection" in selecting characters, performed with the software package SPSS Statistics v21 (IBM, USA) as follows: In a first step, following SEIFERT & al. (2014b), consistently classified nests and wild cards of Nest-Centroid-Ward and Nest-Centroid-K-means with $P > 0.66$ belonging to either hypothesis "1" or "2" were fixed as new calibration set, while all cases with $P \leq 0.66$ were set as wild cards. In a second LDA, cases with $P > 0.58$ were hypothesis-fixed, in a third LDA also cases > 0.5 , so that finally no unassigned case remained. Then, species-pair-wise discordance rates between the Nest-Centroid-clustering-based hypotheses and the DNA-based species hypotheses were calculated.

Geometric morphometrics (GM) of workers and gynes: In 485 workers, we analyzed two-dimensional im-

Fig. 7: Example of Nest-Centroid clustering: CO1 clades *caespitum*, B, U1, U2, and D_w (= *Tetramorium caespitum*) build the upper Nest-Centroid cluster (green), D_e (= *T. staercke* sp.rev.) the lower one (red). One nest of each hypothesized species with discordance between DNA-based and Nest-Centroid-clustering-based species-hypotheses (see arrows).



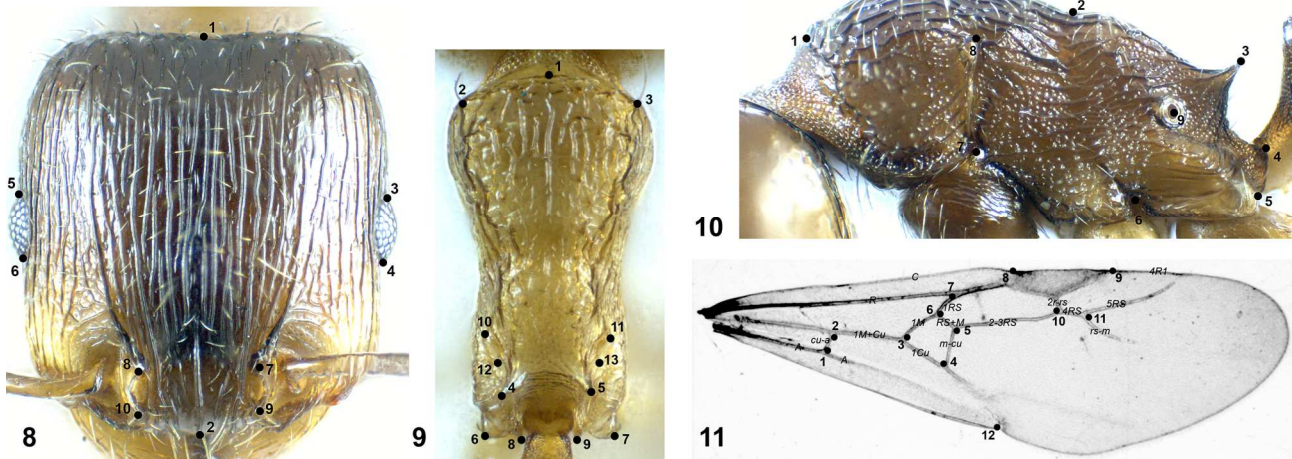


Fig. 8: Position of landmarks on head, frontal view. (1) Median point of posterior margin of head; (2) anteromedian point of clypeus; (3, 5) caudal margins of eyes; (4, 6) frontal margins of eyes; (7, 8) deepest points of antennal fossae; (9, 10) fusion points of margins of frontal lobe and anterior ridges of antennal fossae.

Fig. 9: Position of landmarks on mesosoma, dorsal view. (1) Dorsofrontal corner of pronotal slope (i.e., where coarsely structured dorsal shield meets finely structured pronotal neck); (2, 3) bases of setae frontolateral corners of pronotum; (4, 5) tips of propodeal spines; (6, 7) posterior tips of metapleural glands; (8, 9) posterior tips of propodeal lobes; (10, 11) anterior margins of propodeal spiracles (including wall); (12, 13) posterior margins of propodeal spiracles (including wall).

Fig. 10: Position of landmarks on mesosoma, lateral view. (1) Dorsofrontal corner of pronotal slope (i.e., where coarsely structured dorsal shield meets finely structured pronotal neck); (2) dorsal depression at border of mesonotum and propodeum; (3) tip of propodeal spine; (4) dorsocaudal extreme of propodeal lobe; (5) meeting point of posterior margins of propodeal lobe and metapleural gland opening; (6) ventral notch between metapleuron and mesopleuron; (7) ventral opening of the suture between pronotum and anepisternite; (8) fusing of pronotum, mesonotum and anepisternite (i.e., point where the suture between pronotum and anepisternite is crossed by the first horizontal rugae); (9) center of propodeal spiracle.

Fig. 11: Position of landmarks on gyne forewings. (1) Junction of *cu-a* and *A*, distal edge; (2) junction of *cu-a* and *IM + Cu*, distal edge; (3) junction of *IM* and *1Cu*, distal edge; (4) junction of *m-cu* and *1Cu*, basal edge; (5) junction of *m-cu* and *2-3RS*, distal edge; (6) junction of *RS + M* and *IRS*, distal edge; (7) junction of *R* and *IRS*, basal edge; (8) junction of *C* and pterostigma; (9) junction of pterostigma and *4R₁*; (10) junction of *2r-rs* and *2-3RS*, basal edge; (11) junction of *4RS* and *rs-m*, distal edge; (12) notch of anal fold.

ages of head in frontal view (Fig. 8), mesosoma in dorsal view (Fig. 9), and mesosoma in lateral view (Fig. 10). Pinned dried specimens were put in identical positions using a goniometer. Approximately 15 - 20 images were taken in different focal planes (distance 10 - 20 μm) with a Leica DFC420 camera attached to a Leica Z6 APO microscope. Images were stacked using the software Helicon Focus v5.1. In frontal view of the head, the focus was on the frontal ridge of the antennal fossa. Then the head was tilted until the posterior margin was maximum focused (at ergotubus magnification of 2.0). Lateral orientation was achieved by adjusting the frontal ridge of the eyes in one focal plane (at ergotubus magnification of 3.6; Fig. 8). Mesosoma was adjusted in dorsal view with two anterior and two posterior reference points in focal plane (i.e., at same horizontal level). The anterior reference points were the bases of setae on the frontolateral corners of pronotum. The posterior reference was the horizontal portion of the upper margin of propodeal lobes just before they ascend to subspinal excavation (rough adjustment at ergotubus magnification of 2.0, fine adjustment at ergotubus magnification of 3.6) (Fig. 9). Mesosoma was adjusted in lateral view with the tips of the propodeal spines exactly super-imposed (Fig. 10).

Shape variation of the forewings was analyzed in 148 gynes (Fig. 11). To allow analyses of directional and fluctuating asymmetry, both forewings were detached from the specimen and placed between slides. One of the wings (when available, the right one) was photographed from the dorsal and ventral side, the other only from the dorsal side. To reduce measurement error, Procrustes coordinates across replicates were averaged. Otherwise, the technical procedure and equipment were the same as for workers.

We used tpsDig2 v2.22 (ROHLF 2015) to digitize landmarks: 10 landmarks in head frontal (Fig. 8), 13 in mesosoma dorsal (Fig. 9), 9 in mesosoma lateral (Fig. 10), and 12 in gyne wings (Fig. 11). The nomenclature of veins follows PERFILIEVA (2015). If not indicated otherwise, Procrustes superimposition and all subsequent analyses were performed with MorphoJ v1.06d (KLINGENBERG 2011). Head frontal and mesosoma dorsal were symmetric structures; corresponding landmarks were set at both sides of the symmetry axis and analyzed with the methods of object symmetry (KLINGENBERG & al. 2002). Only the symmetric component of variation was used in the downstream analyses.

For error assessment of the worker dataset, we took two images of mesosoma lateral per specimen in a sample

of 32 workers (16 from each of two putative species, *Tetramorium alpestre* and *T. immigrans*) and digitized the landmarks twice. Procrustes ANOVA (KLINGENBERG & al. 2002) was used to quantify the measurement error in relation to biological factors as follows: As the imaging error was 1.54 times greater than the digitizing error, and variation among individuals was 11.37 times greater than imaging error (Tab. S2), measurement error was considered negligible. Similarly, Procrustes ANOVA of the gyne forewing dataset showed that the most subtle biological aspect, that is, fluctuating asymmetry, was > 5 times greater than the error from imaging the wings from dorsal and ventral side (Tab. S3).

The datasets of the workers were significantly affected by allometry. Centroid size accounted for 5.8%, 4.4%, and 3.4% of the shape variation in head frontal, mesosoma lateral and mesosoma dorsal, respectively (multivariate regression of shape on size, all $p < 0.001$). To correct for allometric effects, regression residuals were used subsequently. Since allometries may differ across species, pooled within-group regression for specific size corrections was used. Allometry was not significant in gyne forewings (1.1% predicted, $p = 0.11$).

A combination of relative warp analysis and LDA was used (following BAGHERIAN YAZDI & al. 2012) to compare the performance of GM with TM in cryptic species delineation. Relative warps (with no weighting with respect to bending energy) were calculated as principal components of Procrustes coordinates (gyne wings) or regression residuals of Procrustes coordinates (head frontal, mesosoma dorsal, mesosoma lateral). The relative warps of the three datasets of the workers were combined in a single matrix (cf. BAGHERIAN YAZDI & al. 2012). This matrix was the input for unsupervised Nest-Centroid clustering (SEIFERT & al. 2014b), as described for TM. The dataset of the gyne wings was analyzed separately.

Reanalyzed linear discriminant analysis (LDA) of morphometric data: After development of final species hypotheses by the integrative-taxonomy approach, all nests were reanalyzed in a supervised approach using the same data as for Nest-Centroid clustering of worker TM, worker GM, and gyne GM. SPSS Statistics v21 was used to perform the LDAs. To avoid overfitting, the number of individuals of each group had to be at least three times larger than the number of characters (MODER & al. 2007 and references therein).

Thermal niches: Standard air temperature (TAS) in °C of sampling sites two meters above ground were used as a rough approximation of ecological niche (STEINER & al. 2010, SEIFERT & al. 2014a). Following SEIFERT & PANNIER (2007), TAS was calculated as mean air temperature from 1 May to 31 August of the nearest three meteorological stations of the years 1961 to 1990 provided by Klimaabteilung der Zentralanstalt für Meteorologie und Geodynamik (1996). Values were corrected for an altitudinal temperature decrease of 0.661 °C per 100 m: $TAS = -0.694 * LAT + 0.078 * LON - 0.00661 * ALT + 52.20$, where LAT = latitude, LON = longitude, and ALT = altitude. TAS was not used in an unsupervised approach for species delimitation but to explore ecological differences in reanalyses. TAS values were tested for species-specific differences using SPSS Statistics v21.

Type material: Since type material of the following

six taxa could not be excluded from conspecificity with European species of the *Tetramorium caespitum* complex based on qualitative morphological and geographical arguments (details in Taxonomy), it was investigated morphometrically: *T. caespitum* var. *immigrans* SANTSCHI, 1927; *T. semilaeve* var. *kutteri* SANTSCHI, 1927; *T. staerckei* KRATOCHVÍL, 1944; *T. caespitum* var. *fusciclava* CONSANI & ZANGHERI, 1952; *T. goniommoide* POLDI, 1979; *T. pelagium* MEI, 1995. After species delimitation, worker types belonging to the *T. caespitum* complex were set as wild cards in an LDA including all morphometric data of the complex.

Results and discussion

Cytochrome C oxidase subunit I (CO1) gene: Sequences of 1257 nests yielded complete data, that is, 1113 bp. Furthermore, sequences of 134 nests contained missing data but allowed assignment to CO1 clades. All 189 singleton HTs were confirmed by sequencing an independent PCR reaction. Our four-step NUMT check led to the interpretation that three of 386 HTs, that is, HT36, HT330, and HT388, were NUMTs. In detail, (I) reviewing electropherograms, we found distinct double peaks in three cases: Firstly, in HT36, belonging to CO1 clade D_w and already published by SCHLICK-STEINER & al. (2006). In this study, HT36 contained overlaid peaks with HTs of CO1 clade *impurum_w* six times (for species affiliation of CO1 clades, see Figs. 12 - 14). Secondly, HT330 contained overlaid peaks identical with HT52 of clade B sensu SCHLICK-STEINER & al. (2006). Thirdly, HT388 contained overlaid peaks of *impurum_e* (Tab. S1). (II) After mitochondrial-DNA enrichment, electropherograms showed a relative decrease of peaks belonging to HT36, HT330, and HT388 as well as a relative prominence of those belonging to *impurum_w*, B, and *impurum_e* sequences. In contrast, there was no change in electropherograms of CO1 clades *alpestre*, *caespitum*, *indocile*, B, D_e, E, H, I, J, U5, and two remaining nests of D_w. (III) The complementary-DNA PCR of workers from nests 18535 and 18538 (Tab. S1), belonging to CO1 clade U2 (= *T. caespitum* in final species hypotheses), showed identical HTs as the standard PCR, that is, HT439 and HT225, respectively. (IV) The use of U2 and *impurum_w* specific primers on all extracts of D_w samples yielded neither U2 nor *impurum_w* sequences. Summarizing these results, we found evidence in the first and second step of our assessment that HT36 (D_w), HT330, and HT388 are NUMTs, and no indication for further NUMTs in the other steps. Hence, the alignment comprised 383 HTs. While two NUMTs represent only HTs of their clades, HT36 is a NUMT clustering basal in the CO1 clade D_w. Sequences retrieved from the same nests resembled HT36 when whole DNA was extracted but five other HTs when extracts enriched for mitochondrial DNA were used. This finding is in line with the higher mutation rate of mitochondrial DNA compared with NUMTs, and HT36 can be seen as an ancestral state from which the current diversity of mitochondrial DNA in D_w evolved (LOPEZ & al. 1997, HAAG-LIAUTARD & al. 2008, HAZKANI-COVO & al. 2010).

Multi-rate Poisson Tree Processes yielded 30 CO1 clades (Figs. 12, 14; for details, see Tabs. S1, S4); compared with other established tree-based delimitation methods, multi-rate Poisson Tree Processes seems to be less

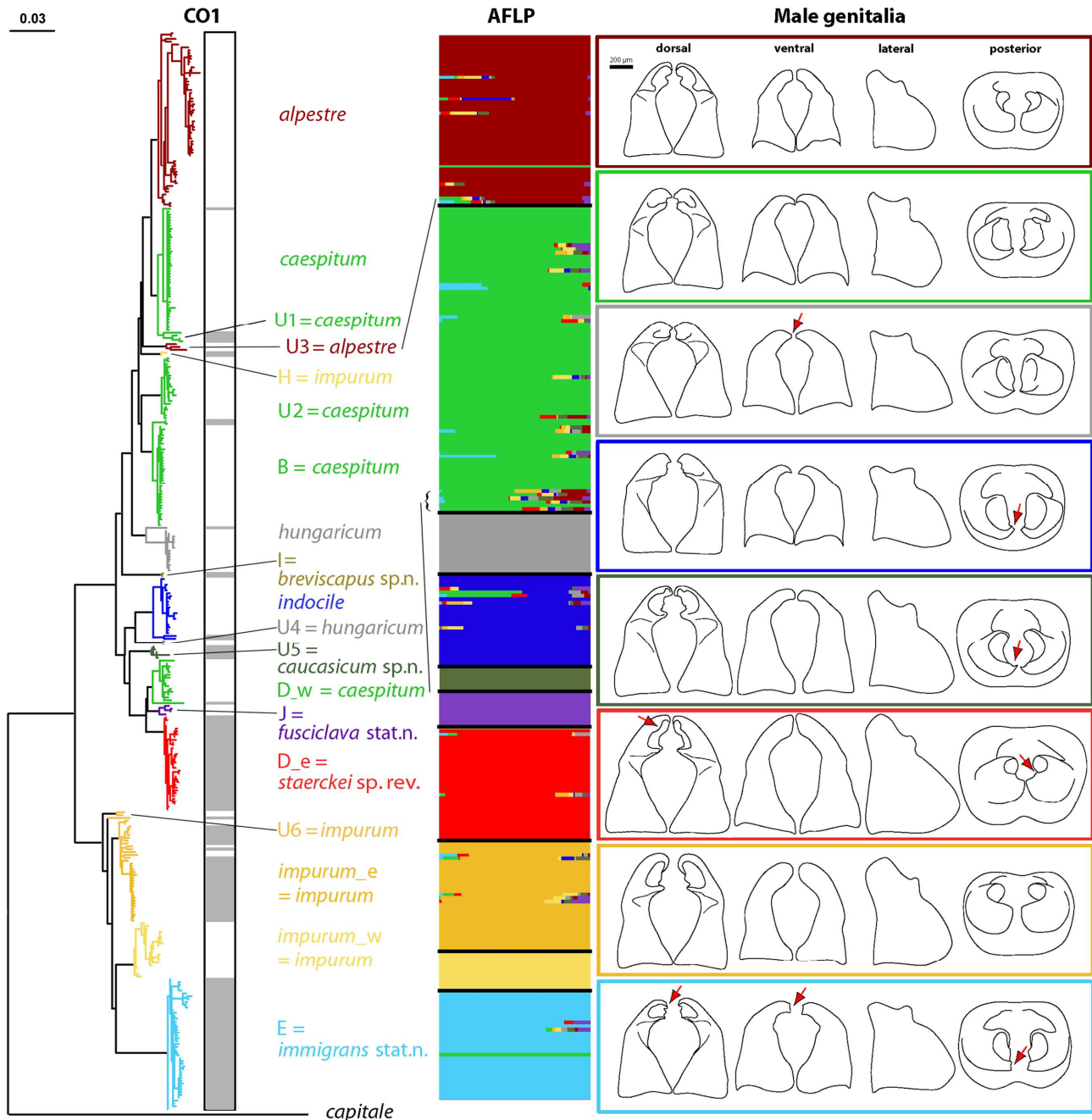


Fig. 12: Cytochrome C oxidase subunit I gene (CO1) phylogeny and species estimation using multi-rate Poisson Tree Processes (30 white and grey bars), amplified fragment-length polymorphism BAPS clusters, and male genital morphology of species. Labels refer to former entity names (SCHLICK-STEINER & al. 2006, STEINER & al. 2010, CSŐSZ & al. 2014b) and entities first delimited here (I, J, H, *impurum_e*, *impurum_w*) as well as final species hypotheses newly established here following equal signs. The final species hypotheses drawn here match in color those of Figures 7, 13, and 14. AFLP data for I = *breviscapus* sp.n. as well as male genital data for I = *T. breviscapus* sp.n. and J = *T. fusciclava* stat.n. are not available.

prone to oversplitting (also in the present case; data not shown) but, in such cases of clades consisting of very few HTs, still seems to tend towards it. Most of these clades were already recovered by SCHLICK-STEINER & al. (2006). However, four CO1 clades are new (H, I, J, and *impurum_w*), and twelve small clades consisting of one or two

HTs (*caespitum2*, B2, D_w1, D_w2, *indocile2*, *hungaricum2*, *impurum_e2* - e7) were split off other clades. Since the latter represent no taxonomic units based on the integrative taxonomic approach (see Integrative-taxonomy approach), we mostly treat these twelve clades under their earlier, more inclusive clade names.

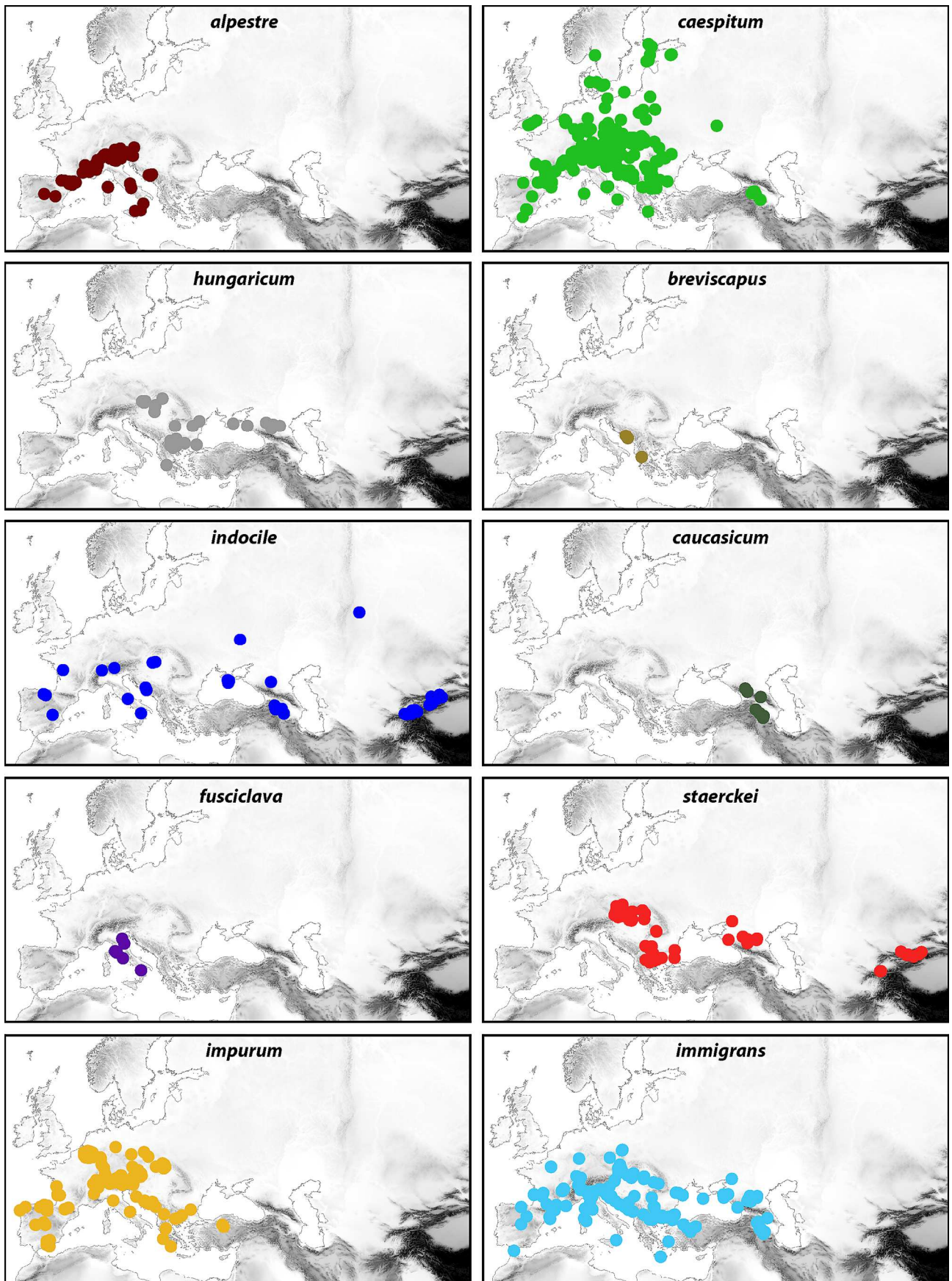


Fig. 13: Geographic distribution of *Tetramorium alpestre*, *T. caespitum*, *T. hungaricum*, *T. breviscapus* sp.n., *T. indocile*, *T. caucasicum* sp.n., *T. fusciclava* stat.n., *T. staerckei* sp.rev., *T. impurum*, and *T. immigrans* stat.n.

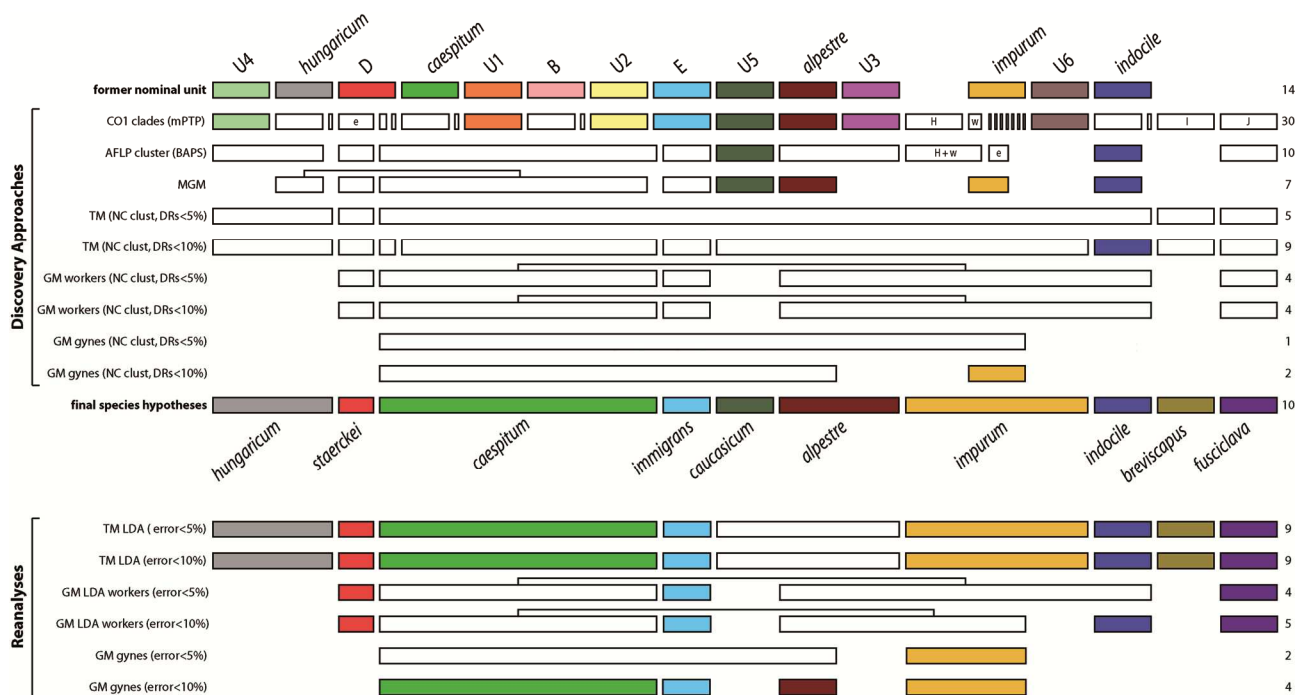


Fig. 14: Summarized results from all discovery approaches and reanalyses after evolutionary interpretation and delimitation of final species hypotheses. Former entity names are shown atop; filled color bars in the unsupervised discovery approaches reflect results matching the former entity limits. Blank bars reflect different groupings; also blank bars connected with lines group together. Final species hypotheses drawn from our integrative-taxonomy approach are shown underneath in colored bars matching colors in Figures 7, 12 and 13. Supervised reanalyses are illustrated below; filled color bars reflect significant and blank bars nonsignificant results. Numbers of species delimited based on a data source are to the right.

Amplified fragment-length polymorphism (AFLP): After quality checks, 269 workers profiles remained. These belonged to 20 of the 30 CO1 clades; for ten clades, each consisting of one or two HTs (Tab. S4), no AFLP data were available. After concatenation of the five primer sets, the final binary matrix contained 890 loci. BAPS identified ten well-separated AFLP clusters (Fig. 12; Tab. S5). Several instances of mitochondrial-nuclear discordance were found, which are discussed under Integrative-taxonomy approach.

Male genital morphology: We found two different basic forms of paramere structure (for specific details of male genital morphology, see Taxonomy, Treatment of species and Key to males of the *Tetramorium caespitum* complex), the *impurum*-like form (incl. AFLP clusters *alpestre*, U5, D_e, *impurum_e*, and *impurum_w*; for species affiliation of CO1 clades, see Figs. 12 - 14) and the *caespitum*-like form (incl. AFLP clusters *caespitum* (incl. U1, U2, B, and D_w), *hungaricum*, *indocile*, and E). Within the *impurum*-like form, AFLP clusters U5 (n = 2 nests), *alpestre* (n = 18), D_e (n = 3), and *impurum_w* / *impurum_e* (n = 20) exhibited distinct differences. However, AFLP clusters *impurum_w* and *impurum_e* differed in only 83% of males (n = 18): Visible in lateral view, ventral paramere lobe in *impurum_w* was typically more rounded, while *impurum_e* had a slightly pronounced corner on dorsal end of ventral paramere lobe (Fig. S1). In the *caespitum*-like form, AFLP clusters *caespitum* / *hungaricum* (n = 20), *indocile* (n = 4), and E (n = 8) exhibited distinct differences. AFLP cluster *hungaricum* typically had a truncated end of ventral lobe in ventral view

(n = 3); because the latter morphology was also found in 11% of *caespitum* (n = 17), we were not able to delimit these two based on male genital morphology.

Traditional and geometric morphometrics (TM, GM): Nest-Centroid clustering had discordance rates < 5% in 78%, 71%, and 60% of hypothesized pairwise species comparisons of worker TM (n = 55, mean discordance rate 2.7%), worker GM (n = 28, mean discordance rate 4.7%), and gyne GM (n = 10, mean discordance rate 7.7%; Tab. 2; raw data in Tabs. S6 - 8), respectively. The worker TM data yielded the strongest support of the DNA-based species hypotheses. The discordance rates of worker GM data were mostly equal to or higher than in TM (Tab. 2). Compared with worker TM and GM, gyne GM data yielded higher discordance rates; however, delimitation of *alpestre* / *caespitum*, *alpestre* / *impurum_e*, and *alpestre* / *impurum_w* was morphometrically supported by gyne GM only (Tab. 2; for species affiliation of CO1 clades, see Figs. 12, 14). Discordance rates varied across hypothesized species: While data of the morphologically hypothesized species *hungaricum*, I, J, D_e, and E conformed largely with DNA-based species hypotheses, *alpestre*, *caespitum*, *indocile*, U5, *impurum_w*, and *impurum_e* provided several times discordance rates > 5% (Tab. 2). Our discordance rates were distinctly higher than TM error rates of other studies on myrmicine ants (CSÖSZ & al. 2014a, 2015, SEIFERT & al. 2014a, SEIFERT & CSÖSZ 2015, CSÖSZ & FISHER 2016). High level of crypsis, that is, interspecific similarity, and intraspecific variability, might cause high discordance rates. However, additionally to morphometric data, here we have a DNA-based background

Tab. 2: Discordance rates between Nest-centroid clustering and DNA-based species hypotheses for pairwise comparisons [%]. *n* = number of nests, *i* = number of individuals. Values in the first row of each species show results of worker traditional morphometric data, in the second row of worker geometric morphometric (GM) data, in the third row of gyne GM data. Missing data are indicated by "-". Values < 5% in bold.

	<i>alpestre</i>	<i>caespitum</i>	<i>hungaricum</i>	<i>breviscapus</i> (= I)	<i>indocile</i>	<i>caucasicum</i> (= U5)	<i>fusciclava</i> (= J)	<i>staerckei</i> (= D_e)	<i>impurum</i> _e	<i>impurum</i> _w	<i>immigrans</i> (= E)	Mean
<i>n / i</i>	73 / 146 48 / 97 12 / 35	145 / 294 87 / 170 42 / 70	23 / 51 - / - - / -	3 / 15 - / - - / -	34 / 89 26 / 52 - / -	10 / 32 - / - - / -	17 / 34 12 / 24 - / -	41 / 81 24 / 48 - / -	50 / 100 16 / 31 11 / 16	28 / 56 8 / 16 6 / 6	40 / 84 24 / 47 6 / 16	
<i>alpestre</i>												
<i>caespitum</i>	6.0 19.7 3.7											
<i>hungaricum</i>	1.0 - -	1.8 - -										
<i>breviscapus</i> (= I)	1.3 - -	0.7 - -	0.0 - -									
<i>indocile</i>	7.8 8.1 -	8.0 8.0 -	1.5 - -	0.0 - -								
<i>caucasicum</i> (= U5)	15.7 - -	9.9 - -	0.0 - -	0.0 - -	5.7 - -							
<i>fusciclava</i> (= J)	0.0 0.0 -	0.0 0.0 -	0.0 - -	0.0 - -	0.0 0.0 -	0.0 - -						
<i>staerckei</i> (= D_e)	1.8 0.0 -	0.5 1.8 -	0.0 - -	0.0 - -	0.0 4.0 -	2.0 - -	0.0 0.0 -					
<i>impurum</i> _e	11.9 9.4 0.0	4.8 11.4 5.7	0.0 - -	1.9 - -	2.2 11.8 -	6.7 - -	0.0 0.0 -	0.0 0.0 -				
<i>impurum</i> _w	15.8 1.8 0.0	3.3 2.4 4.2	0.0 - -	0.0 - -	2.8 11.9 -	7.9 - -	0.0 0.0 -	1.4 0.0 -	16.7 25.0 35.3			
<i>immigrans</i> (= E)	0.0 2.8 11.1	1.1 4.5 16.7	0.0 - -	0.0 - -	0.0 2.0 -	6.0 - -	0.0 2.8 -	0.0 4.2 -	0.0 0.0 0.0	1.5 0.0 0.0		2.7 4.7 7.7

to justify species delimitations (see Integrative-taxonomy approach). The species of the *Tetramorium caespitum* complex could represent more pronounced morphological cypsis than most other ants analyzed.

Integrative-taxonomy approach: Based on the integrative-taxonomy approach combining CO1, AFLP, male genital morphology, and Nest-Centroid-clustering data (Figs. 12 - 14), we present arguments for delimiting ten species, that is, *Tetramorium alpestre*, *T. caespitum*, *T. hungaricum*, *T. sp. I*, *T. indocile*, *T. sp. U5*, *T. sp. J*, *T. sp. D_e*, *T. impurum*, and *T. sp. E* (for the final species names, see Figs. 12 - 14). For one outlier nest, we also consider the results for thermal niches (see Thermal niches). We focus on arguments relevant for species delimitation and discuss discordant results.

(1) *Tetramorium alpestre*: All workers except one of the CO1 clade *alpestre* grouped in one AFLP cluster (Fig. 12). The only outlier (i70) affiliated with the AFLP cluster of *T. caespitum* (Tabs. S1, S5), while it Nest-Centroid-clustered with *T. alpestre*. Since also ecology data (TAS = 8.9 °C, see Thermal niches, Tab. 4) were typical for *T. alpestre*, we suppose a pipetting error during AFLP data generation and treat this nest as *T. alpestre*. Also AFLP data of Iberian and French nests (*n* = 18; in STEINER & al. (2010) labeled with "?") matched this spe-

cies hypothesis well. Differentiation from all other species based on male genital morphology was possible (Fig. 12; Fig. S1: 1 - 4). As CO1 clade U3 weakly affiliated to the *T. alpestre* AFLP cluster (Tab. S5), we consider U3 as an isolated southern relict population of *T. alpestre*. However, the status remains tentative as we lack males and sufficient nest records to establish a solid background for large-scale morphometric investigation. Discordance between Nest-Centroid-clustering and DNA-based species hypotheses (discordance rate > 5%) was recorded for all comparisons of *T. alpestre* with *T. indocile* and *T. sp. U5* (Tab. 2), confirming that *T. alpestre* is one of the most cryptic species of the complex. However, CO1, AFLP, and male genital morphology data support the species status, despite extreme morphological worker similarity.

(2) *Tetramorium caespitum*: AFLP clusters suggested conspecificity of CO1 clades *caespitum*1, B1, U1, U2, and D_w1 (Fig. 12). Three CO1 clades consisting of only one or two HTs each (*caespitum*2, B2, and D_w2) yielded no AFLP and male genital results, however, based on nest-Centroid clustering they belong to *T. caespitum*. Male genital morphology did not differ between CO1 clades *caespitum*1, B1, U1, U2, and D_w1 (Fig. S1: 5 - 8). Nest-Centroid clustering provided discordance rates with DNA-based species hypotheses > 5% with *T. indocile*

and *T. sp.* U5 in all applied morphometric methods; this weakness does not challenge species status and we interpret it as extreme morphological crypsis. *Tetramorium caespitum* is polyphyletic in CO1 (Fig. 12): CO1 clades *caespitum*1, *caespitum*2, and U1 were closer related to *alpestre* than to U2 and B. CO1 clades D_w1 and D_w2 were not close to all other CO1 clades of *T. caespitum*, but to those of *T. sp.* J and *T. sp.* D_e. We identified evolutionary explanations for this CO1 polyphyly (see Reasons for mitochondrial-nuclear discordances).

(3) *Tetramorium hungaricum*: AFLP clusters and discordance rates between Nest-Centroid clustering and DNA-based species hypotheses suggested conspecificity of CO1 clades *hungaricum*1 and U4 (Fig. 12, Tab. 2, Tab. S5). CO1 clade *hungaricum*2 consisting of only one HT yielded no AFLP and male genital results; however, based on Nest-Centroid clustering, it belongs to *T. hungaricum*. Distinct male genital morphology differences from *T. caespitum* were not found (Fig. S1: 9 - 12).

(4) *Tetramorium sp.* I: The CO1 clade was a supported monophylum (Fig. 12). AFLP and male genital data were lacking. Nest-Centroid clustering allowed a safe delimitation from all other taxa (Tab. 2).

(5) *Tetramorium indocile*: All workers of CO1 clade *indocile*1 coincided in one AFLP cluster (Fig. 12); male genital morphology showed the same pattern (Fig. 12, Fig. S1: 13 - 16). CO1 clade *indocile*2 consisting of only two HTs (Tab. S1) yielded no AFLP and male genital results; Nest-Centroid clustering results are doubtful and we tentatively consider it as isolated population of *T. indocile*. Nest-Centroid clustering resulted in discordance rates with DNA-based species hypotheses > 5% with *T. alpestre*, *T. caespitum*, and *T. sp.* U5 (Tab. 2), based on high crypsis and geographic variability. *Tetramorium indocile* is a representative example of a cryptic species showing congruent results in CO1, AFLP, and male genital morphology through its large distribution area from Iberia to Central Asia, despite sympatric occurrence with nearly all species of the complex.

(6) *Tetramorium sp.* U5: We found complete mitochondrial-nuclear concordance (Fig. 12). Additionally, male genital morphology allowed distinguishing this from all other species of the complex (Fig. 12, Fig. S1: 17 - 20). Based on high morphological crypsis and low number of samples, Nest-Centroid clustering led to discordance rates > 5% with DNA-based species hypotheses with *T. alpestre*, *T. caespitum*, *T. indocile*, *T. impurum*, and *T. sp.* E (Tab. 2). However, based on CO1, AFLP, and male genital morphology results, morphological crypsis of workers does not challenge species status.

(7) *Tetramorium sp.* J: All workers of CO1 clade J grouped in one AFLP cluster (Fig. 12). Male genital morphology data are missing, but Nest-Centroid clustering results always matched with DNA-based species hypothesis (Tab. 2).

(8) *Tetramorium sp.* D_e: CO1 clade and AFLP cluster coincided perfectly (Fig. 12). Differentiation from all other species based on male genital morphology was possible (Fig. 12, Fig. S1: 21 - 24); discordance rates between Nest-Centroid clustering and DNA-based species hypotheses supported delimitation from all other species (Tab. 2).

(9) *Tetramorium impurum*: AFLP clusters suggested conspecificity of CO1 clades *impurum_w* and H as well as *impurum_e*1 - e4, respectively (Fig. 12, Tabs. S4, S5); also Nest-Centroid clustering supported affiliation of these CO1 clades to *T. impurum*. Four CO1 clades consisting of only one or two HTs (*impurum_e*5 - 7, U6) yielded no AFLP and male genital results; based on Nest-Centroid clustering, they belong most likely to *T. impurum*. However, the affiliation of some Greek and Anatolian nests is difficult. Here, we consider them as southern relict populations of *T. impurum*. Male genital morphology of *T. impurum* was different from all other species of the complex (Fig. 12, Fig. S1: 25 - 31), discordance rates between Nest-Centroid clustering and DNA-based species hypotheses separated *T. impurum* from all species except *T. sp.* U5. The two main CO1 clades of *T. impurum*, that is, *impurum_w* (incl. H) and *impurum_e*1 - 4, had separate AFLP clusters (Fig. 12, Tab. S5). However, no distinct difference in male genital morphology (error rate 17%) and high discordance rates between DNA-based and Nest-Centroid clustering-based species-hypotheses were found (Tab. 2). To avoid oversplitting (CARSTENS & al. 2013), we set aside describing *impurum_w* as new species. Henceforth, we term intraspecific units of *T. impurum* eastern and western clade.

(10) *Tetramorium sp.* E: All nests except one (i246) of CO1 clade E grouped in a single AFLP cluster (Fig. 12, Tab. S5). Male genital morphology was different from all other species of the complex (Fig. 12, Fig. S1: 32 - 35). Nest-Centroid clustering separated species E well from all other taxa except *T. sp.* U5 (Tab. 2). One nest (18375) with a lack of AFLP data mismatched as *T. caespitum* in Nest-Centroid clustering. The outliers, i246 and 18375, showed mitochondrial-nuclear discordance that we explained biologically (see Reasons for mitochondrial-nuclear discordances).

Reasons for mitochondrial-nuclear discordances:

In five of ten species, that is, *Tetramorium alpestre*, *T. caespitum*, *T. hungaricum*, *T. impurum*, and *T. sp.* E (= *T. immigrans* according to our final species hypotheses), at least one nest showed mitochondrial-nuclear discordance. In identifying reasons for the discordances, the geographic distribution of clades is relevant. Thus, in *T. caespitum*, the five CO1 clades constituted distinct geographic patterns (Fig. S2). Similarly, in *T. alpestre*, *T. hungaricum*, and *T. impurum*, we found rare CO1 clades only close to distribution edges (Tab. S1). Following the argumentation of TOEWS & BRELSFORD (2012), distinct geographic patterns of CO1 clades exclude incomplete lineage sorting as explanation. We hypothesize (I) peripatric speciation or (II) ancient hybridization with subsequent backcrossing of hybrids into parental populations, that is, introgression, as sources of most cases of mitochondrial-nuclear discordance (cf. FUNK & OMLAND 2003, cf. SLOAN & al. 2017). In the latter, introgression might be followed by divergence of mitochondrial DNA from that of the maternal species. As we outline in the following, distinguishing between these explanations is difficult, but all of the possible explanations result in the need to prioritize the nuclear over the mitochondrial DNA results. In more detail: (I) *T. alpestre* could have speciated in peripatry, that is, as a smaller and local population in spatial isolation and under different ecological conditions along the periphery of the

Tab. 3: Error rates of linear discriminant analyses (LDA) / cross-validation LDA results for pairwise species comparisons [%]. *n* = number of nests, *i* = number of individuals. Values in the first row of each species are results of worker traditional morphometric data, in the second row of worker geometric morphometric (GM) data, in the third row of gyne GM data. Missing data indicated by "-". Values < 5% in bold.

	<i>alpestre</i>	<i>caespitum</i>	<i>hungaricum</i>	<i>breviscapus</i> (= I)	<i>indocile</i>	<i>caucasicum</i> (= U5)	<i>fusciclava</i> (= J)	<i>staercke</i> (= D_e)	<i>impurum</i>	<i>immigrans</i> (= E)	Mean
<i>n / i</i>	73 / 146 48 / 97 12 / 35	145 / 294 87 / 170 42 / 70	23 / 51 -/- -/-	3 / 15 -/- -/-	34 / 89 26 / 52 -/-	10 / 32 -/- -/-	17 / 34 12 / 24 -/-	41 / 81 24 / 48 -/-	78 / 156 24 / 47 17 / 22	40 / 84 24 / 47 6 / 16	
<i>alpestre</i>											
<i>caespitum</i>	2.8 / 4.7 11.2 / 13.1 5.7 / 7.6										
<i>hungaricum</i>	0.0 / 0.0 -/- -/-	0.4 / 1.2 -/- -/-									
<i>breviscapus</i> (= I)	1.1 / 1.1 -/- -/-	0.0 / 0.0 -/- -/-	0.0 / 0.0 -/- -/-								
<i>indocile</i>	1.7 / 7.8 8.1 / 8.7 -/-	2.4 / 6.1 9.5 / 10.8 -/-	1.5 / 3.0 -/- -/-	0.0 / 0.0 -/- -/-							
<i>caucasicum</i> (= U5)	11.4 / 15.7 -/- -/-	4.4 / 9.9 -/- -/-	0.0 / 0.0 -/- -/-	0.0 / 0.0 -/- -/-	3.3 / 9.4 -/- -/-						
<i>fusciclava</i> (= J)	0.0 / 0.0 0.0 / 0.0 -/-	0.0 / 0.0 0.5 / 0.5 -/-	0.0 / 0.0 -/- -/-	0.0 / 0.0 -/- -/-	0.0 / 0.0 0.0 / 1.3 -/-	0.0 / 0.0 -/- -/-					
<i>staercke</i> (= D_e)	0.9 / 0.9 0.0 / 1.4 -/-	0.0 / 0.0 0.5 / 1.8 -/-	0.0 / 0.0 -/- -/-	0.0 / 0.0 -/- -/-	0.0 / 0.0 1.0 / 4.0 -/-	0.0 / 0.0 -/- -/-	0.0 / 0.0 0.0 / 1.4 -/-				
<i>impurum</i>	2.7 / 4.9 6.9 / 8.3 0.0 / 0.0	1.5 / 3.6 11.1 / 12.4 2.2 / 3.3	0.0 / 0.0 -/- -/-	0.0 / 0.8 -/- -/-	0.8 / 0.8 9.1 / 10.1 -/-	4.8 / 8.2 -/- -/-	0.0 / 0.0 0.0 / 0.0 -/-	0.0 / 0.8 0.0 / 2.1 -/-			
<i>immigrans</i> (= E)	0.0 / 0.0 1.4 / 2.8 5.9 / 11.8	0.3 / 0.3 4.1 / 5.5 8.1 / 10.5	0.0 / 0.0 -/- -/-	0.0 / 0.0 -/- -/-	0.0 / 0.0 1.0 / 4.0 -/-	1.2 / 3.6 -/- -/-	0.0 / 0.0 0.0 / 0.0 -/-	0.0 / 0.0 4.2 / 6.3 -/-	0.8 / 0.8 0.0 / 0.0 0.0 / 0.0		0.9 / 1.9 3.3 / 4.5 3.7 / 5.5

larger range of the parental species. Under such conditions, the budding population would lose HTs by drift faster than the parental species. As a result, the monophyletic *T. alpestre* (excl. CO1 clade U3) would be embedded in the more widely distributed paraphyletic *T. caespitum*. (II) If U2 and B were the ancient CO1 clades of *T. caespitum* (Fig. 12), the CO1 clade *caespitum* (incl. U1) could have descended from *T. alpestre*. Here, a single introgression event suffices to explain the parapatry between *T. caespitum* (excl. CO1 clade D_w) and *T. alpestre* (excl. CO1 clade U3). If introgressed CO1 clades became fixed, mitochondrial DNA would imply no hints of its heterospecific origin (FUNK & OMLAND 2003). Even low introgression levels may suffice to establish a CO1 clade in a foreign population (TAKAHATA & SLATKIN 1984). Sporadic episodes of hybridization combined with small and patchy populations facilitate the fixation of introgressed HTs (PATTON & SMITH 1994). Other CO1 polyphylies in *T. alpestre*, *T. caespitum* (incl. CO1 clade D_w), *T. impurum*, and *T. hungaricum*, may have resulted from similar processes. Especially the CO1 polyphyly of *T. caespitum*, combined with a distinct geographic pattern of CO1-clade distributions (Fig. S2), but no geographic difference in AFLP data, could be interpreted as resulting from male-biased dispersal and female philopatry (cf. RÜPPELL & al. 2003).

To a lesser extent, recent hybridization is presumably the source for mitochondrial-nuclear discordance: Two nests

of CO1 clade E represented mitochondrial-nuclear discordance: Nest i246 belonged to clade E (HT79), and AFLP cluster as well as Nest-Centroid cluster of *Tetramorium caespitum* (Tab. S1). Similarly, nest 18375 (HT70) Nest-Centroid clustered with *T. caespitum*, and its ecology (TAS = 15.8 °C) differed from that of *T. sp. E* (Tabs. 4, 5). AFLP data are missing here, but as phenotypes are mainly determined by nuclear genes (cf. SMITH 1992), we assume mitochondrial-nuclear discordance. Hybrids of these two species were also found based on microsatellite data (B. Kaufmann & J. Gippet, pers. comm. 2015). Hybridization of these two species might be facilitated by similar male genital morphology (Fig. S1: 5 - 8, 32 - 35), overlapping phenology (see Taxonomy, Redescriptions of species), and frequent syntopic occurrence (Tab. S1), especially in anthropogenically influenced habitats (cf. SEIFERT 1999).

Across all species, our data suggest that hybridization on the individual level is rare (cf. SEIFERT 1999). However, on evolutionary time scales, it may have played a central role in forming these *Tetramorium* species' genomes (cf. ABBOTT & al. 2013).

Reanalyzed linear discriminant analysis (LDA) of morphometric data: The LDA had error rates < 5% in 98%, 71%, and 70% of pairwise species comparisons of worker TM (*n* = 45, mean error 0.9%), worker GM (*n* = 21, mean error 3.3%), and gyne GM (*n* = 10, mean error

Tab. 4: Standard air temperature (TAS) comparison as an overview of ecological niches. Given are arithmetic means of localities \pm standard deviation [lower extreme, upper extreme]; n = number of localities, TAS in °C.

Species	n	TAS
<i>alpestre</i>	181	8.6 \pm 2.1 [5.2, 17.6]
<i>caespitum</i>	465	16.1 \pm 2.0 [7.9, 21.1]
<i>hungaricum</i>	43	20.6 \pm 2.7 [16.2, 26.2]
<i>breviscapus</i> (= I)	3	22.1 \pm 1.4 [20.6, 23.2]
<i>indocile</i>	42	15.6 \pm 3.2 [11.5, 25.4]
<i>caucasicum</i> (= U5)	7	13.5 \pm 2.8 [10.2, 18.2]
<i>fusci-clava</i> (= J)	13	21.3 \pm 1.6 [16.1, 21.8]
<i>staerckei</i> (= D_e)	79	18.1 \pm 3.1 [11.0, 26.4]
<i>impurum</i>	155	14.1 \pm 2.7 [7.7, 21.4]
<i>immigrans</i> (= E)	201	19.9 \pm 2.5 [13.0, 26.7]

3.7%; Tab. 3; raw data in Tabs. S6 - 8), respectively. We got LDA error rates $<$ 5% at least in one morphometric method in all cases except *Tetramorium alpestre* / U5. Due to the small sample size in the smallest class, with only 32 workers in *T. caucasicum*, an LDA reduced to 10 characters had to be performed (MODER & al. 2007).

Thermal niches: Species-specific ecological differences were significant in 34 of 45 pairwise species comparisons (76%) (Tabs. 4 - 5). *Tetramorium alpestre* had by far the lowest TAS values, followed by the four moderately thermophilous species *T. sp. U5* (for final species names, see Figs. 12 - 14), *T. impurum*, *T. indocile*, and *T. caespitum*. Five species were distinctly thermophilous: *T. sp. D_e*, *T. sp. E*, *T. hungaricum*, *T. sp. J*, and *T. sp. I*.

Type material assignment: Type material belonging to the *Tetramorium caespitum* complex was assigned to species based on qualitative morphology, morphometrics, thermal niche, and biogeography (for details, see Taxonomy, Treatment of species): *T. semilaeve* var. *kutteri* and *T. staerckei* var. *gregori* are synonyms of *T. indocile* and *T. impurum*, respectively. Further, types of *T. staerckei* belong to *T. sp. D_e*, those of *T. caespitum* var. *fusci-clava* to *T. sp. J*, and those of *T. caespitum* var. *immigrans* to *T. sp. E*; we redescribe these three species (see Taxonomy, Treatment of species; Figs. 17 - 19). Since no type material proved to be conspecific with *Tetramorium sp. I* and *T. sp. U5*, we newly describe these species as *T. breviscapus* sp.n. and *T. caucasicum* sp.n., respectively (see Taxonomy, Treatment of species; Figs. 15, 16).

Were all data types used necessary for the final species delimitation? We applied six methods using mostly the same ant material (in sexuals, material from the same nests): mitochondrial DNA (CO1 gene), nuclear DNA (AFLP), male genital morphology, traditional worker morphometrics, geometric worker morphometrics, and geometric gyne wing morphometrics. Obviously, (ant) biologists will not perform such comprehensive analyses on all taxonomic problems. Choosing an efficient but still reliable array of methods for future studies will depend on the particular taxonomic problem. In many cases of ant taxonomy, morphometric analysis alone suffices (see SEI-

FERT 2003, SEIFERT & al. 2014a, b, SEIFERT & CSÖSZ 2015). However, single methods can lead to simplified assumptions (e.g., CARSTENS & al. 2013, CLOUSE & al. 2016, SANTOS & al. 2016). Thus, to solve highly intricate problems, we strongly recommend the use of integrative taxonomy combining molecular studies with morphology (see also PULLANDRE & al. 2012). The use of three disciplines seems worthwhile since hereby the error rate should fall below the level of 5% (SCHLICK-STEINER & al. 2010). In doing so, mitochondrial DNA data are helpful to get a first impression of diversity and to select material for further analyses. Furthermore, when combined with nuclear DNA, mitochondrial DNA allows the insight into evolutionary processes such as introgression and thus interspecific gene flow. However, even well-separated mitochondrial DNA clades must not automatically be treated as species. In contrast, nuclear DNA data repeatedly proved reliable in generating species-delimitation hypotheses (recent ant examples: WARD 2011, WARD & SUMNIGHT 2011). In the case of the *Tetramorium caespitum* complex, AFLP results appear authoritative and frequently concur with morphological data and the final species hypotheses. The disadvantage of AFLP is that all samples have to be processed simultaneously due to poor reproducibility; hence, technical and human resources limit the sample size. Next-Generation-Sequencing-based approaches will likely become important in taxonomy, such as restriction site-associated DNA sequencing (animal example: BERNARDI & al. 2017). De novo whole-genome sequencing, as it is becoming more and more affordable (NYGAARD & WURM 2015), might at some point in the future even replace CO1 sequencing and AFLP in taxonomy.

Among the morphological approaches chosen here, qualitative male genital investigations were very successful and relevant. However, in other ant genera, this approach may be less successful either due to a lack of sampled males or of species-specific differences. Carefully collected morphometric data are precious because of the possibilities of multivariate statistics. Traditional morphometrics is time- but not money-intensive if a microscope is available; once data have been published, they can also be taken for future studies of taxonomic or evolutionary research. In the study by BAGHERIAN YAZDI & al. (2012), GM data performed better than TM data in discriminant analyses of cryptic species, but the opposite was true in our study (Tab. 2). Especially in gyne GM, we explain the lower success by the smaller sample size. GM data are useful for species delimitation but have the disadvantage to be available only as principal components (Tabs. S7, S8) and thus are not usable for all kinds of interest (e.g., discriminant functions for keys, individual integration of characters with data from other studies). Nonetheless, distance matrices derived from GM analyses can easily be compared with genetic distances, and subtle shape variation among species can be made visible using GM tools. Anyway, we recommend at least one large-scale morphometric discipline for future taxonomic studies. Morphometric analyses usually are cheaper and easier than molecular-genetic ones, and they were found to have lower failure rates in a literature analysis (SCHLICK-STEINER & al. 2010). Moreover, the linkage between type material or other historical material of interest and operational taxonomic units frequently can only be made with morphometric

Tab. 5: Species-specific Standard air temperature. Significances at $\alpha = 0.05$ Student's t-test after Bonferroni-Holm-correction are labeled with *.

	<i>alpestre</i>	<i>caespitum</i>	<i>hungaricum</i>	<i>breviscapus</i> (= I)	<i>indocile</i>	<i>caucasicum</i> (= U5)	<i>fusciclava</i> (= J)	<i>staerckeii</i> (= D_e)	<i>impurum</i>	<i>immigrans</i> (= E)
<i>alpestre</i>										
<i>caespitum</i>	0.000*									
<i>hungaricum</i>	0.000*	0.000*								
<i>breviscapus</i> (= I)	0.000*	0.000*	0.364							
<i>indocile</i>	0.000*	0.320	0.000*	0.001*						
<i>caucasicum</i> (= U5)	0.000*	0.001*	0.000*	0.001*	0.108					
<i>fusciclava</i> (= J)	0.000*	0.000*	0.314	0.393	0.000*	0.000*				
<i>staerckeii</i> (= D_e)	0.000*	0.000*	0.000*	0.028	0.000*	0.000*	0.000*			
<i>impurum</i>	0.000*	0.000*	0.000*	0.000*	0.003	0.569	0.000*	0.000*		
<i>immigrans</i> (= E)	0.000*	0.000*	0.084	0.132	0.000*	0.000*	0.010	0.000*	0.000*	

analyses (SCHLICK-STEINER & al. 2007a, SEIFERT 2009, SCHLICK-STEINER & al. 2010, CARSTENS & al. 2013, SEIFERT 2016).

Conclusion and outlook

Using integrative taxonomy, we solved a major problem in ant taxonomy and (re)described ten cryptic species of the *Tetramorium caespitum* complex. Data of two molecular and four morphological data types were analyzed in an unsupervised fashion to build species hypotheses independently. The results revealed a surprisingly high number of large-scale discordances, especially between mitochondrial and nuclear DNA. Whether such pattern is an exception, will crystallize when more in-depth studies of cryptic species have become available. Mitochondrial-nuclear discordances allowed insights into evolutionary processes of species. We interpreted them mostly as due to either peripatric speciation or ancient interspecific hybridization but to a lesser extent also as due to recent hybridization. Additionally, based on the investigation of type material, we linked the operational taxonomic units with their valid scientific names. Since only this step enables the stable use of correct species names, we encourage other biologists to publish nomenclatural consequences of species delimitations whenever feasible. Our findings constitute the basis of future research on the evolution of cryptic species itself, for example into the role of stasis and / or convergence. However, we cannot exclude the presence of further, rare cryptic species in southernmost Europe and expect further species outside Europe, for example, in Anatolia. We expect that the increasing trend to discover cryptic species (BICKFORD & al. 2007) will continue. Biologists will have to get increasingly used to them and to handle them in their daily research routine. We hope that integrative taxonomy will disentangle further intricate species complexes to bring us closer to understanding the global species richness and the evolution of species.

Taxonomy

Diagnosis of the *Tetramorium caespitum* complex

BOROWIEC (2014) listed 28 species of the genus *Tetramorium* MAYR, 1855 as native to Europe (Canary Islands

and Cyprus excluded), all belonging to the *T. caespitum* group sensu BOLTON (1979). Four species complexes of this group have been outlined so far: The *T. semilaeve* ANDRÉ, 1883 complex (CSÓSZ & SCHULZ 2010), the *T. ferox* RUZSKY, 1903 complex (CSÓSZ & SCHULZ 2010; 5 taxa), the *T. chefketi* FOREL, 1911 complex (GÜSTEN & al. 2006, CSÓSZ & al. 2007; 11 taxa), and the *T. caespitum* complex (SCHLICK-STEINER & al. 2006). Additionally, there are further species not allocated to any of these complexes, for example, *T. meridionale* EMERY, 1870, *T. brevicorne* BONDROIT, 1918, *T. hippocratis* AGOSTI & COLLINGWOOD, 1987, and *T. pelagium*.

Characters of species of the *Tetramorium caespitum* complex are as follows:

(1) At least some workers of a nest with c-shaped, crinkly, or sinuous hairs arising just behind buccal cavity (Fig. 2, arrow). Most typical character for *Tetramorium caespitum* complex; absent from *T. semilaeve* complex, *T. ferox* complex, *T. chefketi* complex, *T. meridionale*, *T. brevicorne*, *T. hippocratis*, and *T. lucidulum* MENOZZI, 1933, but also present in *T. pelagium* and *T. goniommoide* POLDI, 1979.

(2) Workers with microsculpture on basal part of 1st gastral tergite varying from few, scattered stickman-like to complex reticulate structures (Fig. 4), MC1TG < 30 (error 0.0% in 993 workers). Very complex polygonal structure in *Tetramorium chefketi* complex, MC1TG > 40 (error 0.0% for 34 workers).

(3) Propodeal spines small to medium, PEW / SPST < 2.055 (error 0.0% for 471 nest means), $33.959 * POTCos - 8.569 * PPH + 7.487 * SPST + 649 < 0$ (error 0.4% for 471 nest means). In European species of *Tetramorium ferox* complex and *T. inerme* MAYR, 1877, propodeal spines reduced to slightly developed corners, PEW / SPST > 2.055 (> 2.08 in 11 workers). In *T. brevicorne*, propodeal spines rather long and number of postoculo-temporal costae and costulae high in relation to postpetiole height: $33.959 * POTCos - 8.569 * PPH + 7.487 * SPST + 649 > 0$ (error 0.0% for 9 workers).

(4) Worker head, mesosoma, petiole, and postpetiole surface partly smooth (as in *Tetramorium hungaricum*) to coarsely sculptured (as in *T. staerckeii*), but not largely

smooth (as in *T. inermis*) or very coarsely sculptured as in *T. chefketi* complex and *T. goniommoide*.

(5) Worker head, dorsum, and occiput with longitudinal costae and costulae, but occiput never with transversal costae and costulae as in *Tetramorium meridionale*.

(6) Often dark brown to black. In Benelux, Central Europe, and Balkan mountain areas sometimes light brown (*Tetramorium impurum*); rarely reddish (*T. immigrans*); most species not yellowish (as in *T. diomedea*, *T. lucidulum*, *T. flavidulum* EMERY, 1924) or reddish (as typical in *T. ferox*, *T. punicum* (F. SMITH, 1861)).

(7) Worker eye moderately sized, in nest mean EYE / CS = 0.155 - 0.196 (n = 471), but not > 0.197 as in *Tetramorium pelagium* and *T. biskrense* FOREL, 1904 (n = 8 workers).

(8) Male with ten antennal segments, and not nine as in *Tetramorium pelagium* and *T. biskrense*.

(9) Male paramere length > 843 µm and thus larger than in *Tetramorium semilaeve* complex, *T. ferox*, *T. moravicum*, and *T. pelagium*.

(10) Large sexuals. Gyne MW > 1198 µm and thus larger than in *Tetramorium semilaeve* complex, *T. brevicorne*, *T. punctatum* SANTSCHI, 1927, and *T. pelagium*.

Treatment of species

We evaluated all Palearctic *Tetramorium caespitum* group names listed by BOLTON (2014) concerning their possible affiliation to the *T. caespitum* complex (Tab. S9). Based on information given in the original descriptions and in recent taxonomic revisions (SANETRA & al. 1999, CSŐSZ & MARKÓ 2004, GÜSTEN & al. 2006, SCHLICK-STEINER & al. 2006, CSŐSZ & al. 2007, CSŐSZ & SCHULZ 2010, CSŐSZ & al. 2014b, STEINER & al. 2010, RADCHENKO & SCUPOLA 2015, BOROWIEC & al. 2016), we excluded taxon names using the following criteria: (I) Unavailable names. (II) Names of material outside the *T. caespitum* complex based on original descriptions because of, alone or in combination, (a) workers with yellowish, brownish-yellowish or reddish color, (b) pronounced reticulate structures or longitudinally striato-punctated 1st gastral tergite, (c) general surface smooth, (d) frontal carinae reaching (almost) until the occiput, (e) transversal carinae on head, (f) or head, petiole, postpetiole, or proportions of eye, mesosoma, petiole, and postpetiole in figures different from the *T. caespitum* complex, (g) too small sexuals, or (h) gynes with a deep median incision of petiolar node. (III) Names of material belonging to other species complexes based on (a) SANETRA & al. (1999), (b) GÜSTEN & al. (2006), (c) CSŐSZ & SCHULZ (2010), (d) CSŐSZ & al. (2007), (e) CSŐSZ & al. (2014b), (f) RADCHENKO & SCUPOLA (2015), (g) and BOROWIEC & al. (2016). (IV) Names of material already linked to the operational taxonomic units of the *T. caespitum* complex (*T. hungaricum*: CSŐSZ & MARKÓ 2004; *T. caespitum* and *T. impurum*: SCHLICK-STEINER & al. 2006; *T. alpestre*: STEINER & al. 2010; *T. indocile*: CSŐSZ & al. 2014b). (V) Names of material originating from Great Britain or Fennoscandia (where only *T. caespitum* occurs). (VI) Names of material originating from outside the Palearctic and east of the Johansen line. This line in the Yenisei area at around 85° E represents the most important zoogeographical boundary in the northern Palearctic (JOHANSEN 1955). Since only species with very wide ecological valence cross this zoogeographical

boundary (MÜLLER 1974), we did not expect that type material collected east of it was relevant for this study. Especially the two new species we describe, *T. sp. U5* (= *T. caucasicum*) and *T. sp. I* (= *T. breviscapus*), have restricted distribution areas limited to the Caucasus above 1000 m a.s.l. and to the Western Balkans, respectively. In contrast, *T. sp. E* has been introduced to non-native regions (STEINER & al. 2008), and one could argue its origin might be, for example, east of the Johansen line. However, we found a distinctly higher HT diversity (Tab. S1) in Anatolia and the Caucasus region compared with Europe and North America. High haplotype-diversity in mitochondrial DNA has been frequently used to detect a species' geographical origin (ant examples include SCHLICK-STEINER & al. 2007b, GOTZEK & al. 2015). Following this idea, Anatolia and the Caucasus region are the most likely geographic origin of *T. immigrans*.

After this selection, 16 taxon names remained as possible candidates for valid names of operational taxonomic units: *Tetramorium banyulense* BERNARD, 1983; *T. caespitum* var. *typicum* RUZSKY, 1902; *T. caespitum oxyomma* KARAVAEV, 1912; *T. caespitum tenuicornis* EMERY, 1925; *T. caespitum* var. *immigrans* SANTSCHI, 1927; *T. semilaeve* var. *kutteri* SANTSCHI, 1927; *T. semilaeve* var. *transbaicalense* RUZSKY, 1936; *T. moravicum* var. *caespito-moravicum* KRATOCHVÍL, 1941; *T. staercke* KRATOCHVÍL, 1944; *T. staercke* var. *gregori* KRATOCHVÍL, NOVAK & SNOFLÁK, 1944; *T. caespitum* var. *fusciclava* CONSANI & ZANGHERI, 1952; *T. goniommoide* POLDI, 1979; *T. hippocratis* AGOSTI & COLLINGWOOD, 1987; *T. pelagium* MEI, 1995; *T. persignatum* BOLTON, 1995; and *T. taueret* BOLTON, 1995. Type material of *T. semilaeve* var. *transbaicalense* is lost (RADCHENKO 1992). We did also not receive type material of *T. caespitum* var. *typicum*, *T. moravicum* var. *caespito-moravicum*, and *T. staercke* var. *gregori*, which is not housed in St. Petersburg (Dmitry A. Dubovikoff in litt. 2012), Moscow (Elena Fedoseeva in litt. 2013), or in the private collection of Klára Bezděčková and Pavel Bezděčka (Klára Bezděčková & Pavel Bezděčka in litt. 2013). Probably, type material of *T. caespitum* var. *typicum* was never defined as that author's intention was not to describe a new taxon but simply the "typical" form of *T. caespitum*. In *T. moravicum* var. *caespito-moravicum*, no type material has been defined (KRATOCHVÍL 1941, 1944); because of this and because the description cannot be interpreted, we consider it as nomen dubium. In *T. staercke* var. *gregori*, we tried to interpret a possible synonymy based on information of the original description. *Tetramorium persignatum* BOLTON, 1995 is housed in the Menozzi Collection of DISTA of the University of Bologna. Department policy did not allow to loan types (Mario Marini in litt. 2012). However, transmitted images of type workers allowed the exclusion of this species from the *T. caespitum* complex (see below). We also found distinct morphological characters by qualitative analysis to exclude *T. banyulense*, *T. hippocratis*, *T. oxyomma*, *T. caespitum tenuicornis*, and *T. taueret* from the *T. caespitum* complex. Type material of the six remaining taxa was not excluded from the complex based on qualitative analysis and was investigated in detail:

Tetramorium caespitum var. *fusciclava* [sic!] CONSANI & ZANGHERI, 1952 (2 workers) [Italy]: 2 workers labeled as: "Riccione" [-] SYNTYPI *Tetramorium caes-*

pitum c. var. *fusciclava* C. Emery, 1925 [-] "var fusciclava Emery" [-] MUSEO GENOVA coll. C. Emery (dono 1925) [-] ANTWEB CASENT 904802.

Tetramorium caespitum var. *immigrans* SANTSCHI, 1927 (8 workers) [Chile]: 5 workers labeled as: TYPE [-] "Chili Valparaiso, Miss Edwards" [-] "Tetramorium caespitum L immigrans Sant". SANTSCHI det. 19 "26" [-] Sammlung Dr. F. Santschi Kairouan; [thereof we have chosen the lectotype worker]. 2 workers labeled as: "Chili M. Edwardes [sic!]" [-] "Were found in road could not find next any where" [-] Sammlung Dr. F. Santschi Kairouan.

Tetramorium goniommoide POLDI, 1979 (3 workers) [Turkey]: 2 workers on 2 separate pins in each case labeled as: Sarayköy 4.-15.X.215m. [-] Türkei 1977 C. Baroni Urbani [-] Collezione Bruno Poldi (Mus. St. Nat. Milano) [-] "T. goniommoides [sic!] synTypus". 1 worker labeled as: Sarayköy 4.-15.X.215m [-] Türkei 1977 C. Baroni Urbani [-] "3" [-] "coTypus". [-] Collezione Bruno Poldi (Mus. St. Nat. Milano).

Tetramorium pelagium MEI, 1995 (6 workers, 1 gyne, 1 male) [Italy]: 2 workers labeled as: "T. PELAGE LINOSA 29.IV.91 GIR MEI" [-] Collezione Bruno Poldi (Mus. St. Nat. Milano) [-] "T. pelagium". 2 workers, 1 gyne, and 1 male labeled as: "SICILIA T. PELAGE LINOSA 29.IV.91 MEI" [-] "6". [-] Collezione Bruno Poldi (Mus. St. Nat. Milano).

Tetramorium semilaeve var. *kutteri* SANTSCHI, 1927 (2 workers) [Switzerland]: 2 workers labeled as: Cotypus [-] "Brig Pfingsten 3. VI 1922" [-] "T. semilaeve v. kutteri" [-] GBIFCH 00190422.

Tetramorium staercke KRATOCHVÍL, 1944 (2 workers, 1 gyne, 1 male) [Hungary]: 2 workers labeled as: Hongrie Nagytétény Coll: Rösztler [/] "17. VI. 1935" [-] "500" [-] Typus [-] "Tetramorium caespitum v. hungaricum v. Staercke worker Röbl. Typus! No. 500" [/] PAUL RÖSZLER Baross Gabor-telep HONGRIE – EUROPE.; [thereof we have chosen the lectotype worker]. 1 gyne labeled as: Hongrie Nagytétény Coll: Rösztler [/] "17. VI 1935" [-] 500 [-] Typus [-] "Tetramorium caespitum r. hungarica v. Staercke gyne Röbl. Typus! No 500" [/] PAUL RÖSZLER Baross Gabor-telep HONGRIE – EUROPE. 1 male labeled as: HUNGARIA NAGYTETENY P.ROESZLER [-] 500 [-] Typus [-] "Tetramorium caespitum r. hungarica v. Staercke male Röbl. Typus! No 500" [/] PAUL RÖSZLER Baross Gabor-telep HONGRIE – EUROPE.

Since type material of *Tetramorium persignatum* was not loanable, we investigated images of type workers and excluded this material from our complex by measurements of head and mesosoma (CW / ML = 1.01; in *T. caespitum* complex CW / ML = 0.85 ± 0.05). *Tetramorium goniommoide* was described from Anatolia and seems to be missing in Europe. Like the *T. caespitum* complex, it shows c-shaped, crinkly, or sinuous hairs on the ventral head. However, a strongly developed sculpture, giving the surface a dull impression (like *chefketi* complex; GÜSTEN & al. 2006, CSÓSZ & al. 2007), distinguishes *T. goniommoide* from the species of the *T. caespitum* complex. Sculpture on lateral side of propodeum builds clear and straight lines. Propodeal spines are shorter than in typical workers of the *T. caespitum* complex. With all measurements in μm , a distinct separation for workers is given by the discriminant $D(\text{goni})$: $2.695 * \text{MW} + 17.189 * \text{POTCos}$

+ $5.738 * \text{EYE} - 7.209 * \text{PPW} - 270$. Workers of *T. caespitum* complex have $D(\text{goni}) < 0$ (error 0.0% in 975 workers) and those of *T. goniommoide* $D(\text{goni}) > 0$ (> 120 in 3 type workers). *Tetramorium pelagium*, described from the island Linosa, also has c-shaped, crinkly, or sinuous hairs on ventral head. However, its gynes differ by small size and a depressed mesosoma (as in *T. semilaeve*) clearly from the *T. caespitum* complex. Additionally, males have only nine and not ten antennal segments. With all measurements in μm , a clear separation for workers is given by the discriminant $D(\text{pela})$: $2.813 * \text{HFL} + 16.891 * \text{MC1TG} - 17.610 * \text{POTCos} - 13.020 * \text{EL} + 490$. Workers of the *T. caespitum* complex have $D(\text{pela}) > 0$ (error 0.0% in 975 workers) and those of *T. pelagium* $D(\text{pela}) < 0$ (< -60 in 6 type workers). Type material of *T. caespitum* var. *fusciclava*, *T. caespitum* var. *immigrans*, *T. semilaeve* var. *kutteri*, and *T. staercke* belongs to the *T. caespitum* complex. A wild-card run of morphometric data in a 10-class LDA including all workers investigated by integrative taxonomy in this study clearly assigned *T. staercke* = D e ($p = 1$), *T. caespitum* var. *fusciclava* = J ($p = 1$), and *T. caespitum* var. *immigrans* = E ($p = 1$). We redescribe these species (see Redescriptions below). However, material of *T. semilaeve* var. *kutteri*, consisting of two dwarf workers, is ambiguous, and the results permit conspecificity with either *T. indocile* ($p = 0.81$) or *T. hungaricum* ($p = 0.19$). Based on three arguments, we propose synonymy with *T. indocile*: (I) Biogeography: *T. hungaricum* is limited to Eastern Europe, the Balkans, and the Pannonian zone (see redescription below). There is no record west of 16° E, while the type material of *T. semilaeve* var. *kutteri* originates from 8° E. Contrariwise, we found *T. indocile* on the type locality of *T. semilaeve* var. *kutteri*. (II) Ecology: *T. hungaricum* is thermophilic with TAS $20.6 \pm 2.7^\circ\text{C}$ [16.2, 26.2], while TAS on the type locality is 15.5°C only. Contrariwise, *T. indocile* shows TAS $15.6 \pm 3.2^\circ\text{C}$ [11.5, 25.4]. (III) Qualitative morphology: Head and mesosoma of *T. hungaricum* are typically without sculpture and largely smooth and shining. The type material of *T. semilaeve* var. *kutteri* has moderately pronounced, but distinct lines on head and mesosoma, especially similar to *T. indocile* originating from the type locality of *T. semilaeve* var. *kutteri*. Since type material of *T. staercke* var. *gregori* was not traceable, we aimed at linking the material based on the original description to a species. The male genital morphology drawing 7e in KRATOCHVÍL (1944: 65) shows typical *impurum*-like parameres without a corner like *T. staercke* on the ventral paramere lobe (Fig. 12, Figs. S1: 21 - 31). Hence, we consider *T. staercke* var. *gregori* as a synonym of *Tetramorium impurum*.

***Tetramorium alpestre* STEINER, SCHLICK-STEINER & SEIFERT, 2010** (including U3 sensu SCHLICK-STEINER & al. 2006)

Tetramorium alpestre STEINER, SCHLICK-STEINER & SEIFERT, 2010: 249-250. CO1 gene from material of the type nest investigated.

Type locality. Vent (Austria), 46.8548° N, 10.9097° E, 2000 m a.s.l., leg. H. Müller, 15.VIII.2007.

CO1 gene. Here and in the following, we use two different abbreviations for HTs, "HT" (HTs published by SCHLICK-STEINER & al. 2006, STEINER & al. 2010, KINZNER & al. 2015, and in this study) and "H" (HTs pub-

lished by Csösz & al. 2014b). 65 HTs from 210 nests: HT101 (15.2%), HT102 (12.9%), HT114 (8.1%), HT116 (6.7%), HT169 (4.3%), HT113 (3.3%), HT172, HT258 (each with 2.9%), HT271 (2.4%), HT115, HT170 (each with 1.9%), HT93, HT111, HT173, HT242, HT257, HT263, HT430 (each with 1.4%), HT91, HT96, HT100, HT103, HT231, HT282, HT294, HT367, HT424, HT426, HT429 (each with 1%), HT92, HT94, HT95, HT97 - HT99, HT110, HT112, HT123, HT168, HT171, HT174, HT232, HT241, HT260, HT261, HT264, HT287, HT288, HT297, HT328, HT400, HT415, HT421 - HT423, HT425, HT427, HT428, HT431 - HT433, HT435 - HT437, HT440 (each with 0.5%).

Description of worker. Medium size, CS = 741 ± 51 [605, 850] μm . Dark brown to blackish.

Head moderately elongate, CL / CW = 1.016 ± 0.014 [0.981, 1.049] μm . Eye rather small, EYE / CS = 0.171 ± 0.005 [0.160, 0.182]. Scape length moderate, SLd / CS = 0.775 ± 0.014 [0.738, 0.802]. Mesosoma long and wide, ML / CS = 1.174 ± 0.025 [1.092, 1.225], MW / CS = 0.644 ± 0.012 [0.615, 0.674].

Promesonotal dorsum convex, metanotal groove shallow. – Head dorsum and occiput with longitudinal costae and costulae. Postoculo-temporal area of head with moderate number of longitudinal costae and costulae, POTCos = 8.11 ± 1.45 [4.50, 11.00]. Mesosoma dorsum longitudinally or partly circularly rugulose, lateral side of propodeum with moderately pronounced smooth and shiny area, Ppss = 37.4 ± 14.5 [14.1, 92.3]. Dorsum of petiolar node with sculpture or smooth. General surface appearance on average moderately smooth and shiny compared with other species. – Connected stickman-like or reticulate microsculpture: small units scattered over 1st gastral tergite, MC1TG = 14.12 ± 2.54 [7.03, 20.94]. – Some workers with long c-shaped, crinkly, or sinuous hairs on ventral head posterior to buccal cavity.

Description of male. Paramere structure belongs to *impurum*-like form: rounded ventral paramere lobe without sharp corner in dorsal or ventral view but with clear division of ventral and dorsal paramere lobes, visible by deep emargination between lobes in posterior view. No sharp corner at end of ventral lobe visible in posterior view. Relatively long and sharp-ended dorsal paramere lobe, visible in posterior and dorsal view. Paramere length in lateral view < 991 μm .

Distribution. Iberian mountains, Pyrenees, Massif Central, Mont Ventoux, Corsica, Alps, Apennines, Calabrian Apennines, Monti Nebrodi, Dinaric Alps (Fig. 13).

Ecology. Less thermophilic than all other species of complex (Tab. 5), TAS of 182 sites 8.6 ± 2.1 °C [5.2, 17.6]. In Alps and Pyrenees often above timberline; never below 900 m a.s.l. Southern Italian population more thermophilous, TAS of three sites 14.8 ± 2.9 °C (t-test, $p = 0.000$). In Alps, typical habitats are south-facing, non-forested alpine meadows, subalpine dwarf-shrub heathland, dry pastures, stony embankments, or block fields. In Pyrenees, known from stony pine forests. Nests often under stones, but also in moss, rootage, and dead wood.

Biology. Facultatively polygynous (STEINER & al. 2003, KRAPP & al. 2017).

Phenology. Adult sexuals in nests on 30 July \pm 17d [18 June, 10 September] ($n = 34$).

Social parasites. Here and in the following, the species names of social parasites follow traditional nomenclature, which reflects morphological and biological traits but is questionable from a cladistic point of view (WARD & al. 2015). Extensive nomenclatural changes among social parasites are currently on the way, but not yet broadly implemented in the literature. *Strongylognathus testaceus* (SCHENCK, 1852) ($n = 3$; host sub "*Tetramorium caespitum*" in SANETRA & al. 1999 and Tab. S1), *Strongylognathus alpinus* WHEELER, 1909 ($n = 1$; host sub "*T. caespitum*" in SANETRA & al. 1999), and *Teleutomymex schneideri* KUTTER, 1950 ($n = 1$; Tab. S1) were found associated with *T. alpestre*.

***Tetramorium caespitum* (LINNAEUS, 1758)** (including B, U1, U2, and D partim sensu SCHLICK-STEINER & al. 2006)

Formica caespitum LINNAEUS, 1758: 581; neotype designation: SCHLICK-STEINER & al. 2006: 270. CO1 gene and morphology of material from the neotype nest investigated here.

Myrmica fuscata NYLANDER, 1846: 935; junior synonym of *Tetramorium caespitum*: SMITH 1851: 118; junior synonymy confirmed hereby based on biogeography (type locality: South Finland).

Tetramorium caespitum var. *hammi* DONISTHORPE, 1915: 178; junior synonym of *Tetramorium caespitum*: BOLTON 1995: 408; junior synonymy confirmed hereby based on biogeography (type locality: New Forest, England).

Type locality. Floghult Bohuslan (Sweden), 58.97° N, 11.42° E, 100 m a.s.l., leg. C.A. Collingwood, 21.VI. 2000.

CO1 gene. 129 HTs from 495 nests: HT1 (27.1%), HT15 (10.7%), HT52 (9.9%), HT58 (8.7%), HT225 (4.6%), HT57 (2.2%), HT43 (2.0%), HT184, HT229 (each with 1.2%), HT5, HT181 (each with 1.0%), HT48, HT53, HT191 (each with 0.8%), HT32, HT220, HT222, HT224, HT295, HT396 (each with 0.6%), HT6, HT8, HT17, HT35, HT50, HT56, HT126, HT180, HT183, HT223, HT280, HT296 (each with 0.4%), HT2 - HT4, HT7, HT9 - HT14, HT16, HT18, HT22, HT24, HT26, HT33, HT34, HT42, HT46, HT47, HT49, HT51, HT55, HT70, HT79, HT117, HT124, HT125, HT127 - HT129, HT182, HT190, HT192, HT218, HT219, HT226 - HT228, HT230, HT247, HT255, HT259, HT262, HT269, HT273, HT275, HT279, HT281, HT283, HT286, HT292, HT300, HT302 - HT304, HT309 - HT311, HT313, HT319, HT324, HT325, HT335 - HT342, HT356 - HT358, HT369, HT372, HT373, HT377, HT389 - HT392, HT395, HT398, HT401, HT405, HT410, HT414, HT416, HT417, HT434, HT438, HT439 (each with 0.2%).

Description of worker. Larger than most species of complex, CS = 761 ± 50 [591, 867] μm . Dark brown to blackish.

Head moderately elongate, CL / CW = 1.012 ± 0.015 [0.969, 1.043]. Eye rather small, EYE / CS = 0.171 ± 0.005 [0.158, 0.188]. Scape length moderate, SLd / CS = 0.777 ± 0.015 [0.724, 0.812]. Mesosoma long and wide, ML / CS = 1.172 ± 0.026 [1.104, 1.233], MW / CS = 0.645 ± 0.015 [0.605, 0.687].

Promesonotal dorsum convex, metanotal groove shallow. – Head dorsum and occiput with longitudinal costae and costulae, in Iberia longitudinal costae and costulae of head dorsum sometimes interrupted by smooth and shiny areas. Postoculo-temporal area of head with moderate number of longitudinal costae and costulae, POTCos = 7.45 ± 1.92 [3.38, 12.13]. Mesosoma dorsum longitudinally rugu-

lose, in Iberia longitudinal costae and costulae sometimes interrupted by smooth and shiny areas. Lateral side of propodeum with a moderately pronounced smooth and shiny area, Ppss = 39.9 ± 20.0 [13.3, 107.7]. Dorsum of petiolar node smooth or with slightly microreticulate sculpture. General surface appearance on average moderately smooth and shiny compared with other species. – Connected stickman-like or reticulate microsculpture: small units scattered over 1st gastral tergite, MC1TG = 12.62 ± 2.31 [7.00, 19.58]. – Some workers with long c-shaped, crinkly, or sinuous hairs on ventral head posterior to buccal cavity.

Description of male. Paramere structure belongs to *caespitum*-like form: ventral paramere lobe with one or two sharp corners; without distinct emargination between paramere lobes in posterior view, both paramere lobes reduced in size; in ventro-posterior view, second corner on ventral paramere lobe missing or < 87 μ m apart from first. In posterior view, typically only one sharp corner on ventral lobe.

Distribution. Whole Europe (after SEIFERT 2007 up to 63° N), Caucasus (Fig. 13).

Ecology. Moderately thermophilic, TAS of 465 sites 16.1 ± 2.0 °C [7.9, 21.1], different from all species except *Tetramorium indocile*. Most common species in most of Europe and more euryoecious than other species of complex. Most records from non-forested habitats like meadows, pastures, heaths, arid or semi-arid grasslands, vineyards, fallow grounds, ruderal areas, road embankments, rock heaps, gravel pits, river banks, but also light pine and oak forests. Urban areas like parks, pavements, and roadsides. Nest construction more flexible than in other species: in soil, under stones, rarely in dead wood; only species building soil mounds higher than 10 cm.

Biology. Monogynous (SEIFERT 2007). Hybridizes with *Tetramorium immigrans* (results of this study, samples i246 and 18375).

Phenology. Adult sexuals in nests on 25 June \pm 14d [28 May, 19 August] (n = 67). Direct swarming behavior observed on 14 June, 15 June at 11:05 true solar time, and 30 June at 07:15 true solar time.

Social parasites. *Anergates atratulus* (SCHENCK, 1852) (n = 1; Tab. S1) and *Strongylognathus testaceus* (n = 5; Tab. S1 and SCHLICK-STEINER & STEINER 2006) were found in nests of *Tetramorium caespitum*.

***Tetramorium hungaricum* RÖSZLER, 1935** (including U4 sensu SCHLICK-STEINER & al. 2006 and *Tetramorium* sp. sensu BRAČKO & al. 2014)

Tetramorium caespitum subsp. *hungarica* RÖSZLER, 1935: 78; subspecies of *Tetramorium semilaeve*: KRATOCHVÍL 1941: 86; raised to species rank: RÖSZLER 1951: 88; lectotype designation: CSŐSZ & MARKÓ 2004: 53. Type material not investigated.

Type locality. Nagytétény (Hungary), 47.391° N, 18.987° E, 101 m a.s.l., leg. P. Rösler, 24.VII.1934.

CO1 gene. 10 HTs from 31 nests: HT108 (54.8%), HT105 (9.7%), HT233, HT274 (each with 6.5%), H05, HT104, HT106, HT107, HT109, HT299, HT370 (each with 3.2%).

Description of worker. Smallest species of complex, CS = 657 ± 34 [584, 722] μ m. Dark brown to blackish.

Head moderately elongate, CL / CW = 1.020 ± 0.014 [0.996, 1.051]. Eye large, EYE / CS = 0.184 ± 0.007 [0.170, 0.194]. Scape short, SLd / CS = 0.747 ± 0.015 [0.716, 0.773]. Mesosoma shortest within complex and narrow, ML

/ CS = 1.103 ± 0.018 [1.064, 1.146], MW / CS = 0.628 ± 0.008 [0.608, 0.645].

Promesonotal dorsum convex, metanotal groove shallow. – Smoothest and shiniest surface within complex: longitudinal costae and costulae on head dorsum and occiput usually interrupted by large-scale smooth and shiny areas. Postoculo-temporal area of head with few longitudinal costae and costulae, POTCos = 2.14 ± 1.21 [0.13, 4.50]. Longitudinal costae and costulae on mesosoma interrupted by smooth and shiny areas, lateral side of propodeum with strongly pronounced smooth and shiny area, Ppss = 85.6 ± 36.1 [21.1, 169.5] μ m. Dorsum of petiolar node usually smooth, exceptionally feebly microreticulated. – Connected stickman-like or reticulate microsculpture: small units scattered over 1st gastral tergite, MC1TG = 14.91 ± 2.53 [9.64, 20.85]. – Some workers with long c-shaped, crinkly, or sinuous hairs on ventral head posterior to buccal cavity.

Description of male. Paramere structure belongs to *caespitum*-like form: ventral paramere lobe with one or two sharp corners; without distinct emargination between paramere lobes in posterior view, both paramere lobes reduced in size; in ventro-posterior view, second corner on ventral paramere lobe missing or < 87 μ m apart from first. In posterior view, typically only one sharp corner on ventral lobe.

Distribution. Pannonian zone, Balkans, Eastern Europe (Fig. 13).

Ecology. More thermophilic than all other species except *Tetramorium breviscapus*, *T. fusciclava*, and *T. immigrans*; TAS of 43 sites 20.6 ± 2.7 °C [16.2, 26.2]. Typical habitats are arid meadows, dry grasslands, stony shrubland, gravel pits; also oak forests.

Phenology. Adult sexuals in nests on 20 June \pm 6 [8 June, 24 June] (n = 7).

***Tetramorium breviscapus* sp.n.** (= I as defined in this study)

Etymology. Named after its proportionally short scape, one of the best morphological characters for discrimination from related species. Because "*breviscapus*" is a noun in apposition, "*us*" is the correct ending.

Type locality. Dubrovnik (Croatia), 42.650° N, 18.083° E, 3 m a.s.l., leg. D. Dender, 29.X.2005.

Type material. All type material from one nest, labeled "CRO: 42.650° N, 18.083° E Dubrovnik coast, 3 m D.Dender 2005.10.29-18071". Holotype worker (Fig. 15) and eleven paratype workers in Senckenberg Naturkundemuseum Görlitz (Germany). Five paratype workers in Museum of Comparative Zoology, Cambridge, Massachusetts (USA), five in Natural History Museum in London (UK), five in Natural History Museum Basel (Switzerland), five in Museum of Nature South Tyrol (Bozen, Italy), five in Tiroler Landesmuseum (Hall, Austria), five in Natural History Museum in Vienna (Austria), five in Budapest Hungarian Natural History Museum (Hungary), and five in Schmalhausen Institute of Zoology Kiev (Ukraine). CO1 gene of type nest: HT329. Morphometric data of holotype in μ m: CL = 724, CW = 724, dAN = 197, EL = 130, EW = 99, FL = 276, HFL = 551, MC1TG = 15.7, ML = 789, MPPL = 234, MPSP = 309, MPST = 189, MtpW = 361, MW = 449, PEH = 245, PEL = 149, PEW = 245, PLSP = 168, PLST = 176, PnHL = 172, PoOc = 292, POTCos = 7.8, PPH = 269, PPL = 106, Ppss = 79, PPW = 306, PreOc = 180, RTI = 295, SLd = 512, SPST = 133, SPWI = 200.

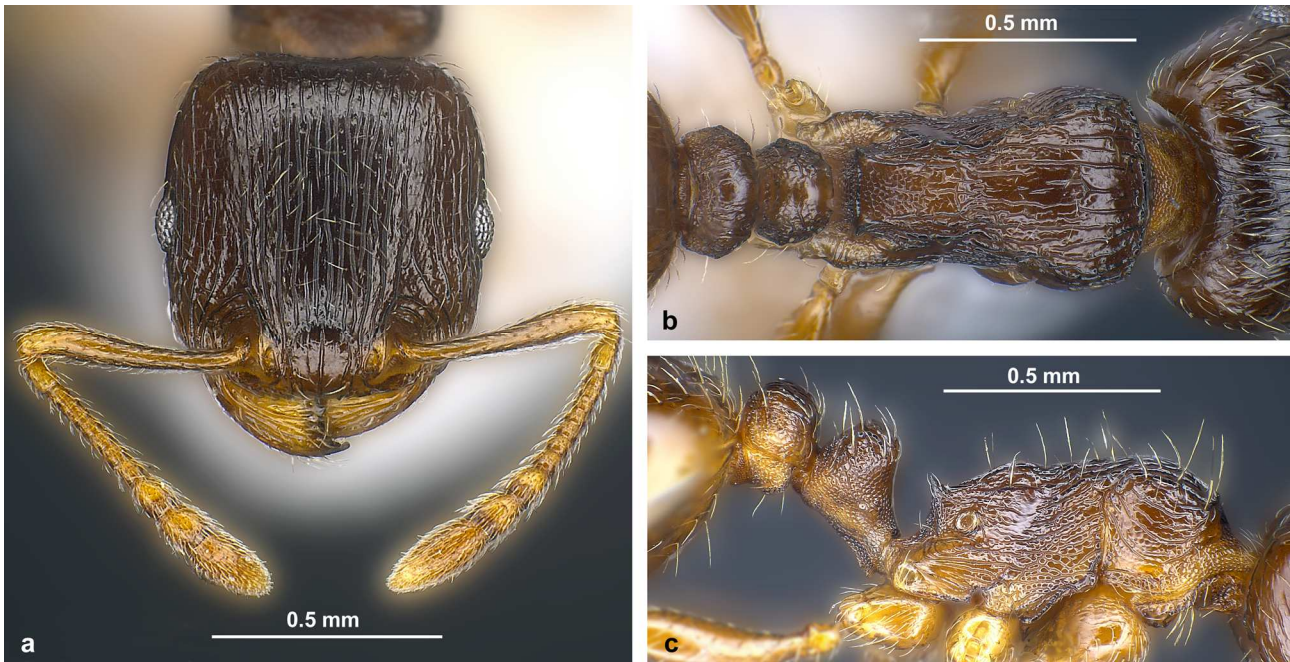


Fig. 15: Holotype of *Tetramorium breviscapus* sp.n. in (A) full face, (B) dorsal, and (C) lateral view.

CO1 gene. 2 HTs from 3 nests: HT329 (66.7%), HT290 (33.3%).

Description of worker. Smaller than most species of complex, CS = 714 ± 26 [689, 740] μm . Dark brown to blackish, mesosoma frequently lighter than head and gaster.

Head rather truncated compared with other species of complex, CL / CW = 1.002 ± 0.012 [0.989, 1.010]. Eye rather small, EYE / CS = 0.169 ± 0.010 [0.163, 0.180]. Scape shortest of complex, SLd / CS = 0.728 ± 0.010 [0.722, 0.739]. Mesosoma short and moderately wide, ML / CS = 1.119 ± 0.013 [1.107, 1.133], MW / CS = 0.631 ± 0.002 [0.629, 0.634].

Promesonotal dorsum convex, metanotal groove shallow. – Head dorsum and occiput with longitudinal costae and costulae. Postoculo-temporal area of head with rather few longitudinal costae and costulae, POTCos = 5.95 ± 0.53 [5.45, 6.50]. Mesosoma dorsum longitudinally rugulose, lateral side of propodeum with large smooth and shiny area, Ppss = 73.6 ± 16.6 [57.9, 91.0]. Dorsum of petiolar node usually smooth, exceptionally microreticulated. General surface appearance rather smooth and shiny compared with other species of complex. – Connected stickman-like or reticulate microsculpture: moderate-sized units scattered over 1st gastral tergite, MC1TG = 15.77 ± 1.20 [14.58, 16.97]. – Some workers with long c-shaped, crinkly, or sinuous hairs on ventral head just posterior to buccal cavity.

Distribution. Croatia, Bosnia-Herzegovina, and Greece (Fig. 13).

Ecology. More thermophilic than *Tetramorium alpestre*, *T. caespitum*, *T. indocile*, *T. caucasicum*, and *T. impurum*; TAS of three sites 22.1 ± 1.4 °C [20.6, 23.2]. Open habitats.

***Tetramorium indocile* SANTSCHI, 1927**

Tetramorium caespitum var. *indocile* SANTSCHI, 1927: 53; raised to species rank: PISARSKI 1969: 304; junior synonym of *T. caespitum*: RADCHENKO 1992: 50; revived from synonymy

and lectotype designation: Csósz & al. 2014b: 477. Morphology of type material investigated.

Tetramorium semilaeve var. *kutteri* SANTSCHI, 1927: 57; junior synonymy fixed hereby based on type investigation and biogeography (type locality: Brig, Switzerland). **Syn.n.**

Type locality. Ssemiretschie, Kasil-Kija'pass (Kyrgyzstan), 40.27° N, 72.13° E, 2100 m a.s.l., leg. N. Kusnezow, 15. VIII.1924.

CO1 gene. 21 HTs from 47 nests: HT87 (25.5%), HT83 (17.0%), HT85 (10.6%), H28, HT82 (each with 6.4%), H27, H29, H30, HT80, HT81, HT86, HT90, HT154, HT155, HT243, HT301, HT354, HT360, HT380, HT412, HT443 (each with 2.1%).

Description of worker. Smaller than most other species of complex, CS = 717 ± 52 [575, 822] μm . Dark brown to blackish.

Head moderately elongate, CL / CW = 1.011 ± 0.014 [0.982, 1.051]. Eye medium-sized, EYE / CS = 0.174 ± 0.005 [0.162, 0.181]. Scape moderately long, SLd / CS = 0.764 ± 0.013 [0.734, 0.790]. Mesosoma moderately long and moderately wide, ML / CS = 1.155 ± 0.020 [1.107, 1.205], MW / CS = 0.637 ± 0.011 [0.609, 0.667].

Promesonotal dorsum convex, metanotal groove shallow. – Head dorsum and occiput with longitudinal costae and costulae. Postoculo-temporal area of head with rather few longitudinal costae and costulae, POTCos = 6.08 ± 1.69 [2.63, 9.75]. Mesosoma dorsum longitudinally rugulose, lateral side of propodeum with rather pronounced smooth and shiny area, Ppss = 50.0 ± 23.8 [17.6, 110.5]. – Dorsum of petiolar node often smooth, rarely feebly microreticulated. General surface appearance on average rather smooth and shiny compared with other species. – Connected stickman-like or reticulate microsculpture: small units scattered over 1st gastral tergite, MC1TG = 14.01 ± 2.44 [6.41, 19.96]. – Some workers with long c-shaped, crinkly, or sinuous hairs on ventral head posterior to buccal cavity.

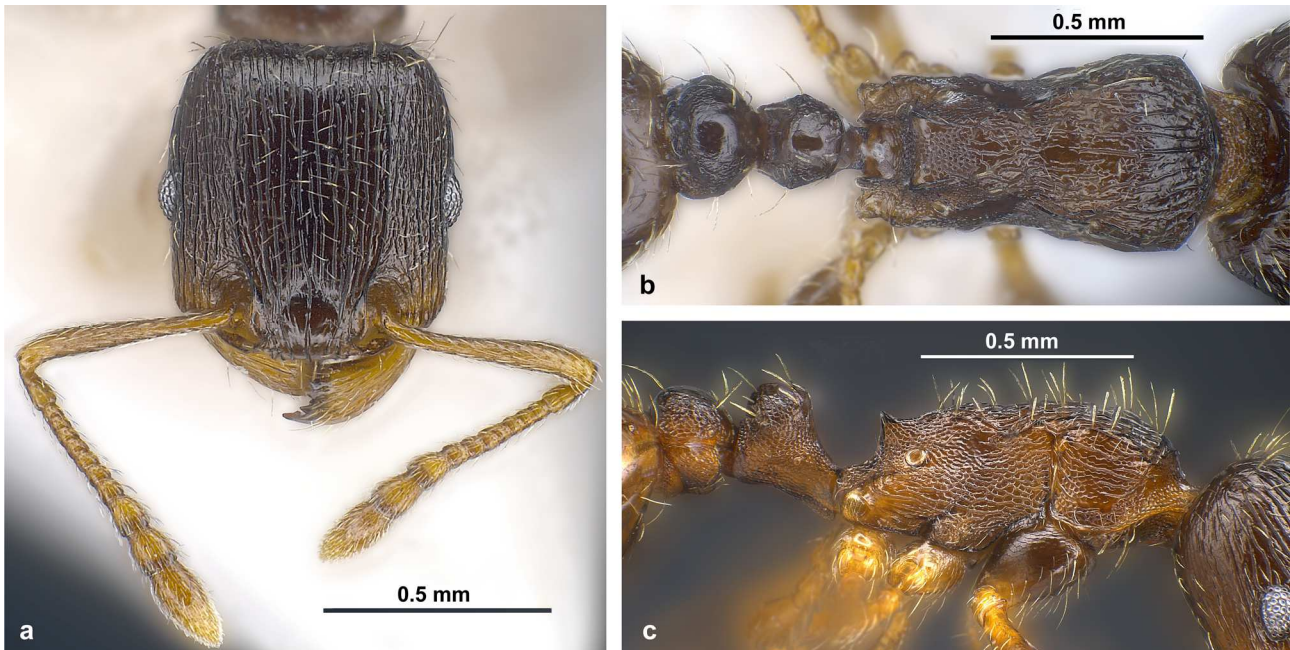


Fig. 16: Holotype of *Tetramorium caucasicum* sp.n. in (A) full face, (B) dorsal, and (C) lateral view.

Description of male. Paramere structure belongs to *caespitum*-like form: ventral paramere lobe with one or two sharp corners; without distinct emargination between paramere lobes in posterior view, paramere lobes reduced in size; in ventro-posterior view, second corner on ventral paramere lobe missing or $< 87 \mu\text{m}$ apart from first. In posterior view, two sharp corners on ventral lobe.

Distribution. Disjunct: Iberia, France, Central Europe, Italy, Balkans, Eastern Europe, Caucasus, Central Asia (Fig. 13).

Ecology. Moderately thermophilic, TAS of 42 sites $15.6 \pm 3.2 \text{ }^\circ\text{C}$ [11.5, 25.4], different from all species except *Tetramorium caespitum* and *T. caucasicum*. In Central Europe rare and in arid habitats like south-facing, fallow, rocky grassland in dry inner-alpine Rhône valley near Brig, on sandy cattle pasture near Mals in Vinschgau, vineyard near Budapest. Replaced by *T. caespitum* in less dry areas of Central Europe. In Armenia in montane steppic meadow, in Chelyabinsk area in steppe, in Kyrgyzstan in meadows, dry grasslands, *Juniperus*-heaths, river banks, stony steppes, semideserts. Nests in soil, often under stones.

Phenology. Adult sexuals in nests on 17 July \pm 24 [20 June, 16 August] (n = 7).

***Tetramorium caucasicum* sp.n.** (= U5)

Etymology. Named after its distribution area, the Caucasus.

Type locality. River Bashil valley (Russia), 43.211° N, 42.987° E, 2206 m a.s.l., leg. Z.M. Yusupov, 18.VI.2009.

Type material. All type material from one nest, labeled "RUS: 43.211° N, 42.987° E River Bashil valley, 2206 m S slope, timberline, under stone Z.M.Yusupov 2009.06.18-17372". Holotype worker (Fig. 16) and two paratype workers in Senckenberg Naturkundemuseum Götting (Germany). Two paratype workers in Museum of Comparative Zoology, Cambridge, Massachusetts (USA), two in Natural History Museum in London (UK), two in Natural History Museum Basel (Switzerland), one in mu-

seum of Nature South Tyrol (Bozen, Italy), one in Tiroler Landesmuseum (Hall, Austria), two in Natural History Museum in Vienna (Austria), two in Budapest Hungarian Natural History Museum (Hungary), and two in Schmalhausen Institute of Zoology Kiev (Ukraine). CO1 gene of type nest: HT234. Morphometric data of holotype in μm : CL = 714, CW = 691, dAN = 205, EL = 131, EW = 97, FL = 270, HFL = 563, MC1TG = 13.5, ML = 798, MPPL = 240, MPSP = 300, MPST = 183, MtpW = 338, MW = 433, PEH = 243, PEL = 157, PEW = 216, PLSP = 151, PLST = 171, PnHL = 183, PoOc = 286, POTCos = 8.5, PPH = 259, PPL = 111, Ppss = 57, PPW = 274, PreOc = 177, RTI = 289, SLd = 546, SPST = 134, SPWI = 185.

CO1 gene. 5 HTs from 7 nests: HT343 (42.9%), HT234 - HT236, HT378 (each with 14.3%).

Description of worker. Larger than most other species of complex, CS = 757 ± 44 [706, 839] μm . Dark brown to blackish.

Head strongly elongate, CL / CW = 1.027 ± 0.021 [0.987, 1.052]. Eye medium-sized, EYE / CS = 0.172 ± 0.005 [0.162, 0.178]. Scape moderately long, SLd / CS = 0.779 ± 0.015 [0.749, 0.798]. Mesosoma moderately long and moderately wide, ML / CS = 1.160 ± 0.022 [1.131, 1.211], MW / CS = 0.637 ± 0.015 [0.612, 0.670].

Promesonotal dorsum convex, metanotal groove shallow. – Head dorsum and occiput with longitudinal costae and costulae. Postoculo-temporal area of head with rather many costae and costulae, POTCos = 8.71 ± 1.44 [6.17, 10.63]. Mesosoma dorsum longitudinally rugulose, lateral side of propodeum with moderately pronounced smooth and shiny area, Ppss = 45.0 ± 20.2 [16.4, 80.4]. Dorsum of petiolar node smooth or with sculpture. General surface appearance on average moderate smooth and shiny compared with other species. – Connected stickman-like or reticulate microsculpture: small units scattered over 1st gastral tergite, MC1TG = 14.47 ± 1.81 [11.64, 17.33]. – Some workers with long c-shaped, crinkly, or sinuous hairs on ventral head posterior to buccal cavity.

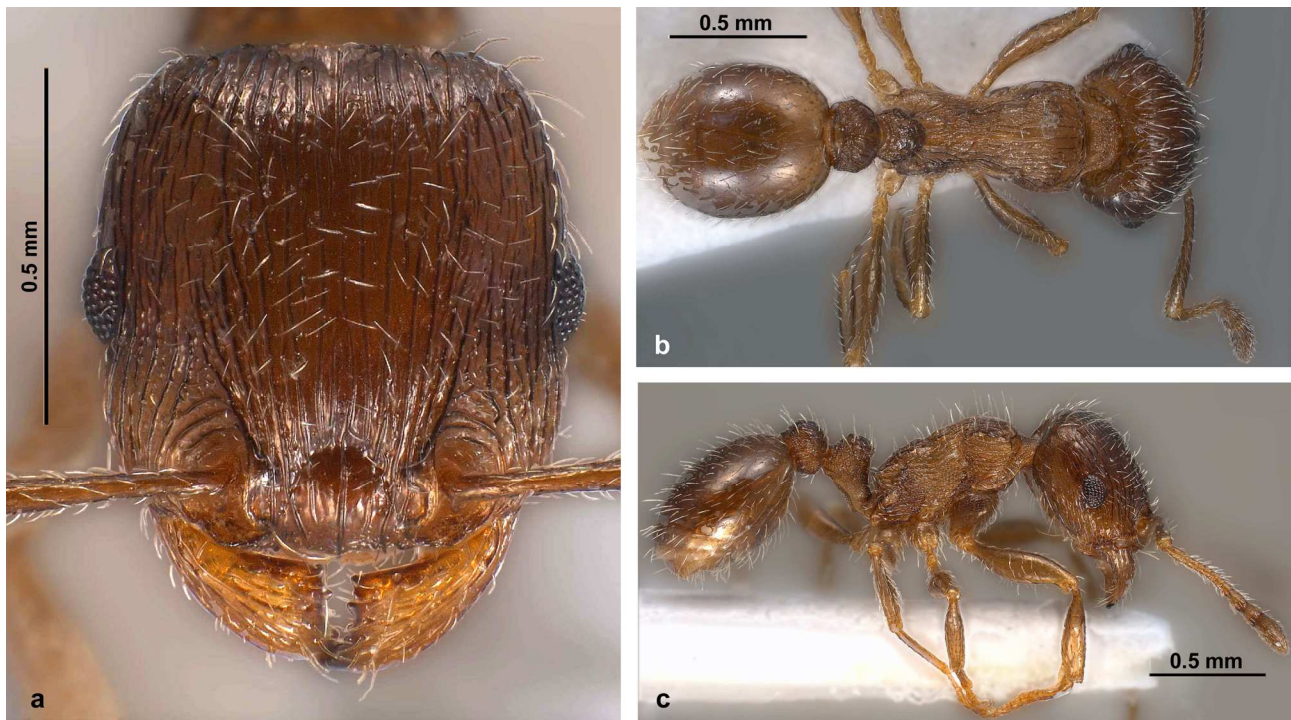


Fig. 17: Lectotype of *Tetramorium fusciclava* stat.n. in (A) full face, (B) dorsal, (C) and lateral view (specimen ANT-WEB1008486 from www.AntWeb.org, photographer Roland Schultz).

Description of male. Paramere structure belongs to *impurum*-like form: rounded ventral paramere lobe without any sharp corner in dorsal or ventral view but with clear division of ventral and dorsal paramere lobes, visible by deep emargination between lobes in posterior view. Sharp corner at end of ventral lobe in posterior view.

Distribution. Caucasus: Southern Russia, Georgia, and Armenia (Fig. 13).

Ecology. Less thermophilic than most other species of complex, TAS of seven sites 13.5 ± 2.8 °C [10.2, 18.2] and different from all species except *Tetramorium indocile* and *T. impurum*. Often above timberline; typical habitats are pastures and steppic meadows.

Phenology. Adult sexuals in nests on 2 August (n = 1).

***Tetramorium fusciclava* CONSANI & ZANGHERI, 1952 stat.n.** (= J as defined in this study)

Tetramorium caespitum caespitum var. *fusciclava* EMERY, 1925: 187 (unavailable name); first available use: *Tetramorium caespitum* var. *fusciclavum* [sic!] CONSANI & ZANGHERI 1952: 42; junior synonym of *Tetramorium caespitum*: SANETRA & al. 1999: 320; revived from synonymy, raised to species rank and lectotype designation hereby.

Type locality. Riccione (Italy), 43.999° N, 12.656° E, 11 m a.s.l., leg. C. Emery, 1925.

Lectotype designation. Top worker of two syntype workers (of two cards on one needle), labeled "Riccione" [-] SYNTYPI *Tetramorium caespitum* c. var. *fusciclava* C. Emery, 1925 [-] "var *fusciclava* Emery" [-] MUSEO GENOVA coll. C. Emery (dono 1925) [-] ANTWEB CASENT 904802, designated as lectotype (Fig. 17). Lectotype worker and one paralectotype worker in Museo Civico di Storia Naturale, Genova (Italy). Morphometric data of lectotype in μm : CL = 701, CW = 697, dAN = 199, EL = 150, EW = 109, FL = 273, HFL = 584, MC1TG =

19.9, ML = 777, MPPL = 228, MPSP = 298, MPST = 190, MtpW = 336, MW = 422, PEH = 244, PEL = 148, PEW = 217, PLSP = 168, PLST = 186, PnHL = 186, PoOc = 275, POTCos = 9, PPH = 252, PPL = 98, Ppss = 23, PPW = 279, PreOc = 167, RTI = 309, SLd = 564, SPST = 133, SPWI = 170.

CO1 gene. 4 HTs from 16 nests: HT189 (56.3%), HT305 (31.3%), HT272, HT404 (each with 6.3%).

Description of worker. Rather small, CS = 724 ± 42 [667, 829] μm . Dark brown to blackish.

Shortest head of complex, CL / CW = 0.996 ± 0.012 [0.976, 1.029]. Largest eye of complex, EYE / CS = 0.188 ± 0.004 [0.183, 0.196]. Scape moderately long, SLd / CS = 0.774 ± 0.006 [0.763, 0.784]. Mesosoma short and narrowest in complex, ML / CS = 1.136 ± 0.021 [1.101, 1.175], MW / CS = 0.615 ± 0.012 [0.596, 0.646].

Promesonotal dorsum convex, metanotal groove shallow. – Head dorsum and occiput with longitudinal costae and costulae. Postoculo-temporal area of head with a moderate number of longitudinal costae and costulae, POTCos = 6.76 ± 2.12 [4.63, 13.50]. Mesosoma dorsum longitudinally rugulose, lateral side of propodeum with pronounced sculpture, Ppss = 30.8 ± 10.5 [15.5, 47.3]. Dorsum of petiolar node typically with few strong costae, sometimes smooth or microreticulated. General surface appearance moderately smooth and shiny compared with other species. – Connected stickman-like or reticulate microsculpture: large units scattered over 1st gastral tergite, MC1TG = 20.57 ± 1.85 [16.34, 23.74]. – Some workers with long c-shaped, crinkly, or sinuous hairs on ventral head posterior to buccal cavity.

Distribution. Italy (Fig. 13).

Ecology. More thermophilic than all species except *Tetramorium hungaricum*, *T. breviscapus*, and *T. immigrans*; TAS of 13 sites 21.3 ± 1.6 °C [16.1, 21.8]. Preference for

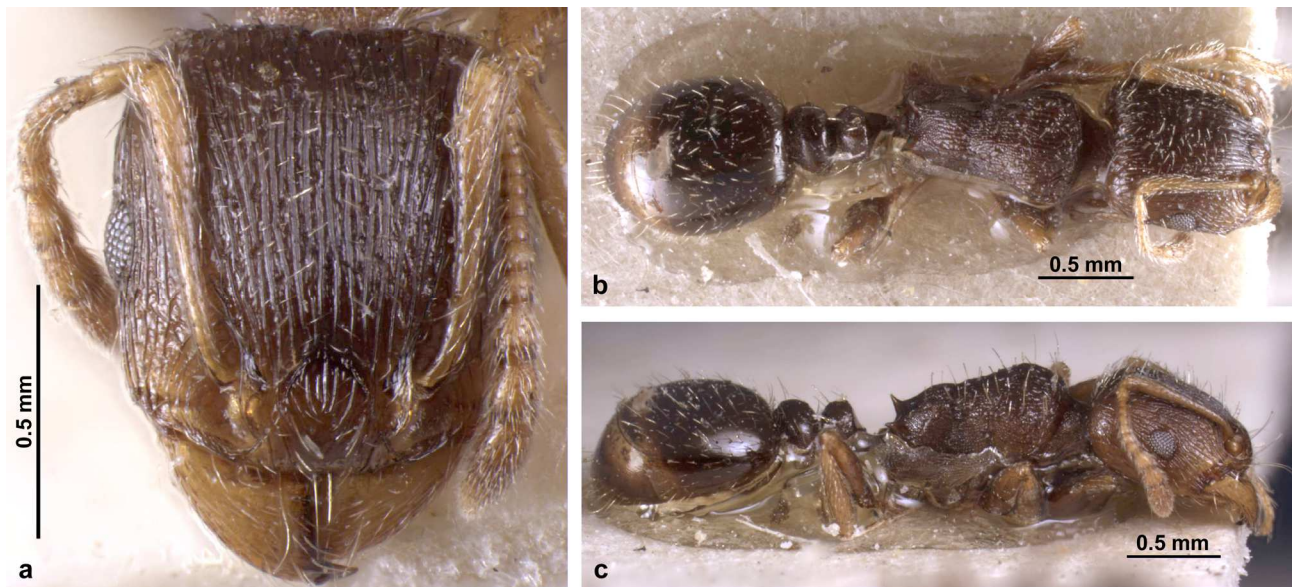


Fig. 18: Lectotype of *Tetramorium staerckei* sp.rev. in (A) full face, (B) dorsal, and (C) lateral view.

coastal areas: Twelve of 13 localities closer than 10 km to sea. Nests in grasslands, cornfield reins, beaches, pine forests; especially on sandy soil.

Phenology. No adult sexuals found, records of sexual larvae and pupae from 13 and 14 May.

***Tetramorium staerckei* KRATOCHVÍL, 1944 sp.rev.**
(= *D* sensu SCHLICK-STEINER & al. 2006 partim)

Tetramorium caespitum ssp. *hungarica* var. *staerckei* RÖSZLER, 1936 (unavailable name); first available use: KRATOCHVÍL 1944: 65; junior synonym of *Tetramorium impurum*: KUTTER 1977: 159; revived from synonymy based on type investigation and lectotype designation hereby.

Type locality. Nagytétény (Hungary), 47.391° N, 18.987° E, 102 m a.s.l., leg. P. Rösler, 17.VI.1935.

Lectotype designation. Worker closer to needle (of two syntype workers of one card), labeled "Hongrie Nagytétény Coll: Rösler [/] "17. VI. 1935" [-] "500" [-] Typus [-] "Tetramorium caespitum v. hungaricum v. Staerckei worker Röbl. Typus! No. 500" [/] "PAUL RÖSZLER Baross Gabor-telep HONGRIE – EUROPE", designated as lectotype (Fig. 18). Lectotype worker, one paralectotype worker, one paralectotype gyne, and one paralectotype male in Museum of Natural History, Sibiu / Hermannstadt (Romania). Morphometric data of lectotype worker in μm : CL = 871, CW = 849, dAN = 266, EL = 181, EW = 133, FL = 350, HFL = 739, ML = 1072, MPPL = 322, MPSP = 396, MPST = 238, MW = 581, PEH = 321, PEL = 203, PEW = 303, PLSP = 201, PLST = 239, PnHL = 241, PoOc = 329, POTCos = 10, PPH = 359, PPL = 126, PPW = 378, PreOc = 212, RTI = 347, SLd = 692, SPST = 186, SPWI = 277.

CO1 gene. 31 HTs from 74 nests: HT38 (18.9%), HT28, HT245, HT347 (each with 9.5%), HT29, HT37, HT39 (each with 4.1%), H20, H21, HT25, HT31, HT188, HT346 (each with 2.7%), H15, H16, HT27, HT30, HT40, HT41, HT144, HT185, HT186, HT244, HT253, HT254, HT268, HT276, HT307, HT371, HT376, HT383 (each with 1.4%).

Description of worker. Rather large compared with other species of complex, CS = 746 ± 57 [655, 878] μm . Dark brown to blackish.

Most elongate head of complex, CL / CW = 1.032 ± 0.014 [1.003, 1.062]. Eye rather large, EYE / CS = 0.178 ± 0.005 [0.168, 0.189]. Longest scape of complex, SLd / CS = 0.787 ± 0.016 [0.750, 0.817]. Mesosoma longest within complex and wide, ML / CS = 1.188 ± 0.025 [1.141, 1.247], MW / CS = 0.645 ± 0.014 [0.614, 0.681].

Promesonotal dorsum convex, metanotal groove shallow. – Head dorsum and occiput with longitudinal costae and costulae. Postoculo-temporal area of head with many costae and costulae, POTCos = 10.53 ± 1.75 [7.38, 13.75]. Mesosoma dorsum longitudinally rugulose, lateral side of propodeum with strongest sculpture of complex, Ppss = 16.9 ± 5.3 [11.3, 33.1]. – Dorsum of petiolar with sculpture or smooth. General surface appearance on average dull compared with other species. – Connected stickman-like or reticulate microsculpture: moderate-sized units scattered over 1st gastral tergite, MC1TG = 15.93 ± 2.35 [11.00, 22.00]. – Some workers with long c-shaped, crinkly, or sinuous hairs on ventral head posterior to buccal cavity.

Description of male. Paramere structure belongs to *impurum*-like form: rounded ventral paramere lobe without any sharp corner in dorsal or ventral view but with clear division of ventral and dorsal paramere lobes, visible by deep emargination between lobes in posterior view. No sharp corner at end of ventral lobe visible in posterior view. Relatively short dorsal paramere lobe, visible in posterior and dorsal view. Paramere structure length in lateral view > 1014 μm . In dorsal and posterior view, distinct corner on ventral paramere lobe between lobe top and emargination with dorsal lobe.

Distribution. Pannonian zone, Balkans, southern Russia, Central Asia (Fig. 13).

Ecology. Thermophilic, TAS of 79 sites 18.1 ± 3.1 °C [11.0, 26.4], different from all species except *Tetramorium breviscapus*. Avoids Mediterranean areas, but occurs on Black Sea coast. Typical European habitats are semi-dry and dry grasslands, semi-arid pastures, road embankments, fallow vineyard, rock heaps, sand dunes; exceptionally urban areas. Might be more salt-tolerant than other species, as it was mentioned under "*Tetramorium* cf. *caespi-*

tum" as most frequent ant species in saline field in Ocna Sibiului (Romania) (TĂUȘAN & MARKÓ 2011; material determined by us). In Kyrgyzstan in meadows, steppes, semi-deserts, groves. Soil nests often under stones, sometimes covered with grass; small soil mounds exist.

Phenology: Adult sexuals in nests on 13 June \pm 10 d [1 June, 27 June] (n = 6).

***Tetramorium impurum* (FOERSTER, 1850)** (including U6 sensu SCHLICK-STEINER & al. 2006)

Myrmica impura FOERSTER, 1850: 48; junior synonym of *Tetramorium caespitum*: CURTIS 1854: 215; revived from synonymy: KUTTER 1977: 159; neotype designation: SCHLICK-STEINER & al. 2006: 267. CO1 gene, AFLP data, and morphology of material from the neotype nest investigated in the present study.

Tetramorium caespitum penninum SANTSCHI, 1927: 54; junior synonym of *Tetramorium impurum*: SANETRA & al. 1999: 321. Morphology of type material investigated.

Tetramorium staerckei var. *gregori* KRATOCHVÍL, 1941: 65; junior synonymy fixed hereby based on description (type locality: Czech Republic). **Syn.n.**

Type locality. Mirwart vic. Saint-Hubert (Belgium), (50.03° N 05.27° E), 360 m a.s.l., leg. Y. Roisin, 4.VIII.2000.

CO1 gene. 61 HTs from 161 nests: HT22 (19.9%), HT21 (19.3%), HT122 (9.9%), HT148 (4.3%), HT147 (2.5%), HT20, HT149, HT152, HT285 (each with 1.9%), HT118, HT143, HT246, HT326, HT353, HT355, HT420 (1.2%), HT19, HT23, HT119 - HT121, HT139, HT140, HT142, HT145, HT146, HT150, HT151, HT153, HT237, HT238, HT248, HT249, HT256, HT266, HT267, HT270, HT277, HT278, HT284, HT289, HT291, HT308, HT315, HT320, HT321, HT323, HT327, HT334, HT351, HT352, HT368, HT374, HT375, HT379, HT385, HT397, HT399, HT402, HT403, HT441 (each with 0.6%).

Description of worker. Medium size, CS = 741 \pm 48 [624, 891] μ m. Light brown to blackish, eastern clade often with lighter mesosoma.

Head moderately elongate, CL / CW = 1.017 \pm 0.017 [0.951, 1.049]. Smallest eye of complex, EYE / CS = 0.168 \pm 0.005 [0.155, 0.181]. Scape moderately long, SLd / CS = 0.779 \pm 0.015 [0.741, 0.820]. Mesosoma short and moderately wide, ML / CS = 1.146 \pm 0.025 [1.082, 1.200], MW / CS = 0.632 \pm 0.011 [0.606, 0.654].

Promesonotal dorsum convex, metanotal groove shallow. – Head dorsum and occiput with longitudinal costae and costulae. Postoculo-temporal area of head with rather many costae and costulae, POTCos = 8.80 \pm 1.78 [5.00, 14.75]. Mesosoma dorsum longitudinally rugulose, lateral side of propodeum with pronounced sculpture, Ppss = 29.4 \pm 14.2 [3.4, 79.5]. – Dorsum of petiolar node usually with stronger costae and often fine transverse or reticulate microsculpture, exceptionally smooth. General surface appearance rather dull compared with other species. – Connected stickman-like or reticulate microsculpture: small units scattered over 1st gastral tergite, MC1TG = 15.25 \pm 2.93 [6.70, 24.92]. – Some workers with long c-shaped, crinkly, or sinuous hairs on ventral head posterior to buccal cavity.

Description of male. Paramere structure belongs to *impurum*-like form: rounded ventral paramere lobe without any sharp corner in dorsal or ventral view but with clear division of ventral and dorsal paramere lobes, vis-

ible by deep emargination between lobes in posterior view. No sharp corner at end of ventral lobe visible in posterior view. Relatively short dorsal paramere lobe, visible in posterior and dorsal view. Paramere structure length in lateral view > 1014 μ m. No corner on ventral paramere lobe between lobe top and emargination with dorsal lobe in dorsal and posterior view.

Distribution. Eastern clade: Anatolia, Balkans, Italy, Central Europe, Benelux northward to 52° N. Western clade: Iberia, western France (Fig. 13).

Ecology. Less thermophilic than most other species of complex, TAS of 155 sites 14.1 \pm 2.7 °C [7.7, 21.4] (n = 155), different from all species except *Tetramorium caespitum*. Temperature difference (t-test, p = 0.000) between eastern (TAS of 124 sites 13.7 \pm 2.7 °C) and western clade (TAS of 31 sites 15.7 \pm 2.3 °C). Eastern clade in Central Europe in mountain areas but also lowlands, in southern Europe on high elevation. Typical habitats are meadows, semi-dry grasslands, rocky pastures, subalpine dwarf-shrub heathland, heaths, gravel pits, rock heaps, road embankments, avalanche trenches, rocky bright forests (pine, spruce, larch). In Central Europe often on loamy soil. Eastern clade of *T. impurum* shows strong affinity to stony habitats, while *T. caespitum* is more frequently collected from meadows. Western clade of *T. impurum* in sandy areas near coast, riverbanks, and oak forests. Nests typically under stones, but small soil mounds exist.

Biology. Monogynous (SEIFERT 2007).

Phenology. Adult sexuals in nests on 23 August \pm 27 [29 June, 14 October] (n = 36).

Social parasites. *Anergates atratulus* (n = 1; Tab. S1), *Strongylognathus testaceus* (n = 1; Tab. S1), and *Strongylognathus alpinus* (n = 1; host sub "*Tetramorium caespitum penninum*" in SANTSCHI 1927) were found in nests of *T. impurum*.

***Tetramorium immigrans* SANTSCHI, 1927 stat.n.** (= E sensu SCHLICK-STEINER & al. 2006)

Tetramorium caespitum var. *immigrans* SANTSCHI, 1927: 54; junior synonym of *T. caespitum*: BOLTON 1979: 171; revived from synonymy, raised to species rank, and lectotype designation hereby.

Type locality. Valparaíso (Chile), 33.05° S, 71.61° W, 18 m, leg. Edwards, 1926.

Lectotype designation. Worker of middle card closer to needle than second worker, labeled "TYPE [-] "Chili Valparaiso, Miss Edwards" [-] "Tetramorium caespitum L immigrans Sant". SANTSCHI det. 19 "26" [-] Sammlung Dr. F. Santschi Kairouan", designated as lectotype (Fig. 19). Lectotype worker and seven paralectotype workers in Naturhistorisches Museum Basel (Switzerland). Morphometric data of lectotype in μ m: CL = 914, CW = 912, dAN = 246, EL = 183, EW = 142, FL = 355, HFL = 783, MC1TG = 25.1, ML = 1100, MPPL = 318, MPSP = 427, MPST = 236, MtpW = 461, MW = 592, PEH = 313, PEL = 218, PEW = 310, PLSP = 223, PLST = 243, PnHL = 238, PoOc = 363, POTCos = 12, PPH = 343, PPL = 144, Ppss = 68, PPW = 379, PreOc = 223, RTI = 359, SLd = 727, SPST = 213, SPWI = 289.

CO1 gene. 44 HTs from 213 nests: HT75 (34.3%), HT79 (18.8%), HT70 (12.2%), HT72 (3.8%), HT60 (2.8%), HT76, HT78 (each with 2.3%), HT61, HT74, HT194 (each with 1.9%), HT64, HT77, HT381, HT382 (each with

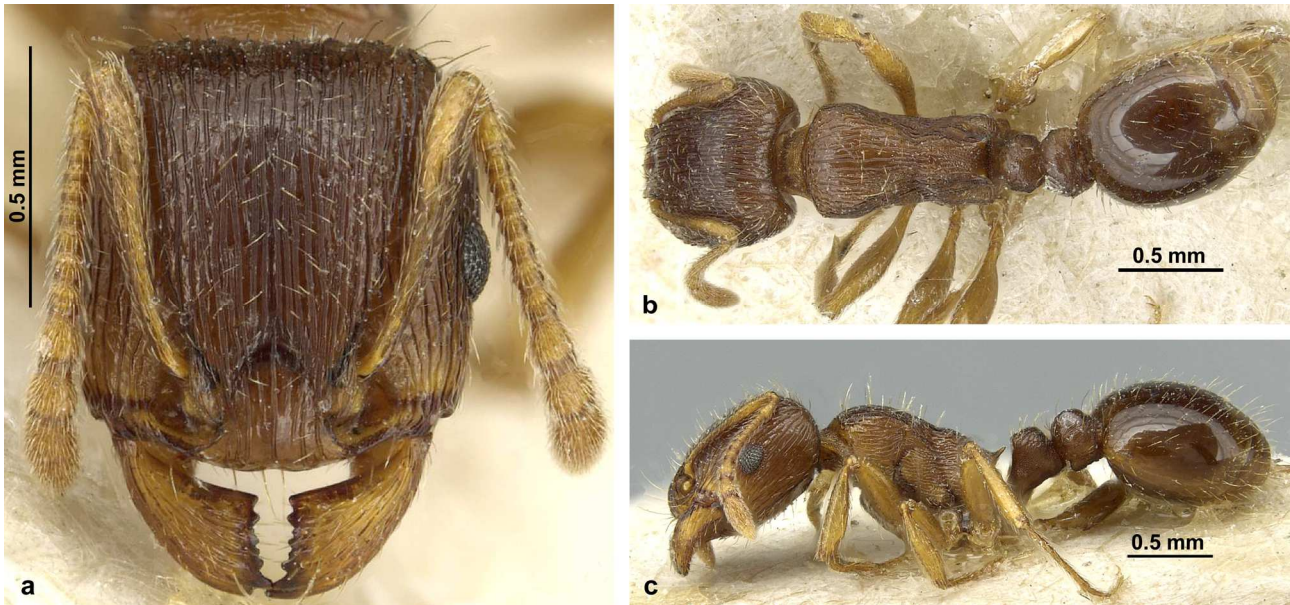


Fig. 19: Lectotype of *Tetramorium immigrans* stat.n. in (A) full face, (B) dorsal, and (C) lateral view (specimen CAS-ENT0913997 from www.AntWeb.org, photographer Zach Lieberman).

0.9%), HT62, HT63, HT65 - HT69, HT71, HT73, HT193, HT195 - HT199, HT202, HT203, HT293, HT312, HT314, HT317, HT318, HT331, HT332, HT345, HT348, HT349, HT384, HT394, HT413 (each with 0.5%).

Description of worker. Largest species of complex, CS = 834 ± 56 [713, 943] μm . Dark brown to blackish, rarely reddish.

Head moderately elongate, CL / CW = 1.012 ± 0.013 [0.985, 1.035]. Eye medium-sized, EYE / CS = 0.176 ± 0.004 [0.167, 0.189]. Scape long, SLd / CS = 0.784 ± 0.014 [0.755, 0.817]. Mesosoma moderately long and narrow, ML / CS = 1.158 ± 0.020 [1.109, 1.201], MW / CS = 0.629 ± 0.012 [0.605, 0.649].

Promesonotal dorsum convex, metanotal groove shallow. – Head dorsum and occiput with longitudinal costae and costulae. Postoculo-temporal area of head with highest number of costae and costulae in complex, POTCos = 12.33 ± 1.67 [8.25, 16.13]. Mesosoma dorsum longitudinally rugulose, lateral side of propodeum with pronounced sculpture, Ppss = 30.5 ± 14.5 [13.6, 63.3]. Dorsum of petiolar with sculpture, reticulate microsculpture, or smooth. General surface appearance rather dull. – Connected stickman-like or reticulate microsculpture: large units scattered over 1st gastral tergite, MC1TG = 21.67 ± 2.68 [16.07, 27.00]. – Some workers with long c-shaped, crinkly, or sinuous hairs on ventral head posterior to buccal cavity.

Description of male. Paramere structure belongs to *caespitum*-like form: ventral paramere lobe with one or two sharp corners; without distinct emargination between paramere lobes in posterior view, both paramere lobes reduced in size. In ventro-posterior view, second corner on ventral paramere lobe > 87 μm apart from first. In posterior view, two corners on ventral lobe.

Distribution. Mediterranean, Western Europe, Central Europe, Balkans, Eastern Europe, Anatolia, Caucasus (Fig. 13), introduced to North (STEINER & al. 2008) and South America (SANTSCHI 1927).

Ecology. More thermophilic than all species except *Tetramorium hungaricum*, *T. breviscapus*, and *T. fusciclava*; TAS of 201 sites 19.9 ± 2.5 °C [13.0, 26.7]. In France and partially Central Europe synanthropic: roadsides, ruderal areas, parks, gardens, pavements, railway constructions, stone pits, balconies, inside of buildings. In Pannonian zone, Mediterranean, and Caucasus most common species in anthropogenic areas, but also primary habitats like semi-arid and arid grasslands, rocky and sandy grasslands, beaches, river banks, rock walls. Bulgarian records from forests. Nests often between cracks of concrete, asphalt, rocks, as well as under stones; small soil mounds exist.

Biology. Hybridizes with *Tetramorium caespitum* (results of this study).

Phenology. Adult sexuals on 27 June \pm 39d [17 March, 29 September] (n = 16).

Social parasites. *Anergates atratulus* (n = 1; Tab. S1) was found in a nest of *Tetramorium immigrans*.

Key to workers of the *Tetramorium caespitum* complex

We present a dichotomous key for Europe (incl. Caucasus and Ural) and Kyrgyzstan here and an online identification key at <https://webapp.uibk.ac.at/ecology/tetramorium>. The application of this key requires magnifications of at least 100 \times and good lighting conditions. Morphometric characters are always in μm . Arithmetic means and standard deviations of indices always refer to means of nest means. Species-specific means for further characters are available in Table S10. The online identification key necessitates morphometric and geographic data of workers and provides correct classifications in 88.0% of individual workers and 97.4% of nest means of two workers.

- 1 British Isles (excl. Channel Islands), Fennoscandia, Baltic. *T. caespitum*
- Central Europe north of 53° N. *T. caespitum*
- Alps or Pyrenees > 2100 m a.s.l. *T. alpestre*

- Italy south of Alps. 2
- Pannonian zone, Balkans (incl. Slovenia and Romania), Eastern Europe. 3
- Other regions. 5
- 2 Eye very large: EL / CS = 0.218 ± 0.005, EW / CS = 0.159 ± 0.003. Distance between outer margins of spines very small and spines short: SPWI / CS = 0.237 ± 0.010, SPST / CS = 0.171 ± 0.008. Petiole and postpetiole narrow: PEW / CS = 0.297 ± 0.009, PPW / CS = 0.391 ± 0.011. Petiole short: PEL / CS = 0.219 ± 0.005. Ridges frontal antennal fossae wider apart: RTI / CS = 0.417 ± 0.010. Stickman-like or reticulate microstructure on first gastral tergite pronounced: MC1TG = 20.57 ± 1.85. Number of postoculo-temporal costae and costulae moderate: POTCos = 6.76 ± 2.12. Discriminant D1 (error 0.0% in 34 workers): 164.05 * SPWI / CS + 95.81 * PEL / CS - 65.61 * RTI / CS - 197.30 * EL / CS + 6.3 < 0. Thermophilic. ***T. fusciclava* stat.n.**
- Eye smaller: EL / CS = 0.196 ± 0.007, EW / CS = 0.147 ± 0.005. Distance between outer margins of spines larger and spine longer: SPWI / CS = 0.286 ± 0.020, SPST / CS = 0.199 ± 0.015. Petiole and postpetiole wider: PEW / CS = 0.324 ± 0.012, PPW / CS = 0.413 ± 0.014. Petiole longer: PEL / CS = 0.235 ± 0.009. Ridges frontal antennal fossae closer together: RTI / CS = 0.399 ± 0.012. D1 > 0 (error 0.5% in 775 workers and 0.0% in 379 nest means of Italian species). 5
- 3 Sculpture on head and mesosoma reduced and large parts smooth and shiny. Very few postoculo-temporal costae and costulae: POTCos = 2.14 ± 1.21. Lateral face of propodeum anterior propodealstigma often smooth: Ppss = 85.6 ± 36.1. Eye large: EL / CS = 0.211 ± 0.009, EW / CS = 0.156 ± 0.006. Postpetiole narrow: PPW / CS = 0.382 ± 0.013. Mesosoma short: ML / CS = 1.103 ± 0.018. Hind femur short: HFL / CS = 0.770 ± 0.011. Discriminant D2 (error 7.8% in 51 workers and 0.0% in 23 nest means): 3.606 * PPW + 27.209 * POTCos + 6.072 * PEL + 1.375 * PnHL - 11.221 * EYE - 886 < 0. Thermophilic. ***T. hungaricum***
- Sculpture on head often well developed, extending over most parts of dorsal head surface. Number of postoculo-temporal costae and costulae higher: POTCos = 8.5 ± 2.4. Lateral face of propodeum anterior propodealstigma often not smooth: Ppss = 35.6 ± 19.3. Eye smaller: EL / CS = 0.196 ± 0.007, EW / CS = 0.147 ± 0.005. Postpetiole wider: PPW / CS = 0.413 ± 0.014. Mesosoma longer: ML / CS = 1.117 ± 0.027. Hind femur longer: HFL / CS = 0.812 ± 0.026. D2 > 0 (error 1.1% in 903 workers and 0.5% in 433 nest means of all species except *T. fusciclava*). 4
- 4 Balkans only. Scape very short: SLd / CS = 0.730 ± 0.013. Petiole and mesosoma short: PEL / CS = 0.215 ± 0.002, ML / CS = 1.121 ± 0.014. Sculpture on large parts of head and mesosoma pronounced, but often distinct smooth and shiny area on lateral face of propodeum anterior the propodeal stigma: Ppss = 73.6 ± 16.6. Number of postoculo-temporal costae and costulae small to moderate: POTCos = 5.95 ± 0.53. Discriminant D3 (error 0.0% in 15 workers): 5.405 * SLd + 6.028 * PEH + 8.718 * PEL - 5.216 * CS - 5.462 * PEW - 4.074 * PLSP - 53 < 0. Thermophilic. ***T. breviscapus* sp.n.**
- All regions. Scape longer: SLd / CS = 0.778 ± 0.016. Petiole and mesosoma longer: PEL / CS = 0.235 ± 0.008, ML / CS = 1.167 ± 0.027. Contrast between smooth and shiny area on lateral face of propodeum and other regions not always obvious. Number of postoculo-temporal costae and costulae moderate to large: POTCos = 8.48 ± 2.40. D3 > 0 (error 0.8% in 922 workers and 0.2% in 447 nest means of all species except *T. hungaricum*). 5
- 5 Sculpture well developed, number of postoculo-temporal costae and costulae large, smooth area on lateral face of propodeum anterior propodeal stigma small: POTCos = 10.53 ± 1.75, Ppss = 16.9 ± 5.3. Eye larger: EL / CS = 0.202 ± 0.006, EW / CS = 0.153 ± 0.004. Discriminant D4 (error 3.7% in 81 workers and 0.0% in 41 nest means of *staerckei*): 13.144 * ML + 89.666 * dAN + 304.936 * POTCos + 123.574 * EYE + 57.722 * PLST + 106.414 * MC1TG - 40.588 * MtpW - 50.045 * CW - 21.122 * RTI - 46.477 * PLSP + 2800 > 0. Thermophilic. 6
- Sculpture strongly reduced to well developed. Eye smaller: EL / CS = 0.195 ± 0.007, EW / CS = 0.146 ± 0.005. D4 < 0 (error 2.0% in 789 workers and 0.3% in 375 nest means of all species except *T. fusciclava* and *T. immigrans*). 7
- 6 Stickman-like or reticulate microsculpture on first gastral tergite moderate: MC1TG = 15.93 ± 2.35. Distance between antennal fossae larger: dAN / CS = 0.300 ± 0.005. Mesosoma longer: ML / CS = 1.188 ± 0.025. Smaller: CS = 746 ± 57. Discriminant D5 (error 1.2% in 81 workers and 0.0% in 41 nest means): 58.624 * MtpW + 58.287 * CL + 84.382 * CW - 57.153 * ML - 51.265 * PPW - 159.873 * dAN - 28593 < 0. Often natural habitats. ***T. staerckei* sp.rev.**
- Stickman-like or reticulate microsculpture on first gastral tergite pronounced: MC1TG = 21.67 ± 2.68. Distance between antennal fossae smaller: dAN / CS = 0.280 ± 0.007. Mesosoma shorter: ML / CS = 1.158 ± 0.020. Larger: CS = 834 ± 56. D5 > 0 (error 0.0% in 84 workers). Often in anthropogenically influenced, vegetation-free, and even concreted habitats, but also rocky natural habitats. ***T. immigrans* stat.n.**
- 7 Kyrgyzstan. ***T. indocile***
- Other regions. 8
- 8 Stickman-like or reticulate microsculpture on first gastral tergite pronounced: MC1TG = 21.67 ± 2.68. Number of postoculo-temporal costae and costulae large, POTCos = 12.33 ± 1.67. Distance between outer margins of spines smaller: SPWI / CS = 0.269 ± 0.020. Eye larger: EL / CS = 0.201 ±

- 0.005, EW / CS = 0.152 ± 0.004. Postocular distance smaller: PoOc / CS = 0.387 ± 0.006. Discriminant D6 (error 8.3% in 84 workers and 2.5% in 40 nest means): 3.348 * CL + 23.130 * POTCos + 9.953 * EW + 2.235 * PPH + 3.133 * PLST + 19.914 * MC1TG - 1.869 * SPWI - 4.364 * MW - 3.172 * PoOc - 1.967 * PPL - 3.243 * PLSP - 0.047 * ALT - 1295 > 0. Thermophilic. In Europe < 1000 m a.s.l. Often in anthropogenically influenced, vegetation-free, and even concreted habitats, but also rocky natural habitats. *T. immigrans* stat.n.
- Stickman-like or reticulate microsculpture on first gastral tergite reduced: MC1TG = 13.71 ± 2.73. Number of postoculo-temporal costae and costulae often smaller, POTCos = 7.74 ± 1.96. Distance between outer margins of spines larger: SPWI / CS = 0.288 ± 0.019. Eye smaller: EL / CS = 0.195 ± 0.007, EW / CS = 0.146 ± 0.005. Postocular distance larger: PoOc / CS = 0.398 ± 0.010. D6 < 0 (error 0.7% in 717 workers and 0.3% in 349 nest means of *T. alpestre*, *T. caespitum*, *T. indocile*, *T. caucasicum*, and *T. impurum*). 9
 - 9 Iberian Peninsula, mainland western France, Balearic Islands, Corsica, Sardinia, British Channel Islands. 10
 - Mainland eastern France, Switzerland, Austria, mainland Italy, Sicily, Balkans (incl. Slovenia and Romania). > 900 m a.s.l. 11
 - Mainland eastern France, Switzerland, Austria, mainland Italy, Sicily, Balkans (incl. Slovenia and Romania). < 900 m a.s.l. 13
 - Benelux, Germany, Poland, Czechia, Slovakia, Hungary. 13
 - Eastern Europe, Caucasus. 16
 - 10 Mesosoma shorter and narrower: ML / CS = 1.131 ± 0.023, MW / CS = 0.627 ± 0.010. Postocular distance larger: PoOc / CS = 0.408 ± 0.010. Longest hair on frontolateral corner of pronotum shorter: PnHL / CS = 0.244 ± 0.023. Discriminant D7 (error 7.1% in 56 workers and 0.0% in 28 nest means of *impurum* western clade): 3.518 * HFL + 2.918 * ML + 6.601 * MW + 4.883 * dAN + 2.229 * PnHL - 4.404 * CS - 3.962 * SLd - 24.810 * POTCos - 5.711 * PEL - 11.518 * MPST - 5.995 * SPST - 9.220 * MC1TG + 22.761 * LAT + 0.109 * ALT - 215 < 0. *T. impurum*
 - Mesosoma longer and wider: ML / CS = 1.164 ± 0.023, MW / CS = 0.643 ± 0.013. Postocular distance smaller: PoOc / CS = 0.397 ± 0.009. Longest hair on frontolateral area of pronotum longer: PnHL / CS = 0.272 ± 0.021. D7 > 0 (error 4.5% in 132 workers and 1.5% in 65 nest means of *T. alpestre*, *T. caespitum*, and *T. indocile* in the region defined in 9a). 14
 - 11 Petiole wider, distance between outer margins of propodeal spines larger: PEW / CS = 0.334 ± 0.011, SPWI / CS = 0.303 ± 0.021. Petiole higher: PEH / CS = 0.356 ± 0.009. Longest hair on frontolateral area of pronotum shorter: PnHL / CS = 0.248 ± 0.025. Distance between antennal fossae smaller: dAN / CS = 0.281 ± 0.006. Discriminant D8 (error 4.5% in 88 workers and 0.0% in 44 nest means of *T. alpestre* in the region defined in 9-11): 2.810 * ML + 5.130 * PPW + 1.876 * SPWI + 4.863 * PreOc + 1.182 * Ppss - 2.349 * MtpW - 2.908 * CW - 2.565 * SLd - 8.968 * POTCos - 1.265 * PnHL - 4.676 * MPST + 0.186 * ALT + 109 > 0. ... 12
 - Petiole narrower, distance between outer margins of propodeal spines smaller: PEW / CS = 0.322 ± 0.011, SPWI / CS = 0.282 ± 0.017. Petiole lower: PEH / CS = 0.346 ± 0.009. Longest hair on frontolateral corner of pronotum longer: PnHL / CS = 0.276 ± 0.020. Distance between antennal fossae larger: dAN / CS = 0.288 ± 0.007. D8 < 0 (error 4.5% in 222 workers and 0.9% in 111 nest means of *T. caespitum* and *T. indocile* in the region defined in 9-11). 13
 - 12 Sculpture on dorsum of petiole and postpetiole often less developed; interspaces between the stronger rugae and rugulae frequently smooth or with faint microsculpture. Dorsum of postpetiole often with shiny areas. Rugae and rugulae on paramedian and lateral areas of dorsal postpetiole weaker and with more longitudinal orientation. Pigmentation of mesosoma varying from brown to black. Longest hair on frontolateral corner of pronotum shorter: PnHL / CS = 0.248 ± 0.025. Postpetiole wider: PPW / CS = 0.424 ± 0.011. Eye wider: EW / CS = 0.146 ± 0.004. Discriminant D9 (error 6.8% in 88 workers and 2.3% in 44 nest means in the region defined in 9b): 3.370 * ML + 5.764 * PPW + 11.408 * EYE + 4.184 * PEL + 4.097 * PPL + 3.508 * Ppss - 3.533 * PoOc - 6.001 * CW - 2.123 * SLd - 20.511 * POTCos - 3.151 * MPSP + 0.135 * ALT + 270 > 0. *T. alpestre*
 - Sculpture on dorsum of petiole and postpetiole often more developed; interspaces between stronger rugae and rugulae with fine transverse or reticulate microsculpture. Dorsum of postpetiole often rather dull; shiny areas can occur, but only on small patch on dorsomedian postpetiole. Rugae and rugulae on paramedian and lateral areas of dorsal postpetiole coarser and semicircular. Mesosoma in adult workers usually light to dark brown, never black. Longest hair on frontolateral corner of pronotum longer: PnHL / CS = 0.260 ± 0.026. Postpetiole narrower: PPW / CS = 0.411 ± 0.012. Eye narrower: EW / CS = 0.142 ± 0.004. D9 < 0 (error 5.2% in 96 workers and 2.1% in 48 nest means in *T. impurum* eastern clade). *T. impurum*
 - 13 Sculpture on dorsum of petiole and postpetiole often more developed; interspaces between stronger rugae and rugulae with fine transverse or reticulate microsculpture. Dorsum of postpetiole often rather dull; shiny areas can occur, but only on small patch on dorsomedian postpetiole. Rugae and rugulae on paramedian and lateral areas on dorsum of postpetiole coarser and semicircular. Mesosoma usually light to dark brown, never black. Distance between antennae fossae smaller: dAN / CS = 0.278 ± 0.006. Eye shorter: EL / CS = 0.189 ± 0.006. Discriminant D10 (error 3.1% in 96 workers and

- 0.0% in 48 nest means of *T. impurum* eastern clade): $1.589 * SPWI + 2.086 * CW + 3.926 * SLd + 13.758 * POTCos + 5.145 * PreOc + 7.708 * PEH + 2.675 * MPSP + 3.374 * PLSP - 2.670 * HFL - 1.564 * ML - 3.056 * MtpW - 7.396 * dAN - 11.118 * EYE - 3.098 * PPH - 1.105 * PnHL - 3.373 * PLST + 11.700 * LAT + 0.118 * ALT - 556 > 0$ ***T. impurum***
- Sculpture on dorsum of petiole and postpetiole often less developed; interspaces between stronger rugae and rugulae frequently smooth or with only suggested microsculpture. Dorsum of postpetiole often with shiny areas. Rugae and rugulae on parame-dian and lateral areas on dorsum of postpetiole weaker and with more longitudinal orientation. Pig-mentation of mesosoma varying from brown to black. Distance between antennae fossae larger: $dAN = 0.288 / CS \pm 0.006$. Eye longer: $EL / CS = 0.196 \pm 0.006$. $D10 < 0$ (error 4.0% in 277 workers and 0.7% in 138 nest means of European *T. caespitum* eastern clade and European *T. indocile*). **17**
 - 14 Maximum distance between outer margins of pro-podeal spines larger: $SPWI / CS = 0.301 \pm 0.017$. Petiole and postpetiole higher: $PEH / CS = 0.360 \pm 0.010$, $PPH / CS = 0.373 \pm 0.011$. Discriminant $D11$ (error 1.9% in 54 workers and 0.0% in 27 nest means in the region defined in 9-10): $5.135 * PPW + 5.411 * SPWI + 29.459 * POTCos + 6.689 * PEH - 5.368 * PPL - 2.306 * PnHL - 17.061 * MPST - 3.016 * SPST + 0.146 * ALT - 48 > 0$. > 1000 m a.s.l. ***T. alpestre***
 - Maximum distance between outer margins of pro-podeal spines smaller: $SPWI / CS = 0.278 \pm 0.016$. Petiole and postpetiole lower: $PEH / CS = 0.345 \pm 0.008$, $PPH / CS = 0.361 \pm 0.010$. $D11 < 0$ (er-ror 2.7% in 75 workers and 2.7% in 37 nest means of *T. caespitum* and *T. indocile* in the region defined in 9-10). **15**
 - 15 Mainland France (excl. Pyrenees), British Channel Islands. **17**
 - Iberian Peninsula, French Pyrenees, Balearic Is-lands, Corsica, Sardinia. **18**
 - 16 Caucasus only. Distance between frontal carinae and antennal fossae smaller: $FL / CS = 0.382 \pm 0.008$, $dAN / CS = 0.283 \pm 0.005$. Distance be-tween propodeal stigma and dorsocaudal end of pro-podeal lobe smaller: $PLST / CS = 0.252 \pm 0.008$. Discriminant $D12$ (error 0.0% in 32 workers): $4.043 * SPWI + 5.776 * CL + 4.686 * PPH + 1.199 * Ppss + 11.585 * MC1TG - 3.593 * PPW - 3.318 * FL - 4.665 * PreOc - 1.017 * PnHL - 6.289 * MPSP - 3.502 * PLST + 14.909 * LAT + 0.227 * ALT - 1870 > 0$. > 1000 m a.s.l. ...***T. caucasicum* sp.n.**
 - Distance between frontal carinae and antennal fos-sae larger: $FL / CS = 0.391 \pm 0.008$, $dAN / CS = 0.289 \pm 0.006$. Distance between propodeal stigma and dorsocaudal end of propodeal lobe larger: $PLST / CS = 0.262 \pm 0.008$. $D12 < 0$ (error 0.8% in 122 workers and 0.0% in 61 nest means of *T. caespitum* and *T. indocile* in the region defined in 9-16). **17**
 - 17 Hind femur and scape longer: $HFL / CS = 0.826 \pm 0.023$, $SLd / CS = 0.779 \pm 0.014$. Mesosoma longer and metapleuron wider: $ML / CS = 1.179 \pm 0.021$, $MtpW / CS = 0.504 \pm 0.012$. Postpetiole longer: $PPL / CS = 0.169 \pm 0.008$. Longest hair on frontolateral corner of pronotum longer: $PnHL / CS = 0.279 \pm 0.020$. Larger: $CS = 770 \pm 47$. Sculpture on head and mesosoma developed. Dis-criminant $D13$ (error 3.3% in 242 workers and 0.8% in 121 nest means of *T. caespitum* eastern clade): $4.272 * CS + 3.883 * CL + 7.783 * dAN + 4.929 * PEH + 2.350 * Ppss + 4.209 * MPSP + 8.733 * MC1TG - 6.570 * MtpW - 7.246 * PoOc - 7.085 * FL - 3.367 * RTI - 3.459 * SLd - 10.625 * PPL + 247 < 0$ ***T. caespitum***
 - Hind femur and scape shorter: $HFL / CS = 0.791 \pm 0.023$, $SLd / CS = 0.764 \pm 0.013$. Mesosoma shorter and metapleuron narrower: $ML / CS = 1.155 \pm 0.020$, $MtpW / CS = 0.488 \pm 0.009$. Postpetiole shorter: $PPL / CS = 0.157 \pm 0.005$. Longest hair on frontolateral corner of pronotum shorter: $PnHL / CS = 0.254 \pm 0.023$. Smaller: $CS = 717 \pm 52$. Sculpture on head and mesosoma sometimes reduced and large parts smooth and shiny. $D13 > 0$ (error 10.1% in 79 workers and 2.8% in 36 *T. indocile* nest means without Iberian population). ***T. indocile***
 - 18 Head longer: $CL / CW = 1.012 \pm 0.007$. Posttem-poral distance larger: $PoOc / CS = 0.405 \pm 0.010$. Distance between antennal fossae smaller: $dAN / CS = 0.278 \pm 0.009$. Eye smaller: $EL / CS = 0.195 \pm 0.008$, $EW / CS = 0.145 \pm 0.004$. Propodeal spines shorter: $SPST / CS = 0.185 \pm 0.007$. Discriminant $D14$ (error 23.1% in 52 workers, and 4.2% in 24 *T. caespitum* nest means from Iberia): $6.532 * CW + 10.326 * SPST + 8.118 * PLSP - 17.560 * PoOc - 19.893 * PreOc + 1195 < 0$ ***T. caespitum***
 - Head shorter: $CL / CW = 1.003 \pm 0.006$. Posttem-poral distance smaller: $PoOc / CS = 0.391 \pm 0.011$. Distance between antennal fossae larger: $dAN / CS = 0.288 \pm 0.007$. Eye larger: $EL / CS = 0.203 \pm 0.005$, $EW / CS = 0.150 \pm 0.003$. Propodeal spines longer: $SPST / CS = 0.194 \pm 0.010$. $D14 > 0$ (error 12.5% in 24 workers and 0.0% in 12 nest means of Western and Central European *T. indocile*). .. ***T. indocile***
- Key to males of the *Tetramorium caespitum* complex**
- This dichotomous key considers Europe (incl. Caucasus and Ural) and Kyrgyzstan. The male genital morphology remains unknown for *Tetramorium fusciclava* stat.n. and *T. breviscapus* sp.n., which are endemic to Italy and the Balkans, respectively. Figures S3 - 5 show typical exam-ples of paramere structure; for further examples, see Figure S1; "n" is always the number of nests investigated.
- 1 Ventral view: one or two corners visible on ven-tral paramere lobe (Fig. S3a - d, arrows). Posterior view: no distinct emargination between paramere lobes (Fig. S4a - d, A arrows); *caespitum*-like form. .. **2**
 - Ventral view: no corner but rounded ends on ven-tral paramere lobe (Fig. S3e - h, arrows). Posterior view: distinct division of ventral and dorsal lobe by

- deep emargination between paramere lobes (Fig. S4e - h, A arrows); *impurum*-like form. 4
- 2 Ventro-posterior view: ventral paramere lobe with two corners, > 87 μm apart (101 ± 16 ; $n = 8$) (here in posterior view: Fig. S4d, B arrow). Often in anthropogenically influenced, vegetation-free, and even concreted habitats. In Europe nesting < 1000 m a.s.l. *T. immigrans* stat.n.
- Ventro-posterior view: ventral paramere lobe has one corner or two corners, < 87 μm apart (here in posterior view: Fig. S4a - c, B arrow). All regions and habitats. 3
- 3 Posterior view: two sharp corners on ventral paramere lobe (Fig. S4c, B arrow, $n = 5$). Corner between ventral and dorsal lobe often missing or small and positioned more ventral (Fig. S4c, C arrow). In Europe rare and < 51° N. *T. indocile*
- Posterior view: usually one corner on ventral paramere lobe (Fig. S4a - b, B arrows, $n = 41$). Corner between ventral and dorsal lobe often large and positioned more median (Fig. S4a, b, A arrows), but sometimes missing or small. *T. caespitum* (whole Europe) and *T. hungaricum* (Pannonian zone, Balkans, Eastern Europe)
- 4 Posterior view: sharp corner at end of ventral paramere lobe (Fig. S4f, B arrow, $n = 2$). Caucasus only. Nesting > 1000 m a.s.l. *T. caucasicum* sp.n.
- Posterior view: rounded margin at end of ventral paramere lobe (Fig. S4e, g, h, B arrows). 5
- 5 Lateral view: paramere length < 991 μm ($n = 11$). Posterior view: dorsal and ventral paramere lobes often longer and narrower (Fig. S4e). Dorsal view: dorsal paramere lobe often longer and sharp-ended (Fig. S5a, A arrow). Nesting > 900 m a.s.l. ... *T. alpestre*
- Lateral view: paramere length > 1014 μm ($n = 21$). Posterior view: dorsal and ventral paramere lobes often shorter and wider (Fig. S4g, h). Dorsal view: dorsal paramere often shorter and with round end (Fig. S5b, c, A arrow). Nesting < 2000 m a.s.l. 6
- 6 Dorsal or posterior view: ventral paramere lobe with distinct corner between lobe top and emargination with dorsal paramere lobe (Fig. S4g, C arrow; Fig. S5b, B arrow, $n = 3$). Pannonian zone, Balkans, Eastern Europe, Central Asia. *T. staerckei* sp.rev.
- Dorsal or posterior view: ventral paramere lobe without corner between lobe top and emargination with dorsal paramere lobe (Fig. S4h, C arrow; Fig. S5c, B arrow, $n = 18$). Iberia, Western Europe, Central Europe, Balkans, Anatolia. *T. impurum*

Acknowledgments

We thank 156 collectors for generously sharing *Tetramorium* material (Tab. S1); Philipp Andesner, Clemens Folterbauer, Martin-Carl Kinzner, Jasmin Klarica, Anna Kluibenschedl, Patrick Krapf, Elisabeth Mayr, and Andrea Peskoller for assistance in the laboratory; Thomas Dejaco and Paschalia Kapli for assistance in analyzing genetic data; Katharina Spiß for drawing most of the male genital images; Karl Moder for assistance in statistics; Christian

Haider for coding large parts of the online identification key; Isabelle Zürcher-Pfander (Naturhistorisches Museum Basel), Alexander G. Radchenko (Museum and Institute of Zoology, Kiev), Fabrizio Rigato (Museo Civico di Storia Naturale, Milano), Maria Tavano (Museo Civico di Storia Naturale, Genova), Anne Freitag (Musée cantonal de zoologie, Lausanne), Ionut Tăușan (Museum of Natural History, Sibiu / Hermannstadt) for loans of type material; Fabrizio Santi (Dipartimento di Biologia Evoluzionistica Sperimentale, Bologna) for photographs of type material; Roland Schultz (Senckenberg Museum of Natural History Görlitz) for making and processing z-stack photographs of type material; ad-hoc Editor-in-Chief Herbert Zettel, reviewer Marek Borowiec, and an anonymous reviewer for extensive input that helped to improve this paper. Research of HCW and CM was supported by the University of Innsbruck and the Austrian Science Fund (FWF, P23409).

References

- ABBOTT, R., ALBACH, D., ANSELL, S., ARNTZEN, J.W., BAIRD, S.J.E., BIERNE, N., BOUGHMAN, J., BRELSFORD, A., BUERKLE, C.A., BUGGS, R., BUTLIN, R.K., DIECKMANN, U., EROUKHMANOFF, F., GRILL, A., CAHAN, S.H., HERMANSEN, J.S., HEWITT, G., HUDSON, A.G., JIGGINS, C., JONES, J., KELLER, B., MACZEWSKI, T., MALLETT, J., MARTINEZ-RODRIGUEZ, P., MÖST, M., MULLEN, S., NICHOLS, R., NOLTE, A.W., PARISOD, C., PFENNIG, K., RICE, A.M., RITCHIE, M.G., SEIFERT, B., SMADJA, C.M., STELKENS, R., SZYMURA, J.M., VÄINÖLÄ, R., WOLF, J.B.W. & ZINNER, D. 2013: Hybridization and speciation. – *Journal of Evolutionary Biology* 26: 229-246.
- ARTHOFFER, W. 2010: tinyFLP and tinyCAT: software for automatic peak selection and scoring of AFLP data tables. – *Molecular Ecology Research* 10: 385-388.
- ARTHOFFER, W., RAUCH, H., THALER-KNOFLACH, B., MODER, K., MUSTER, C., SCHLICK-STEINER, B.C. & STEINER, F.M. 2013: How diverse is *Mitopus morio*? Integrative taxonomy detects cryptic species in a small-scale sample of a widespread harvestman. – *Molecular Ecology* 22: 3850-3863.
- ARTHOFFER, W., SCHLICK-STEINER, B.C. & STEINER, F.M. 2011: optiFLP: software for automated optimization of amplified fragment length polymorphism scoring parameters. – *Molecular Ecology Resources* 11: 1113-1118.
- BAGHERIAN YAZDI, A., MÜNCH, W. & SEIFERT, B. 2012: A first demonstration of interspecific hybridization in *Myrmica* ants by geometric morphometrics (Hymenoptera: Formicidae). – *Myrmecological News* 17: 121-131.
- BERNARDI, G., LONGO, G.C. & QUIROS, T.E.A.L. 2017: *Altrichthys alelia*, a new brooding damselfish (Teleostei, Perciformes, Pomacentridae) from Busuanga Island, Philippines. – *Zookeys* 675: 45-55.
- BICKFORD, D., LOHMAN, D.J., SODHI, N.S., NG, P.K.L., MEIER, R., WINKER, K., INGRAM, K.K. & DAS, I. 2007: Cryptic species as a window on diversity and conservation. – *Trends in Ecology & Evolution* 22: 148-155.
- BOLTON, B. 1979: The ant tribe Tetramoriini (Hymenoptera: Formicidae). The genus *Tetramorium* MAYR in the Malagasy region and in the New World. – *Bulletin of the British Museum (Natural History)*. Entomology 38: 129-181.
- BOLTON, B. 1995: A new general catalogue of the ants of the world. – Harvard University Press, Cambridge, MA, 504 pp.
- BOLTON, B. 2014: New general catalogue of the ants of the world, and synopsis of taxonomic publications on Formicidae. – <http://antwiki.org/wiki/images/0/0a/NGC_July_2014.pdf>, retrieved on 15 July 2017.

- BOROWIEC, L. 2014: Catalogue of ants of Europe, the Mediterranean Basin and adjacent regions (Hymenoptera: Formicidae). – Genus 25: 1-340.
- BOROWIEC, L., GALKOWSKI, C. & SALATA, S. 2016: Redescription of *Tetramorium atlante* CAGNIANT, 1970, new status (Hymenoptera: Formicidae: Myrmicinae). – Annales Zoologici 66: 43-52.
- BRAČKO, G., WAGNER, H.C., SCHULZ, A., GIOAHIN, E., MATIČIĆ, J. & TRATNIK, A. 2014: New investigation and a revised checklist of the ants (Hymenoptera: Formicidae) of the Republic of Macedonia. – North-Western Journal of Zoology 10: 10-24.
- CARSTENS, B.C., PELLETIER, T.A., REID, N.M. & SATLER, J.D. 2013: How to fail at species delimitation. – Molecular Ecology 22: 4369-4383.
- CLOUSE, R.M., BLANCHARD, B.D., GIBSON, R., WHEELER, W.C. & JANDA, M. 2016: Taxonomic updates for some confusing Micronesian species of *Camponotus* (Hymenoptera: Formicidae: Formicinae). – Myrmecological News 23: 139-152.
- COLLINGWOOD, C.A. 1979: The Formicidae (Hymenoptera) of Fennoscandia and Denmark. – Fauna Entomologica Scandinavica 8: 1-174.
- CONSANI, M. & ZANGHERI, P. 1952: Fauna di Romagna. Imenotteri – Formicidi. – Memorie della Società Entomologica Italiana 31: 38-48.
- CORANDER, J., SIRÉN, J. & ARJAS, E. 2008: Bayesian spatial modeling of genetic population structure. – Computational Statistics 23: 111-129.
- CSŐSZ, S. & FISHER, B.L. 2016: Taxonomic revision of the Malagasy members of the *Nesomyrmex angulatus* species group using the automated morphological species delineation protocol NC-PART-clustering. – PeerJ 4: art. e1796.
- CSŐSZ, S., HEINZE, J. & MIKÓ, I. 2015: Taxonomic synopsis of the ponto-mediterranean ants of *Temnothorax nylanderii* species-group. – Public Library of Science One 10: art. e0140000.
- CSŐSZ, S. & MARKÓ, B. 2004: Redescription of *Tetramorium hungaricum* RÖSZLER, 1935, a related species of *T. caespitum* (LINNAEUS, 1758) (Hymenoptera: Formicidae). – Myrmecologische Nachrichten 6: 49-59.
- CSŐSZ, S., RADCHENKO, A. & SCHULZ, A. 2007: Taxonomic revision of the Palearctic *Tetramorium chefketi* species complex (Hymenoptera: Formicidae). – Zootaxa 1405: 1-38.
- CSŐSZ, S. & SCHULZ, A. 2010: A taxonomic review of the Palearctic *Tetramorium ferox* species-complex (Hymenoptera: Formicidae). – Zootaxa 2401: 1-29.
- CSŐSZ, S., SEIFERT, B., MÜLLER, B., TRINDL, A., SCHULZ, A. & HEINZE, J. 2014a: Cryptic diversity in the Mediterranean *Temnothorax lichtensteini* species complex (Hymenoptera: Formicidae). – Organisms Diversity & Evolution 14: 75-88.
- CSŐSZ, S., WAGNER, H.C., BOZSÓC, M., SEIFERT, B., ARTHOFER, W., SCHLICK-STEINER, B.C., STEINER, F.M. & PÉNZES, Z. 2014b: *Tetramorium indocile* SANTSCHEI, 1927 stat. rev. is the proposed scientific name for *Tetramorium* sp. C sensu SCHLICK-STEINER & al. (2006) based on combined molecular and morphological evidence (Hymenoptera: Formicidae). – Zoologischer Anzeiger 253: 469-481.
- CURTIS, J. 1854: On the genus *Myrmica* and other indigenous ants. – Transactions of the Linnean Society of London 21: 211-220.
- DE QUEIROZ, K. 2007: Species concepts and species delimitation. – Systematic Biology 56: 879-886.
- DEJACO, T., GASSNER, M., ARTHOFER, W., SCHLICK-STEINER, B.C. & STEINER, F.M. 2016: Taxonomist's nightmare ... evolutionist's delight: an integrative approach resolves species limits in jumping bristletails despite widespread hybridization and parthenogenesis. – Systematic Biology 65: 947-974.
- EMERY, C. 1925: Notes critiques de Myrmécologie. – Extrait des Annales & Bulletin de la Société Entomologique de Belgique 64: 177-191.
- FUNK, D.J. & OMLAND, K.E. 2003: Species-level paraphyly and polyphyly: Frequency, causes, and consequences, with insights from animal mitochondrial DNA. – Annual Review of Ecology, Evolution, and Systematics 34: 397-423.
- GOTZEK, D., AXEN, H.J., SUAREZ, A.V., CAHAN, S.H. & SHOEMAKER, D. 2015: Global invasion history of the tropical fire ant: a stowaway on the first global trade routes. – Molecular Ecology 24: 374-388.
- GÜSTEN, R., SCHULZ, A. & SANETRA, M. 2006: Redescription of *Tetramorium forte* FOREL, 1904 (Insecta: Hymenoptera: Formicidae), a western Mediterranean ant species. – Zootaxa 1310: 1-35.
- HAAG-LIAUTARD, C., COFFEY, N., HOULE, D., LYNCH, M., CHARLESWORTH, B. & KEIGHTLEY, P.D. 2008: Direct estimation of the mitochondrial DNA mutation rate in *Drosophila melanogaster*. – Public Library of Science Biology 6: 1706-1714.
- HAZKANI-COVO, E., ZELLER, R.M. & MARTIN, W. 2010: Molecular poltergeists: mitochondrial DNA copies (numts) in sequenced nuclear genomes. – Public Library of Science Genetics 6: art. e1000834.
- JOHANSEN, H. 1955: Die Jenissei-Faunenscheide. – Zoologische Jahrbücher, Abteilung für Systematik, Ökologie und Geographie der Tiere 83: 237-247.
- KAPLI, P., LUTTEROPP, S., ZHANG, J., KOBERT, K., PAVLIDIS, P., STAMATAKIS, A. & FLOURI, T. 2017: Multi-rate Poisson tree processes for singlelocus species delimitation under maximum likelihood and Markov chain Monte Carlo. – Bioinformatics: 331630-331638.
- KINZNER, M.-C., WAGNER, H.C., PESKOLLER, A., MODER, K., DOWELL, F.E., ARTHOFER, W., SCHLICK-STEINER, B.C. & STEINER, F.M. 2015: A near-infrared spectroscopy routine for unambiguous identification of cryptic ant species. – PeerJ 3: art. e991.
- KLINGENBERG, C.P. 2011: MorphoJ: an integrated software package for geometric morphometrics. – Molecular Ecology Resources 11: 353-357.
- KLINGENBERG, C.P., BARLUENGA, M. & MEYER, A. 2002: Shape analysis of symmetric structures: quantifying variation among individuals and asymmetry. – Evolution 56: 1909-1920.
- KRAPF, P., RUSSO, L., ARTHOFER, W., MÖST, M., STEINER, F.M. & SCHLICK-STEINER, B.C. 2017: An Alpine ant's behavioural polymorphism: monogyny with and without internest aggression in *Tetramorium alpestre*. – Ethology Ecology & Evolution, doi: 10.1080/03949370.2017.1343868.
- KRATOCHVÍL, J. 1941: [Untitled. New species, *Tetramorium moravicum*, attributed to KRATOCHVÍL.]. p. 86.– In: NOVÁK, V. & SADIL, J. 1941: Klíč k urcování mravencu střední Evropy se zvláštním zretelem k mravenci zvěre Cech a Moravy. – Entomologické listy 4: 65-115.
- KRATOCHVÍL, J. 1944: [Untitled.] – In: KRATOCHVÍL, J., NOVÁK, V. & ŠNOFLÁK, J. 1944: Mohelno. Soubor prací venovaných studiu významné památky přírodní. 5. Hymenoptera – Aculeata. Formicidae – Apidae – Vespidae. – Archiv Svazu na Ochranu Přírody a Domoviny na Morave 6: 1-155.
- LANFEAR, R., CALCOTT, B., HO, S.Y.W. & GUINDON, S. 2012: PartitionFinder: combined selection of partitioning schemes and substitution models for phylogenetic analyses. – Molecular Biology and Evolution 29: 1695-1701.
- LOPEZ, J.V., CULVER, M., STEPHENS, J.C., JOHNSON, W.E. & O'BRIEN, S.J. 1997: Rates of nuclear and cytoplasmic mitochondrial DNA sequence divergence in mammals. – Molecular Biology and Evolution 14: 277-286.

- LUNT, D.H., ZHANG, D.-X., SZYMURA, J.M. & HEWLT, O.M. 1996: The insect cytochrome oxidase I gene: Evolutionary patterns and conserved primers for phylogenetic studies. – *Insect Molecular Biology* 5: 153-165.
- MALLET, J. 1995: A species definition for the modern synthesis. – *Trends in Ecology & Evolution* 10: 294-299.
- MODER, K., SCHLICK-STEINER, B.C., STEINER, F.M., CREMER, S., CHRISTIAN, E. & SEIFERT, B. 2007: Optimal species distinction by discriminant analyses: comparing established methods of character selection with a combination procedure using ant morphometrics as case study. – *Journal of Zoological Systematics and Evolutionary Research* 45: 82-87.
- MÜLLER, P. 1974: Aspects of zoogeography. – W. Junk, The Hague, 216 pp.
- NEUMEYER, R. 2008: Ergänzungen zur Artenliste der frei lebenden Ameisen (Hymenoptera: Formicidae) in der Schweiz. – *Entomo Helvetica* 1: 43-48.
- NYGAARD, S. & WURM, Y. 2015: Ant genomics (Hymenoptera: Formicidae): challenges to overcome and opportunities to seize. – *Myrmecological News* 21: 59-72.
- PATTON, J.L. & SMITH, M.F. 1994: Paraphyly, polyphyly, and the nature of species boundaries in pocket gophers (genus *Thomomys*). – *Systematic Biology* 43: 11-26.
- PERFILIEVA, K.S. 2015: The evolution of diagnostic characters of wing venation in representatives of the subfamily Myrmecinae (Hymenoptera: Formicidae). – *Entomological Review* 95: 1000-1009.
- PISARSKI, B. 1969: Myrmicidae und Formicidae. Ergebnisse der zoologischen Forschungen von Dr. Z. Kaszab in der Mongolei (Hymenoptera). – *Faunistische Abhandlungen* 2: 295-316.
- PULLANDRE, N., MODICA, M.V., ZHANG, Y., SIROVICH, L., BOISELIER, M.C., CRUAUD, C., HOLFORD, M. & SAMADI, S. 2012: Large-scale species delimitation method for hyperdiverse groups. – *Molecular Ecology* 21: 2671-2691.
- R DEVELOPMENT CORE TEAM 2012: R: a language and environment for statistical computing. – R Foundation for Statistical Computing, Vienna.
- RADCHENKO, A.G. 1992: Ants of the genus *Tetramorium* (Hymenoptera: Formicidae) of the USSR fauna. Report 2. – *Zoologicheskij Zhurnal* 71: 50-58.
- RADCHENKO, A.G. & SCUPOLA, A. 2015: Taxonomic revision of the *striativentre* species group of the genus *Tetramorium* (Hymenoptera: Formicidae). – *Vestnik zoologii* 49: 219-244.
- RAMBAUT, A., SUCHARD, M.A., XIE, D. & DRUMMOND, A.J. 2014: Tracer v1.6. – <<http://beast.bio.ed.ac.uk/Tracer>>, retrieved on 15 July 2017.
- ROHLF, F. 2015: tpsDig2, version 2.22. A program for digitizing landmarks and outlines for geometric morphometric analyses. – Department of Ecology and Evolution, State University of New York, Stony Brook, New York, NY.
- RONQUIST, F., TESLENKO, M., VAN DER MARK, P., AYRES, D.L., DARLING, A., HOHNA, S., LARGET, B., LIU, L., SUCHARD, M.A. & HUELSENBECK, J.P. 2012: MrBayes 3.2: efficient Bayesian phylogenetic inference and model choice across a large model space. – *Systematic Biology* 61: 539-542.
- RÖSZLER, P. 1936: Beiträge zur Kenntnis der Ameisenfauna von Siebenbürgen und Ungarn. – *Verhandlungen und Mitteilungen des Siebenbürgischen Vereins für Naturwissenschaften zu Hermannstadt* 83-84: 72-83.
- RÖSZLER, P. 1951: Myrmecologisches aus dem Jahre 1938. – *Zoologischer Anzeiger* 146: 88-96.
- RÜPPELL, O., STRÄTZ, M., BAIER, B. & HEINZE, J. 2003: Mitochondrial markers in the ant *Leptothorax rugatulus* reveal the population genetic consequences of female philopatry at different hierarchical levels. – *Molecular Ecology* 12: 795-801.
- SANETRA, M., GÜSTEN, R. & SCHULZ, A. 1999: On the taxonomy and distribution of Italian *Tetramorium* species and their social parasites (Hymenoptera: Formicidae). – *Memorie della Societa Entomologica Italiana* 77: 317-357.
- SANTOS, I.S., MARIANO, C.S.F., DELABIE, J.H.C., COSTA, M.A., CARVALHO, A.F. & SILVA, J.G. 2016: "Much more than a neck": karyotype differentiation between *Dolichoderus attelaboides* (FABRICIUS, 1775) and *Dolichoderus decollatus* F. SMITH, 1858 (Hymenoptera: Formicidae) and karyotypic diversity of five other Neotropical species of *Dolichoderus* LUND, 1831. – *Myrmecological News* 23: 61-69.
- SANTSCHI, F. 1927: A propos du *Tetramorium caespitum* L. – *Folia Myrmecologica et Termitologica* 4/5: 52-58.
- SCHLICK-STEINER, B.C. & STEINER, F.M. 2006: Die Ameisen der Sattnitz: gestern, heute und morgen. – In: GOLOB, B. & ZWANDER, H. (Eds.): *Die Sattnitz. Konglomerat der Natur im Süden Kärntens. Ein Naturführer.* – Naturwissenschaftlicher Verein für Kärnten, Klagenfurt, pp. 237-242.
- SCHLICK-STEINER, B.C., STEINER, F.M., MODER, K., SEIFERT, B., SANETRA, M., DYRESON, E., STAUFFER, C. & CHRISTIAN, E. 2006: A multidisciplinary approach reveals cryptic diversity in Western Palearctic *Tetramorium* ants (Hymenoptera: Formicidae). – *Molecular Phylogenetics and Evolution* 40: 259-273.
- SCHLICK-STEINER, B.C., STEINER, F.M., SANETRA, M., HELLER, G., STAUFFER, C., CHRISTIAN, E. & SEIFERT, B. 2005: Queen size dimorphism in the ant *Tetramorium moravicum* (Hymenoptera: Formicidae): morphometric, molecular genetic and experimental evidence. – *Insectes Sociaux* 52: 186-193.
- SCHLICK-STEINER, B.C., SEIFERT, B., STAUFFER, C., CHRISTIAN, E., CROZIER, R.H. & STEINER, F.M. 2007a: Without morphology, cryptic species stay in taxonomic crypsis following discovery. – *Trends in Ecology & Evolution* 22: 391-392.
- SCHLICK-STEINER, B.C., STEINER, F.M., SANETRA, M., SEIFERT, B., CHRISTIAN, E. & STAUFFER, C. 2007b: Lineage specific evolution of an alternative social strategy in *Tetramorium* ants (Hymenoptera: Formicidae). – *Biological Journal of the Linnean Society* 91: 247-255.
- SCHLICK-STEINER, B.C., STEINER, F.M., SEIFERT, B., STAUFFER, C., CHRISTIAN, E. & CROZIER, R.H. 2010: Integrative taxonomy: a multisource approach to exploring biodiversity. – *Annual Review of Entomology* 55: 421-438.
- SEIFERT, B. 1999: Interspecific hybridisations in natural populations of ants by example of a regional fauna (Hymenoptera: Formicidae). – *Insectes Sociaux* 46: 5-52.
- SEIFERT, B. 2002: How to distinguish most similar insect species – improving the stereomicroscopic and mathematical evaluation of external characters by example of ants. – *Journal of Applied Entomology* 126: 445-454.
- SEIFERT, B. 2003: The ant genus *Cardiocondyla* (Insecta: Hymenoptera: Formicidae) – a taxonomic revision of the *C. elegans*, *C. bulgarica*, *C. batesii*, *C. nuda*, *C. shuckardi*, *C. stambuloffii*, *C. wroughtonii*, *C. emeryi*, and *C. minutior* species groups. – *Annalen des Naturhistorischen Museums Wien, Serie B* 104: 203-338.
- SEIFERT, B. 2007: Die Ameisen Mittel- und Nordeuropas. – Lutra Verlags- und Vertriebsgesellschaft, Tauer/Görlitz, 386 pp.
- SEIFERT, B. 2009: Cryptic species in ants (Hymenoptera: Formicidae) revisited: We need a change in the alpha-taxonomic approach. – *Myrmecological News* 12: 149-166.
- SEIFERT, B. 2014: A pragmatic species concept applicable to all eukaryotic organisms independent from their mode of reproduction or evolutionary history. – *Soil Organisms* 86: 85-93.
- SEIFERT, B. 2016: Analyzing large-scale and intranidal phenotype distributions in eusocial Hymenoptera – a taxonomic tool

- to distinguish intraspecific dimorphism from heterospecificity. – *Myrmecological News* 23: 41-59.
- SEIFERT, B. & CSÖSZ, S. 2015: *Temnothorax crasecundus* sp. n. – a cryptic Eurocaucasian ant species (Hymenoptera: Formicidae) discovered by Nest Centroid Clustering. – *ZooKeys* 479: 37-64.
- SEIFERT, B., CSÖSZ, S. & SCHULZ, A. 2014a: NC-Clustering demonstrates heterospecificity of the cryptic ant species *Temnothorax luteus* (FOREL, 1874) and *T. racovitzai* (BONDROIT, 1918) (Hymenoptera: Formicidae). – *Contributions to Entomology* 64: 47-57.
- SEIFERT, B. & PANNIER, L. 2007: A method for standardized description of soil temperatures in terrestrial ecosystems. – *Abhandlungen und Berichte des Naturkundemuseums Görlitz* 78: 151-182.
- SEIFERT, B., RITZ, M. & CSÖSZ, S. 2014b: Application of Exploratory Data Analyses opens a new perspective in morphology-based alpha-taxonomy of eusocial organisms. – *Myrmecological News* 19: 1-15.
- SLOAN, D.B., HAVIRD, J.C. & SHARBROUGH, J. 2017: The on-again, off-again relationship between mitochondrial genomes and species boundaries. – *Molecular Ecology* 26: 2212-2236.
- SMITH, F. 1851: List of the specimens of British animals in the collection of the British Museum. Part VI. Hymenoptera, Aculeata. – British Museum, London, 134 pp.
- SMITH, G.R. 1992: Introgression in fishes: significance for paleontology, cladistics, and evolutionary rates. – *Systematic Biology* 41: 41-57.
- SMITH, M.A., RODRIGUEZ, J.J., WHITFIELD, J.B., DEANS, A.R., JANZEN, D.H., HALLWACHS, W. & HEBERT, P.D.N. 2008: Extreme diversity of tropical parasitoid wasps exposed by iterative integration of natural history, DNA barcoding, morphology, and collections. – *Proceedings of the National Academy of Sciences of the United States of America* 105: 12359-12364.
- SONG, H., BUHAY, J.E., WHITING, M.F. & CRANDALL, K.A. 2008: Many species in one: DNA barcoding overestimates the number of species when nuclear mitochondrial pseudogenes are coamplified. – *Proceedings of the National Academy of Sciences of the United States of America* 105: 13486-13491.
- STEINER, F.M., SCHLICK-STEINER, B.C. & BUSCHINGER, A. 2003: First record of unicolonial polygyny in *Tetramorium* cf. *caespitum* (Hymenoptera: Formicidae). – *Insectes Sociaux* 50: 98-99.
- STEINER, F.M., SCHLICK-STEINER, B.C. & MODER, K. 2006a: Morphology-based cyber identification engine to identify ants of the *Tetramorium caespitum/impurum* complex (Hymenoptera: Formicidae). – *Myrmecologische Nachrichten* 8: 175-180.
- STEINER, F.M., SCHLICK-STEINER, B.C., NIKIFOROV, A., KALB, R. & MISTRIK, R. 2002: Cuticular hydrocarbons of *Tetramorium* ants from Central Europe: analysis of GC-MS data with self-organizing maps (SOM) and implications for systematics. – *Journal of Chemical Ecology* 28: 2569-2584.
- STEINER, F.M., SCHLICK-STEINER, B.C., SANETRA, M., LJUBOMIROV, T., ANTONOVA, V., CHRISTIAN, E. & STAUFFER, C. 2005: Towards DNA-aided biogeography: an example from *Tetramorium* ants (Hymenoptera, Formicidae). – *Annales Zoologici Fennici* 42: 23-35.
- STEINER, F.M., SCHLICK-STEINER, B.C., TRAGER, J.C., MODER, K., SANETRA, M., CHRISTIAN, E. & STAUFFER, C. 2006b: *Tetramorium tsushimae*, a new invasive ant in North America. – *Biological Invasions* 8: 117-123.
- STEINER, F.M., SCHLICK-STEINER, B.C., VANDERWAL, J., REUTHER, K.D., CHRISTIAN, E., STAUFFER, C., SUAREZ, A.V., WILLIAMS, S.E. & CROZIER, R.H. 2008: Combined modelling of distribution and niche in invasion biology: a case study of two invasive *Tetramorium* ant species. – *Diversity and Distributions* 14: 538-545.
- STEINER, F.M., SEIFERT, B., MODER, K. & SCHLICK-STEINER, B.C. 2010: A multisource solution for a complex problem in biodiversity research: description of the cryptic ant species *Tetramorium alpestre* sp.n. (Hymenoptera: Formicidae). – *Zoologischer Anzeiger* 249: 223-254.
- TAKAHATA, N. & SLATKIN, M. 1984: Mitochondrial gene flow. – *Proceedings of the National Academy of Sciences of the United States of America* 81: 1764-1767.
- TAMURA, K. & AOTSUKA, T. 1988: Rapid isolation method of animal mitochondrial DNA by the alkaline lysis procedure. – *Biochemical Genetics* 26: 815-819.
- TAMURA, K., PETERSON, D., PETERSON, N., STECHER, G., NEI, M. & KUMAR, S. 2011: MEGA5: Molecular evolutionary genetics analysis using maximum likelihood, evolutionary distance, and maximum parsimony methods. – *Molecular Biology and Evolution* 28: 2731-2739.
- TĂUȘAN, I. & MARKÓ, B. 2011: Too salty? Not for *Tetramorium* cf. *caespitum*. Ant community of the Ocna Sibiului salina, Romania. – 4th Central European Workshop of Myrmecology, Cluj-Napoca, Romania (Poster).
- TOEWS, D.P.L. & BRELSFORD, A. 2012: The biogeography of mitochondrial and nuclear discordance in animals. – *Molecular Ecology* 21: 3907-3930.
- VOS, P., HOGERS, R., BLEEKER, M., REIJANS, M., VAN DE LEE, T., HORNES, M., FRIJTERS, A., POT, J., PELEMAN, J. & KUIPER, M. 1995: AFLP: a new technique for DNA fingerprinting. – *Nucleic Acids Research* 23: 4407-4414.
- WACHTER, G.A., ARTHOFER, W., DEJACO, T., RINNHOFER, L.J., STEINER, F.M. & SCHLICK-STEINER, B.C. 2012: Pleistocene survival on central Alpine nunataks: genetic evidence from the jumping bristletail *Machilis pallida*. – *Molecular Ecology* 21: 4983-4995.
- WAGNER, H.C. 2009: Ameisen (Formicidae) & der Rotbraune Keulenkäfer *Claviger testaceus* am Tamischbachturm. – *Schriften des Nationalparks Gesäuse* 4: 149-160.
- WAGNER, H.C. 2011a: Die Ameisen (Formicidae) einer Lawenrinne im Nationalpark Gesäuse (Steiermark). – *Schriften des Nationalparks Gesäuse* 6: 123-136.
- WAGNER, H.C. 2011b: Tag der Artenvielfalt – Die Ameisen (Hymenoptera: Formicidae) im Botanischen Garten Graz. – *Mitteilungen des naturwissenschaftlichen Vereines für Steiermark* 141: 235-240.
- WAGNER, H.C. 2012: Revision der Ameisensammlung (Hymenoptera: Formicidae) des Kärntner Landesmuseums. – *Carinthia II* 202/122: 545-600.
- WAGNER, H.C., AMBACH, J. & GLASER, F. 2010: 10 Erstmeldungen von Ameisen (Hymenoptera: Formicidae) für die Steiermark (Österreich). – *Joannea Zoologie* 11: 19-30.
- WAGNER, H.C., KOMPOSCH, C., AURENHAMMER, S., DEGASPERI, G., KORN, R., FREI, B., VOLKMER, J., HEIMBURG, H., IVENZ, D., RIEF, A., WIESMAIR, B., ZECHMEISTER, T., SCHNEIDER, M., DEJACO, T., NETZBERGER, R., KIRCHMAIR, G., GUNCZY, L.W., ZWEIDICK, O., KUNZ, G., PAILL, W., PFEIFER, J., ARTHOFER, P., HOLZER, E., BOROVSKY, R., HUBER, E., PLATZ, A., PAPERBERG, E., SCHIED, J., RAUSCH, H.R., GRAF, W., MUSTER, C., GUNCZY, J., FUCHS, P., PICHLER, G.A., ALLSPACH, A., PASS, T., TEISCHINGER, G., WIESINGER, G. & KREINER, D. 2016: Bericht über das zweite ÖEG-Insektencamp: 1019 Wirbellose Tierarten aus dem Nationalpark Gesäuse (Obersteiermark). – *Entomologica Austriaca* 23: 207-260.
- WARD, P.S. 2011: Integrating molecular phylogenetic results into ant taxonomy (Hymenoptera: Formicidae). – *Myrmecological News* 15: 21-29.
- WARD, P.S., BRADY, S.G., FISHER, B.L. & SCHULTZ, T.R. 2015: The evolution of myrmicine ants: phylogeny and biogeography

- of a hyperdiverse ant clade (Hymenoptera: Formicidae). – Systematic Entomology 40: 61-81.
- WARD, P.S. & SUMNIGHT, T.P. 2012: Molecular and morphological evidence for three sympatric species of *Leptanilla* (Hymenoptera: Formicidae) on the Greek island of Rhodes. – Myrmecological News 17: 5-11.
- WIENS, J.J. & SERVEDIO, M.R. 2000: Species delimitation in systematics: inferring diagnostic differences between species. – Proceedings of the Royal Society B-Biological Sciences 267: 631-636.
- ZWICKL, D. J. 2006: Genetic algorithm approaches for the phylogenetic analysis of large biological sequence datasets under the maximum likelihood criterion. – Ph.D. dissertation, The University of Texas at Austin, TX, USA, 115 pp.